CSIR

Division of Earth, Marine and Atmospheric Science and Technology

Report to the

WATER RESEARCH COMMISSION

on

INTERACTION BETWEEN THE BOUNDARY LAYER AND KENDAL POWER STATION NATURAL-DRAUGHT DRY-COOLING TOWER

by

D J deV Swanepoel

and

M Zunckel

WRC Report No. 452/1/93
ISBN 1 86845 015 5

PRETORIA
September 1993

INTERACTION BETWEEN THE BOUNDARY LAYER AND KENDAL POWER STATION NATURAL-DRAUGHT DRY-COOLING TOWER

by

D J deV Swanepoel

and

M Zunckel

EXECUTIVE SUMMARY

With water being a scarce commodity in South Africa, natural-draught dry-cooling has been employed at a number of South African power stations as an alternative cooling process to water evaporation. Naturally, with the enormous heat exchange in such cooling towers, significant effects of the tower on the stable atmospheric boundary layer are expected, and has led to intensive investigative research.

Much of this research was conducted at the Grootvlei Power Station in 1984 and 1985. There, the natural-draught dry-cooling towers each service a 200 MW power-generating unit. These cooling towers were found to influence the stable atmospheric boundary layer within a region of one tower height from the tower periphery. They were found to entrain an average of 50% of the nocturnal temperature inversion into the tower inlet. This implied that the air being entrained into the tower for the cooling process was considerably warmer than the air at 1,2 m above ground level (AGL). This is the standard height at which meteorological screen temperatures are measured. The entrainment of warmer air under stable boundary layer conditions implies decreased tower efficiency.

In 1990, research was carried out at a natural-draught dry-cooling tower at the Kendal Power Station, serving a 600 MW generating unit. This work was somewhat inconclusive, due to unfavourable weather conditions. Nevertheless, the results indicate that the tower significantly affects the stable boundary layer up to a distance of about two tower heights from the tower periphery. An average inversion entrainment of 50% to 78% was observed. This work concluded with a number of recommendations, which formed the basis of a follow-up proposal to the Water Research Commission. It was, inter alia, recommended to repeat the experiment in 1992 under favourable stable boundary layer conditions and to examine possible scaling effects between the findings at the smaller Grootvlei Power Station and those at Kendal.

The project was awarded to the CSIR with the objective of determining the region of influence of Kendal's No. 1 cooling tower under stable boundary layer conditions and the degree of inversion entrainment. To this end, five nocturnal field excursions were conducted at Kendal. During these, temperature and wind profiles in six planes over the entire height of the tower intake region were monitored. The two-dimensional temperature field was monitored between

ground level and the top of the tower. Tethered balloon soundings were conducted from suitable sites upwind and downwind of the cooling tower, and temperature and wind profiles were measured up to 96 m AGL at a site 685 m north of the tower. Tower performance data were recorded and made available to the CSIR by Eskom.

This study found that, under calm or light wind conditions, the stable boundary layer is significantly distorted around the cooling tower. The region of influence of the cooling tower was most pronounced within a distance of one tower height from its periphery. Some boundary layer distortion was evident at two tower heights distance. No evidence of air entering the tower intake area from outside the distorted stable boundary layer was found. Observed entrainment factors in excess of 100% of the ambient temperature inversion indicated that the air entering the tower is often twice as warm as the air at 1,2 m AGL in the undisturbed boundary layer.

Under prevailing wind conditions, the cooling tower heat plume was found to be advected both downward and downwind. The resultant effect on the stable boundary layer was most pronounced within two tower heights distance from the cooling tower on the downwind side. Almost no effect was found upwind of the cooling tower or elsewhere outside of the direct downwind plane. Entrainment factors in the order of 70% of the ambient temperature inversion were observed. This implies that the air entrained into the cooling tower under prevailing wind conditions is somewhat warmer than that measured at 1,2 m AGL in the undisturbed stable boundary layer.

Using characteristic performance curves for the cooling tower, the efficiency of the cooling tower was assessed for the various ambient weather conditions. While the stable boundary layer was significantly distorted around the cooling tower, the cooling tower did not cool the coolant water to the temperatures indicated by the characteristic curves. This deviation was greater during lower operation levels of unit 1 through the cooling tower than at near maximum operation. The direction of the prevailing wind seemed to play a role in the cooling tower's performance. The cooling tower cooled the coolant water to temperatures below those determined using the characteristic curves with easterly winds, but performed less favourably with northwesterly winds.

ACKNOWLEDGEMENTS

The authors wish to thank the following persons and organisations:

- The Water Research Commission for funding the project.

- Personnel at Eskom Rosherville and Kendal Power Station for tower data and valued information on tower characteristics and performance. Kendal Power Station personnel are also thanked for some logistical support.

- Ematek's Y Hong, I Danford, E Erasmus, S O'Beirne and K Brassel for tethersonde soundings, often carried out in trying conditions. K Brassel is also thanked for the diagrams contained in this report. D Pum and H Langenberg for assistance with field instrumentation. C Roos for assistance during field excursions.

- Miss K van Möllendorff of the Weather Bureau for supplying synoptic weather information.

- Mrs S G Good for the high standard of typing contained in this report.

CONTENTS

LIST OF TABLES

LIST OF FIGURES

1. INTRODUCTION

With water being a scarce commodity in South Africa, much investigation into the efficiency of natural-draught dry-cooling towers, as an alternative cooling process for power stations, has been undertaken over the last number of years. These studies examined, inter alia, the interaction of the cooling towers with the stable boundary layer (SBL) at various power stations on the Transvaal highveld (see: Surridge, 1981; Surridge and Hayton, 1984 and 1985; Swanepoel and Held, 1990). The 1985 study showed that significant interaction occurs between the cooling towers of the Grootvlei Power Station, each servicing a 200 MW generating unit, and the nocturnal SBL. Distortion of the SBL was found to occur within a region of influence of the dry-cooling tower that extended one tower height from the periphery of the tower, within which about 50% of the observed temperature inversion was entrained into the cooling tower. This increased the mean coolant air temperature of the cooling tower intake region to above that indicated by surface measurements.

Swanepoel and Held (1990) attempted to examine the effects of scale by studying the cooling towers at the Kendal Power Station, each servicing 660 MW power generators. Unfortunately, weather conditions during the field experiment were not suitable and the aims of the study, namely

- to determine the percentage of the SBL which is entrained into the cooling tower,
- to determine the region of influence of the cooling tower leading to optimum tower spacing, and
- provide experimental data to the University of Stellenbosch for validation of a theoretical model describing the operation of dry-cooling systems,

could not be answered satisfactorily. The limited quantitative results obtained, indicated that the natural-draught dry-cooling tower at Kendal affected the SBL, and possibly reduces the tower efficiency under certain weather conditions.

This somewhat inconclusive study proposed a number of recommendations to answer key questions. These recommendations formed the basis of a proposal made to the Water Research Commission (WRC) to conduct further field studies at Kendal Power Station under stable nocturnal boundary layer conditions to attempt to answer the issues. The aims of the proposed study to the WRC which are addressed in this report are:

- To repeat the 1990 experiment under typical winter Highveld nocturnal SBL conditions.
- To monitor temperature and wind flow profiles at a number of positions within the intake region of the cooling tower to determine the intake temperature, irrespective of ambient winds.
- To monitor temperature and wind profiles over the 25 m vertical extent of the cooling tower intake region.
- To use tethersonde systems to measure temperature, wind speed and wind direction profiles- up and downwind of the cooling tower.
- To use cooling tower performance data for comparison with various environmental conditions.
- To provide the University of Stellenbosch with suitable data for model evaluation.

2. INSTRUMENTATION AND DATA ACQUISITION

Eskom's Kendal Power Station is situated on the Eastern Transvaal Highveld at 28° 28'S and 26° 05'E. The power station consists of six 660 MW coal-fired power generating units, each cooled by a natural-draught dry-cooling tower. Experimental field work was carried out in and around cooling tower 1 (CT1) which was suitably rigged for the investigations. Figure 2.1 shows a scale plan view of the experimental area at the Kendal Power Station.

Instrumentation used during the field experiment included existing Eskom equipment and additionally installed CSIR equipment. Instrumentation used in the field experiment in the vicinity of CT1 are:

2.1 Four 22 m instrumented intake masts

Four instrumented 22 m masts located within the intake area, on the northern, eastern, southern and western sides of the cooling tower. Temperature and tangential and radial wind speeds were measured at 2 m, 5 m, 8 m, 11 m, 16 m and 22 m above ground level (AGL). Figures 2.2(a) and 2.2(b) illustrate the positions of the masts in the tower intake region and show the elevations of the temperature and wind sensors. One of the masts and an instrument level are illustrated in the photographs in Figure 2.2(c). Temperatures were recorded with

YSI Thermilinear® Component YSI 44202 sensors (Operating range -5 to 45°C). Orthogonally mounted propeller anemometers, described in Surridge (1982), were used to measure the horizontal northerly and easterly components of the wind speeds. Data were logged on in-house data loggers, calculating 10 minute means.

Calibration tests were carried out for each of the anemometers used in the experiment in the wind tunnel facility at Aerotek, CSIR. Relevant corrections were applied to all data. Details of the calibration regression fit to each of the anemometers are included in Appendix 1, with an example of the calibration curve for one sensor. Similarly, the 24 temperature sensors used in the experiment were calibrated in a temperature test chamber facility at Ematek, CSIR. Relevant corrections were applied to all the data. Details of the regression fit to each sensor are included in Appendix 2, with an example of the calibration curve of one sensor.

2.2 Two-dimension (2-D) temperature profiler:

Four lines consisting of 19 serially mounted YSI Thermilinear® Component YSI 44202 temperature sensors, provided a two-dimensional temperature field in a radial vertical plane on the southeastern side of CT1, Figure 2.1. The sensor lines, anchored at a common point at the top of the cooling tower, extended to points 10 m, 40 m, 70 m and 100 m from the base of the tower. A schematic of the two-dimensional temperature profiler illustrating the position of the 19 temperature sensors on the four guy-lines is given in Figure 2.3. A complete cycle of the 19 temperatures, hence a two-dimensional temperature profile from ground level to the top of the cooling tower, was completed every two minutes and logged throughout the nocturnal field excursions.

Calibration tests were performed on the sensors in the temperature test chamber facility at Ematek, CSIR, and relevant corrections were applied to the data. Details of the calibration regression fit are included in Appendix 3, and an example of the calibration curve for one sensor is shown.

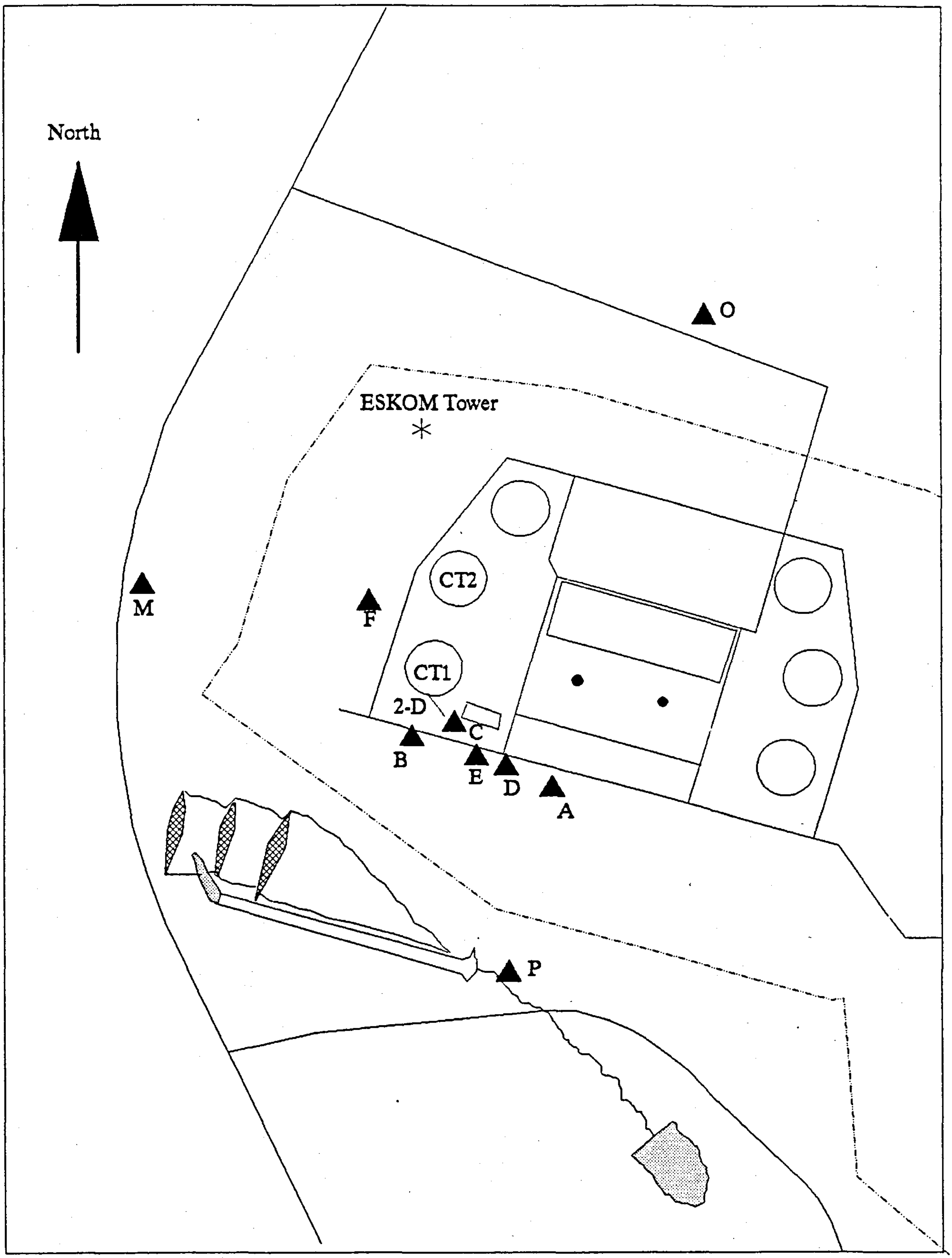

Figure 2.1 Plan view of the experimental area

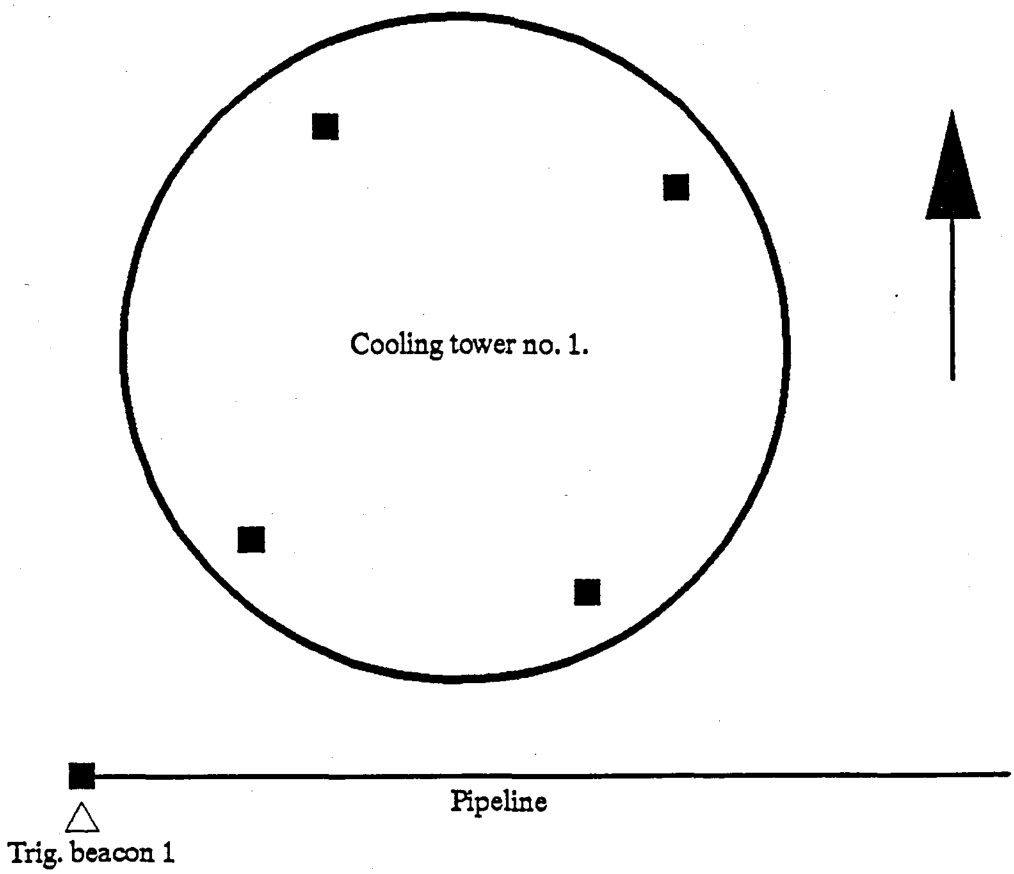

Figure 2.2(a) Position of the 22 m masts in the cooling tower intake region.

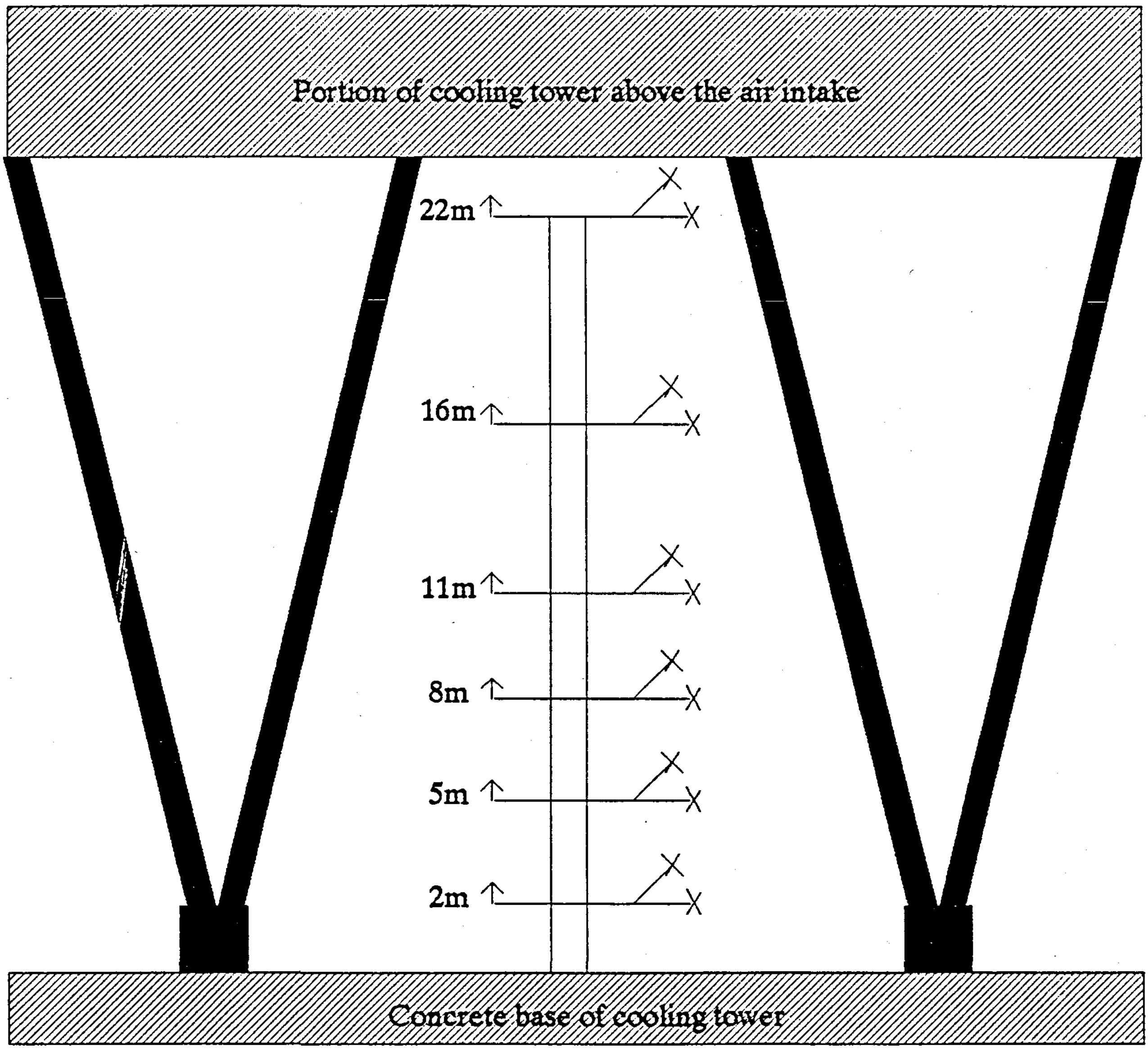

Figure 2.2(b): Schematic of the 22 metre mast in the cooling tower air intake.

2.3 Tethersondes

Two tethersonde balloons were operated from various sites upwind and downwind from CT1. Soundings were carried out frequently and simultaneously from suitably unobstructed sites, determined by the prevailing wind. The sites are shown in Figure 2.1. Vertical profiles of temperature, humidity and wind speed and direction were obtained from the soundings within and out of the immediate field of influence of the cooling tower. Generally, the profiles provided information of the background SBL to heights above the top of the cooling tower or higher when wind speeds were less than 10 $m.s^{-1}$. Information on the extent of the cooling towers field of influence was gleaned from these soundings.

Unfortunately one sonde was lost at the end of the field experiment before calibration tests could be performed. However, surface dry bulb and wet bulb temperatures, determined using a whirling psychrometer before each sounding, were used as initial values.

Wind direction during a tether sounding is obtained by the orientation of a magnetic compass, housed in the sonde, relative to the tethered balloon. Wind directions were corrected for the magnetic declination at Kendal, 16° W.

2.4 96 m Eskom mast

A 96 m mast, situated 680 m north of CT1 (Figure 2.1), measures ambient meteorological parameters continuously. The mast is equipped by Eskom and measures temperature at 1 m, 2 m, 2,5 m, 5 m, 10 m, 20 m, 40 m, 65 m, and 96 m AGL. Three-dimensional anemometers are positioned at 10 m, 20 m, 40 m 65 m and 96 m AGL. A complete set of data was recorded every six minutes. All the temperature and wind sensors were calibrated on 8 June 1992, prior to the commencement of the field work. YSI Thermilinear® Component YSI 44201 temperature sensors (Operational range 0 to 100°C) were used on the 96 m tower.

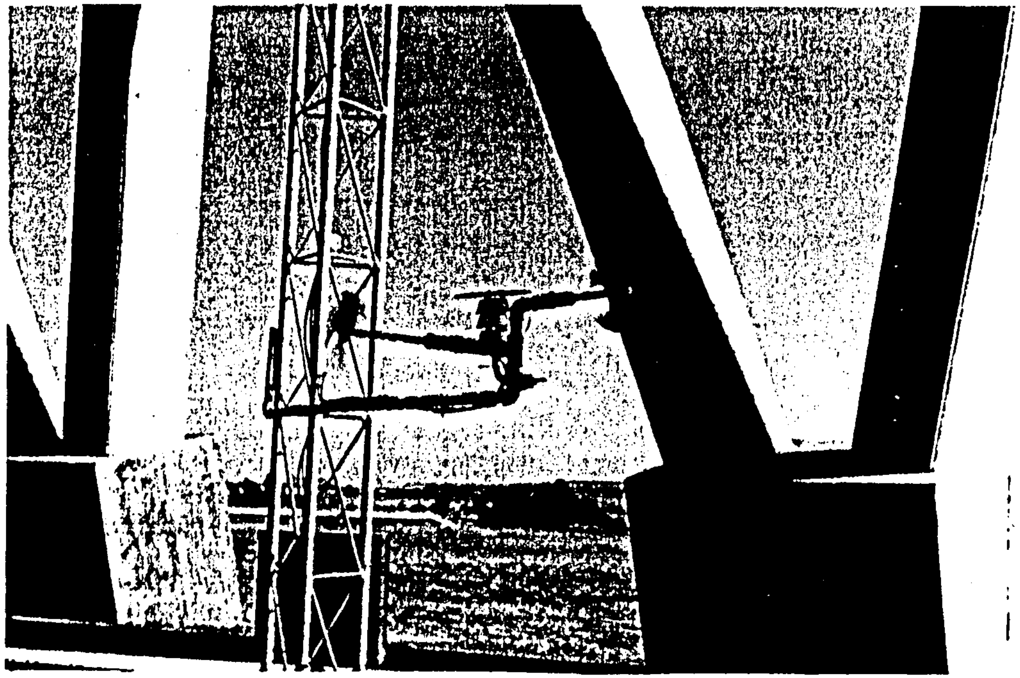

Figure 2.2(c):

Shown above are a set of temperature and wind sensors and on the right is a 22m instrumented mast.

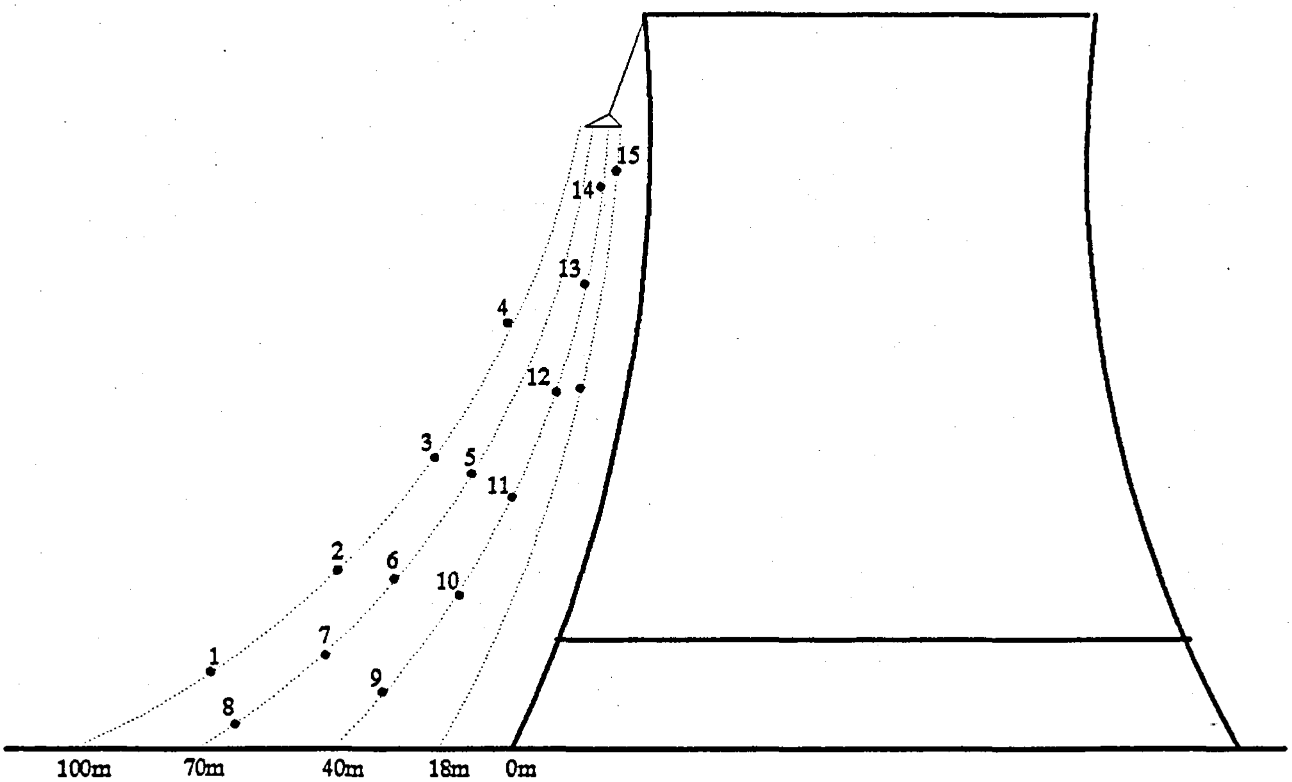

Height of sensors above ground level.

1. - 20m	9. - 13m
2. - 45m	10. - 37m
3. - 70m	11. - 60m
4. - 100m	12. - 85m
5. - 65m	13. - 110m
6. - 40m	14. - 130m
7. - 22m	15. - 135m
8. - 5m	

Figure 2.3 Schematic of the 2-D temperature profiler

2.5 Air outflow

Twelve temperature sensors and three wind sensors, measuring the vertical component only, were installed by Eskom in the exit plane of the cooling tower. The position of the sensors on one of four sensor lines is illustrated by the schematic in Figure 2.4.

2.6 Coolant water

Eskom supplied sensors to measure the temperature of the coolant water into and out of the heat exchanger at four points on each leg. The total power generated by unit 1 and related data during the nocturnal field excursions were monitored and supplied by Kendal Power Station personnel.

2.7 Cooling tower internal temperature profile

Four temperature sensors were mounted on the cooling tower heat exchanger platform, between two A-frame bundles, one each for each concentric ring of the bundles. A cycle was recorded every two minutes. These were installed to facilitate input for the model used by the University of Stellenbosch. A schematic of the above is illustrated in Figure 2.5.

The 28 sensors mentioned in paragraphs 2.5 to 2.7 were linked by Ematek personnel to their CR-10 data logger. These sensors were calibrated by TRI (Eskom).

3. EXPERIMENTAL PERIOD: CASE STUDIES

3.1 Introduction

The highest frequency of nocturnal surface inversions on the Eastern Transvaal Highveld (ETH), indicative of stable boundary layer conditions, occurs during the winter months of June to August (Tyson *et al.*, 1976). However, during these months the frequency of intense cold front intrusions across the ETH, followed by ridging of the Indian Ocean Anticyclone (IOA) is also highest. These are conditions most likely to upset the SBL. With these factors in mind, a number of nocturnal field excursions were planned for June and July 1992 to determine the effect of CT1 on the SBL.

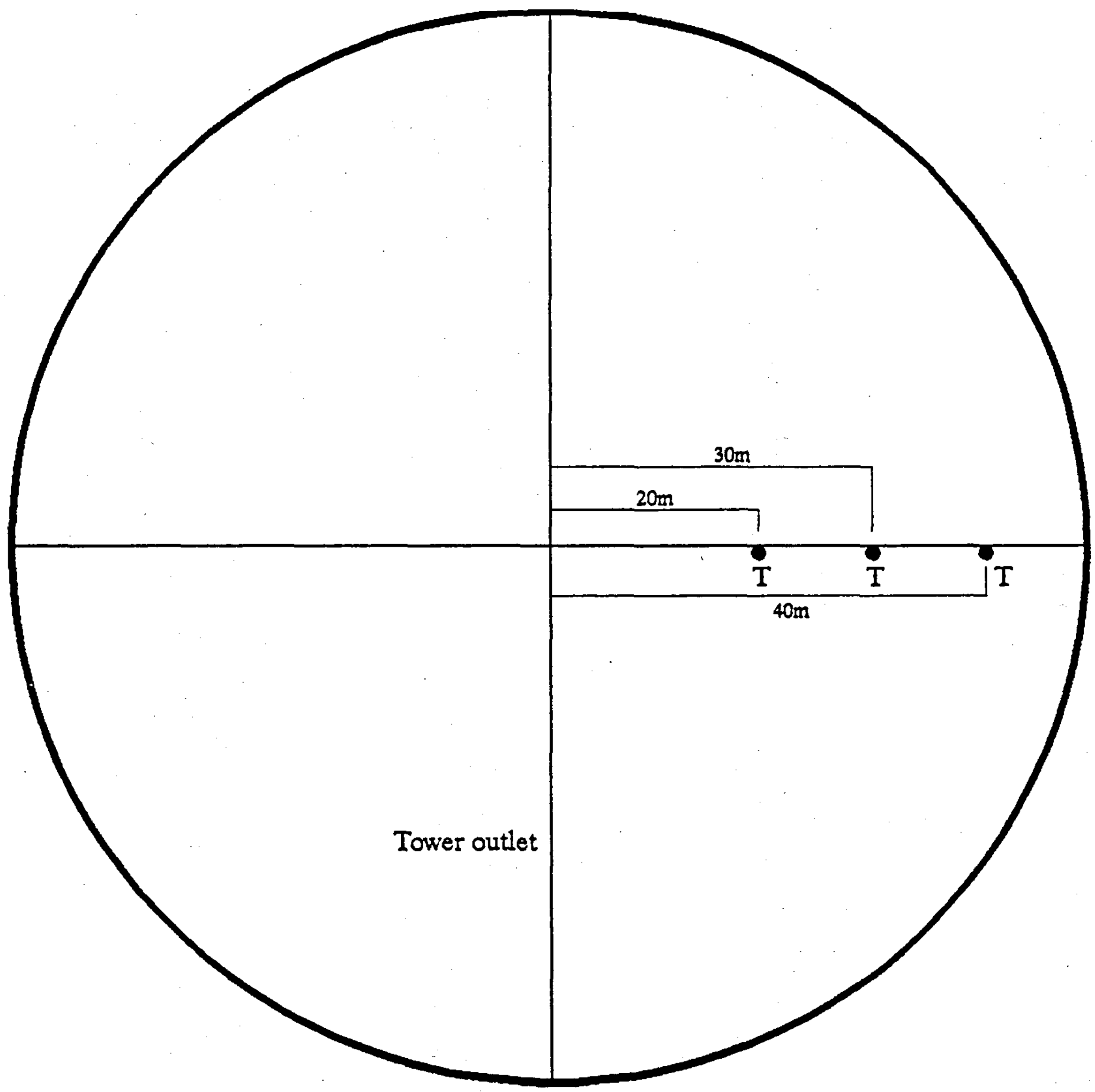

Figure 2.4 Instrumentation in the exit plane of cooling tower no. 1 (CT1).

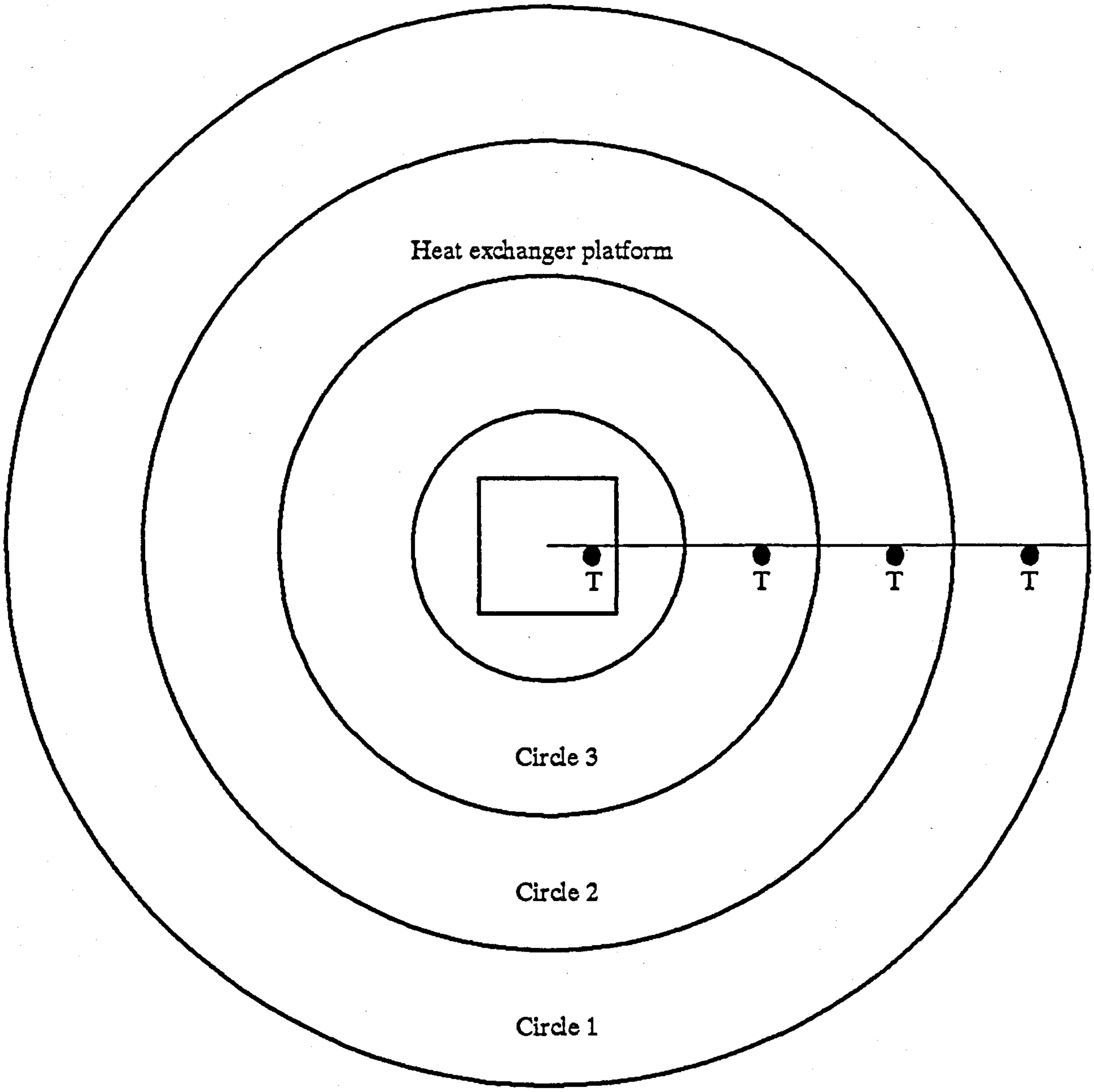

Figure 2.5 Schematic of the Stellenbosch temperature profiler on the tower heat exchanger platform. The A-frame radiators are situated concentrically around each of the circles 1 to 3 as well as the central square. The temperature sensors are positioned as shown between the A-framed radiators. They are approximately in line with the CSIR profiler for external temperature measurements.

To facilitate smooth operation during the field excursions, preparation of equipment and its installation in and around CT1 took place from March to May 1992.

Typical winter stable boundary conditions on the ETH were often disturbed during June and July 1992 by the passage of cold fronts, and the subsequent intrusion of maritime air from the east due to ridging of the IOA, and this occurred more often than expected by the Ematek team. As a result, opportunity for field excursions to monitor SBL conditions were limited. A further limitation was placed on the field program through national power cut-backs. During the period 26 June 1992 to 8 July 1992, Kendal Power Station was placed in cold storage by Eskom. This is a non-operational situation.

In order to determine the extent of the interaction of CT1 on the SBL, power generating unit 1 was required to operate at above 70% of its capacity. Due to relaxed national industrial activity from Friday afternoon to Monday morning, the power station operates at well below its maximum potential during this period, hence below the level required for this study. This situation placed a further constraint on field work opportunities.

Relaxed industrial activity at night usually permits the power station to operate at below full capacity. For the duration of the field work Eskom endeavoured to operate unit 1 at above 70% of its full capacity.

Despite these inhibiting factors, five nocturnal field excursions were undertaken during June and July and data capture was achieved with a varying degree of success. These excursions are discussed chronologically as case studies in Sections 3.2 to 3.6. The data upon which the case studies are based were collected between 21:00 and 03:00. This period was chosen to eliminate the twilight periods and the transition from day to night, and vice versa, and to facilitate comparative studies with similar studies at Grootvlei (Surridge and Hayton, 1985) and at Kendal (Swanepoel and Held, 1990). In some case study discussions, the nocturnal period is sub-divided into shorter periods of interest. The shorter periods were selected either because of a marked change in generating output of unit 1, or because of the occurrence of a significant change in a background SBL parameter. The case study results are summarised collectively in Section 3.7 where common features are highlighted.

The function used to describe the percentage of the observed nocturnal temperature inversion that is entrained into the dry-cooling tower inlet is defined as (Surridge and Hayton, 1985):

$$\frac{\theta_{Inlet} - \theta_{Inv.min}}{\Delta\theta_{Inv.}} * 100 \qquad (3.1.1)$$

where $\theta_{Inv.min}$ is the minimum potential temperature of the observed inversion, $\Delta\theta_{Inv.}$ is the magnitude of the inversion, i.e. temperature difference between the top of the inversion and the bottom. θ_{Inlet} is the mean inlet potential temperature. Potential temperature of a parcel of air is conservative during vertical displacement of the parcel. Since vertical motions of air are considered in the case study discussions, potential temperature, rather than actual temperature, is used when calculating entrainment and boundary layer distortion.

Surridge and Hayton (1984) showed the radial air flow profile into a cooling tower to be non-linear. Therefore, the air temperature measured at different heights in the intake region of a cooling tower must be appropriately weighted to produce a realistic mean. The radial inlet air flow into the cooling tower in considered isotropic, i.e. independent of direction, hence radial air flow at the four intake positions is weighted equally. The mean intake potential temperature is given by Equation 3.1.2:

$$\theta_{Inlet} = \sum_{i=1}^{6} w_i \left(\sum_{j=1}^{4} \frac{\theta_{ij}}{4} \right) / \sum_{i=1}^{6} w_i \qquad (3.1.2)$$

In this equation, θ indicates potential temperatures, j indicates the four profile positions of each mast, i indicates the six monitoring heights on the masts and w_i indicates the appropriate weighting factor for each height. The divisor 4 corresponds to the number of temperature profiles, and the normalisation divisor is the sum of the weighting factors.

The entrainment function in Equation 3.1.1 indicates that region of the undisturbed background inversion which serves as the main source of coolant air. The increase in temperature of the entrained air above that measured at 1,2 m AGL is expressed as a percentage of the inversion magnitude. If an entrainment factor of 60% was calculated for an observed inversion of 5°C, the mean inlet temperature would be 3°C higher than the temperature measured at 1,2 m AGL in the background inversion.

In the case study discussions, the output of unit 1 is considered as a percentage of maximum operational output, i.e. percentage of 660 MW. The abscissa in the relevant figures shows the day number and the time as the decimal. For example, 00:00 and 12:00 on 31 January would be indicated as 31,00 and 31,50, respectively.

3.2 Case Study 1: 8 June 21:00 - 9 June 03:00

Strong eastward ridging of the Atlantic Ocean Anticyclone on 6 June 1992 resulted in the formation of its Indian Ocean counterpart by 8 June 1992. This anticyclone extended across the central parts of southern Africa in the form of a strong high at 850 hPa. This high dominated the synoptic scale circulation over the study region during the nocturnal period 8-9 June 1992. The 14:00 synoptic chart on 8 June 1992 is shown in Figure 3.2.1.

The temperature and wind measurements at the 96 m Eskom tower were stable throughout the study period. However, gradual changes did occur due to intensification of the surface inversion. At the start of the nocturnal period, the surface temperature of 10°C increased with height to 12,4°C at 65 m AGL. This 2,4°C inversion increased to 5,9°C by the end of the period. The tethered balloon sounding at 02:00 showed the top of the inversion to occur above 96 m AGL, i.e. above the top of the Eskom mast. The mean wind direction remained consistently easterly throughout the nocturnal period. At ground level, light wind occurred, but increased consistently with height to reach maximum speeds of more than 8 $m.s^{-1}$ at 65 m AGL. The mean temperature and wind profiles are shown in Figure 3.2.2 for the period 21:00 - 03:00, 8-9 June 1992. The relatively small standard deviations indicate the stable nature of these parameters during the nocturnal period.

Generating output of unit 1 during the case study was stable and the mean output was 73,5% of the maximum capacity. The percentage of maximum generating capacity is plotted against time in Figure 3.2.3 for the nocturnal period.

One tethersonde sounding was carried out from site A, Figure 2.1, at 02:00. Site A is located 420 m southeast of CT1. With prevailing easterly winds, this site is situated approximately upwind of CT1 at 02:00. The Kendal Power Station complex prevented selection of a tethersonde site due east of CT1. This sounding produced background temperature and wind profiles up to a height of 420 m AGL. A surface temperature inversion of 3,2°C was observed, from 9,6°C at ground level to 12,8°C at the inversion top. Above this level, the temperature profile was mostly isothermal to the top of the sounding. The additional information gleaned from the tether sounding over that obtained from the

Eskom mast is the height and temperature at the top of the surface inversion. These temperature profiles compare well through to 96 m AGL. It can therefore be assumed that the mean background surface inversion is somewhat stronger and deeper than indicated in Figure 3.2.2 by the Eskom mast. The temperature profile at site A is shown in Figure 3.2.4.

The lowest 100 m of the wind profile at site A, Figure 3.2.4, closely resembles the Eskom wind profiles, Figure 3.2.2. Wind speeds increased from light winds, 2 to 4 $m.s^{-1}$, at ground level to a maximum of about 9 $m.s^{-1}$ at 70 m AGL. Above this level, the speed decreases consistently to the top of the sounding. Wind direction is easterly through the profile.

Temperatures and the tangential and radial wind components at the four 22 m monitoring masts in the intake region of CT1 are listed in Table 3.2.1. As expected with prevailing easterlies, the strongest inflow occurs at the eastern side of CT1. This inflow shows a maximum between 8 and 15 m AGL. In the section of the intake region above 22 m AGL, the radial component decreases markedly. So much so that at 22 m AGL, a slight outflow occurs at the northern side of CT1. The strongest tangential winds occur at the southern side of CT1. This might be expected as the clockwise orientated tangential component at this point is due east, coinciding with the prevailing wind. Generally, little vertical temperature gradient through the 22 m extent of the tower intake masts occurs. However, at the western side a much colder layer of air was observed below 5 m AGL. This air was 4°C colder than the rest of the air intake column.

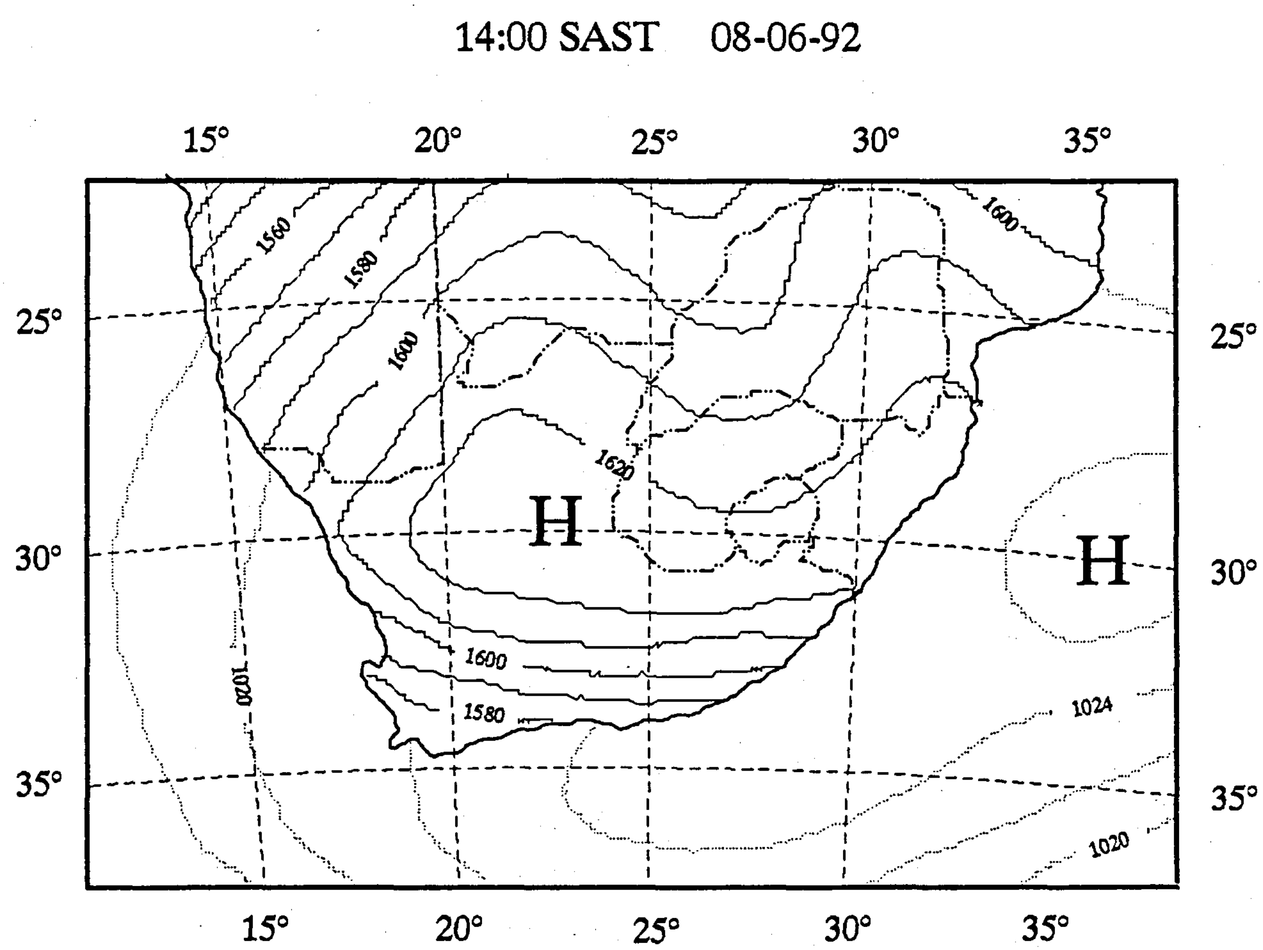

Figure 3.2.1: 14:00 synoptic chart on 8 June 1992. Isobars are shown over the ocean and 850hPa height contours over the land.

ESKOM 96m MAST

MEAN NOCTURNAL PERIOD 8-9 JUNE 1992

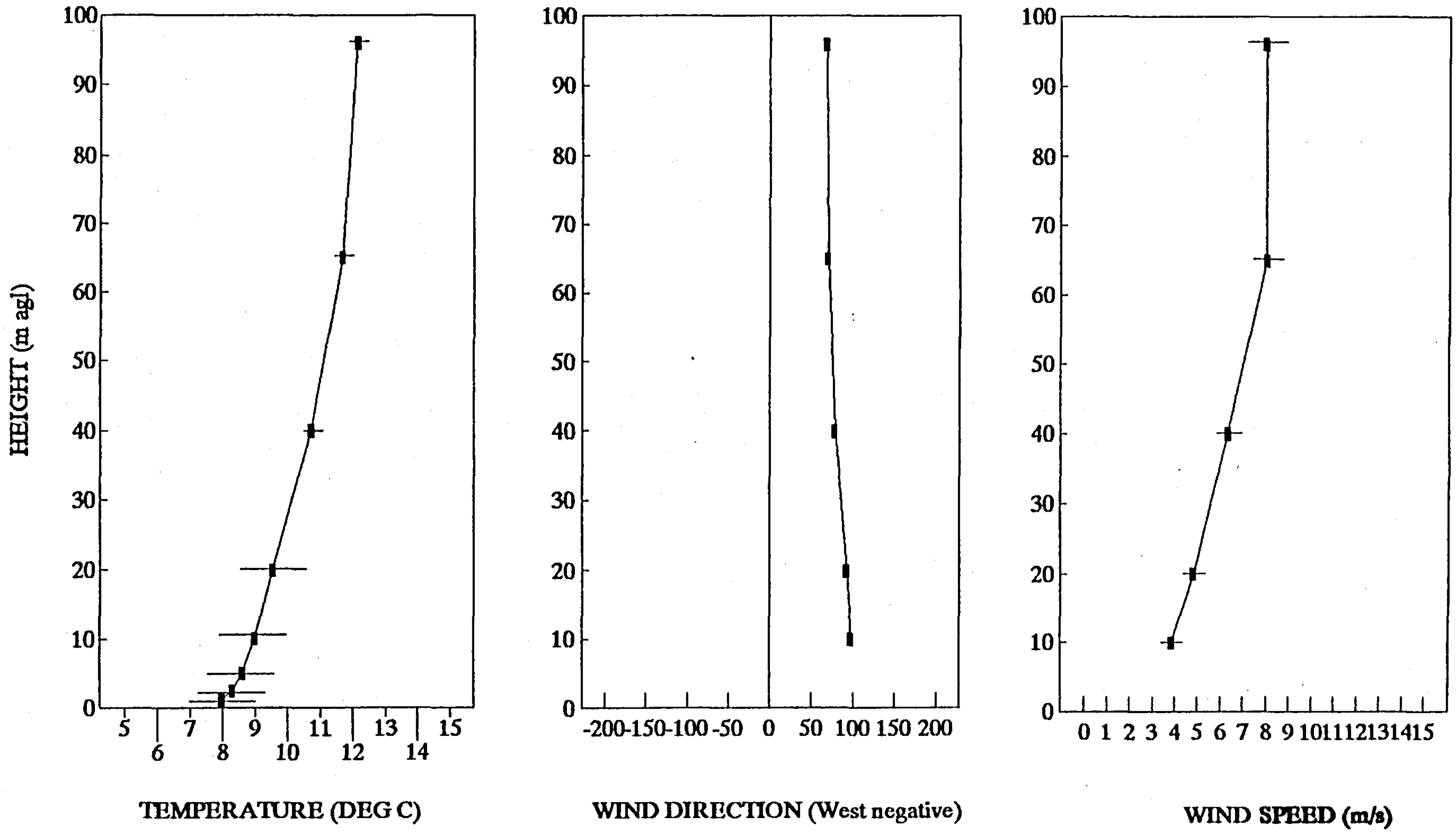

Figure 3.2.2: Mean temperature, wind direction and wind speed profiles for the nocturnal period 8 to 9 June 1992. The bars are standard deviations.

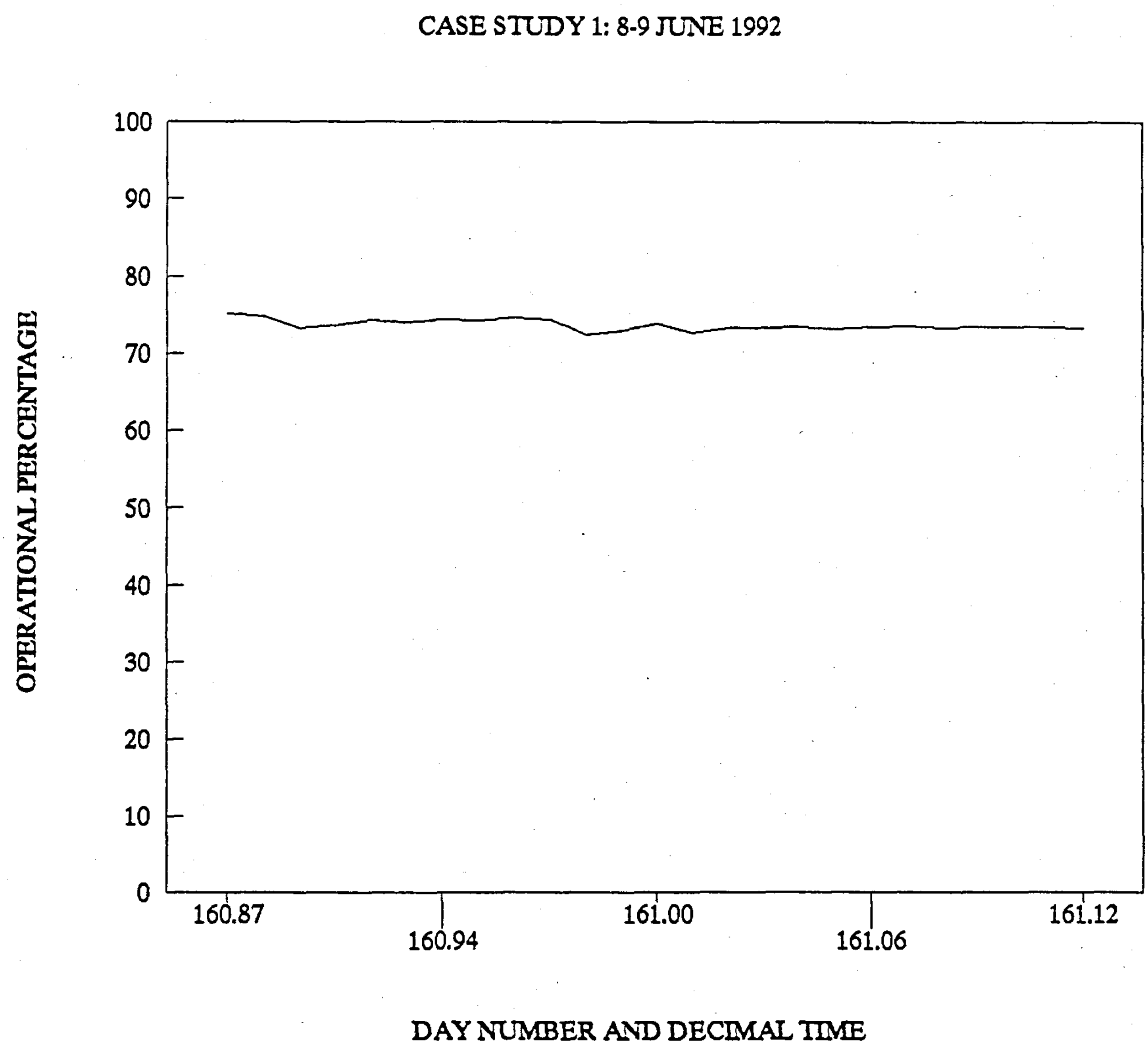

Figure 3.2.3: Percentage of maximum generation output of unit 1 during the nocturnal period 8 to 9 June 1992.

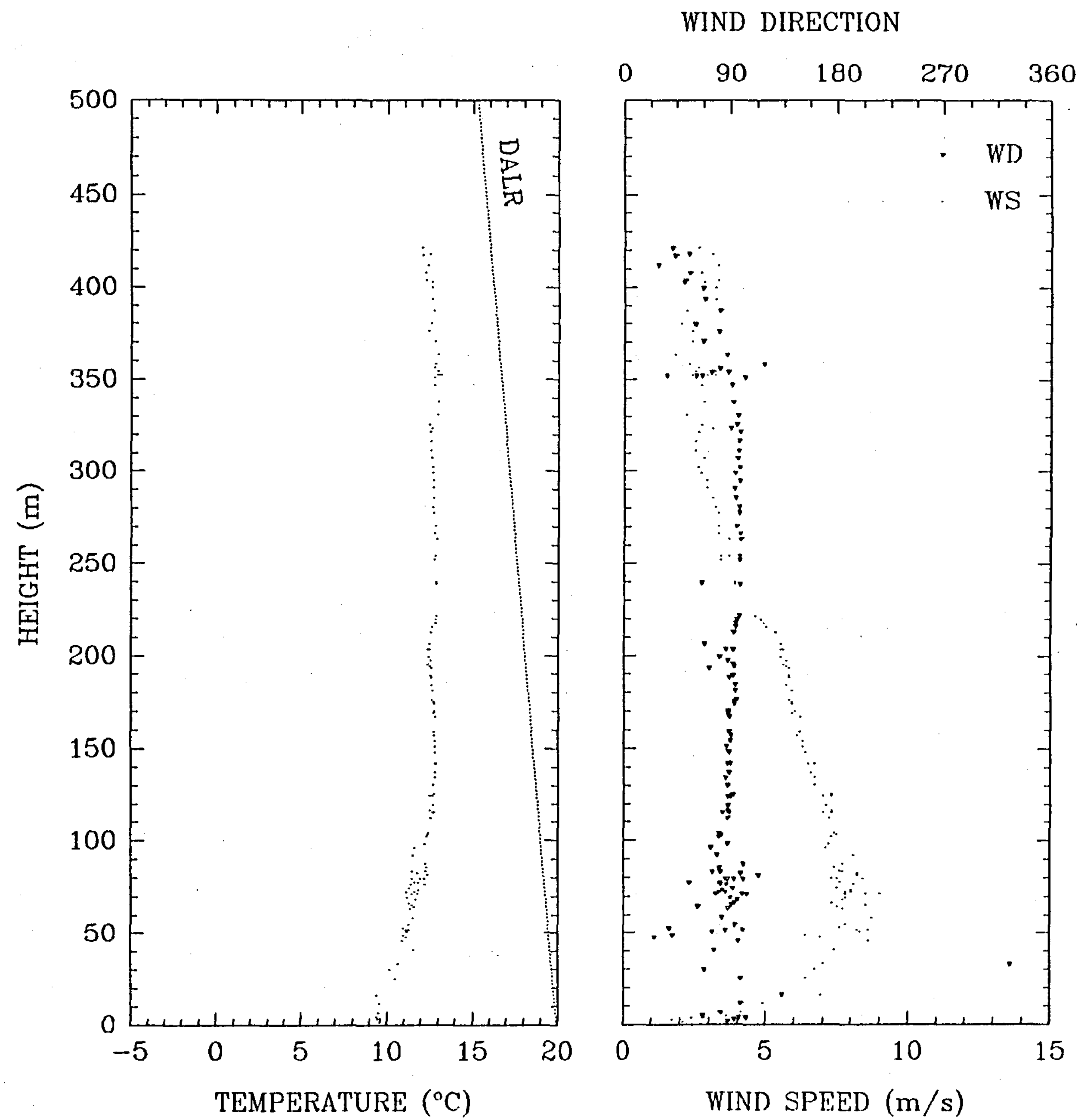

Figure 3.2.4: Tethersonde profiles at site A at 02:00 on the 9 June 1992.

Table 3.2.1 Mean potential temperature (T_θ) in °C, tangential wind speed (V_T) and radial wind speed (V_R) both m.s^{-1}, at the four 22 m intake masts during the period 21:00 to 03:00, 8-9 June 1992. Heights are m AGL, V_T is positive clockwise and V_R is positive into the tower. NRS are normalised radial wind speeds.

Height		N	E	S	W	Mean
22 m	T_θ	11,6	12,0	11,7	11,6	11,7
	V_T	2,2	0,2	2,0	2,2	1,4
	V_R	-0,9	1,2	1,0	2,1	0,9
	NRS	0,29	0,17	0,48	0,60	0,38
16 m	T_θ	12,1	-	-	11,7	11,9
	V_T	2,2	1,0	-	1,5	1,6
	V_R	-0,1	7,4	-	2,3	3,2
	NRS	1,0	1,0	-	0,65	0,88
11 m	T_θ	11,9	11,8	11,5	-	11,7
	V_T	2,1	0,5	4,4	1,4	2,1
	V_R	0,7	6,9	1,	2,5	3,0
	NRS	0,92	0,93	0,907	0,72	0,87
8 m	T_θ	11,7	11,9	11,7	11,5	11,7
	V_T	1,4	0,6	-	1,1	1,0
	V_R	1,4	6,3	-	2,4	3,2
	NRS	0,49	0,95	-	0,68	0,71
5 m	T_θ	12,1	11,3	11,5	7,3	10,6
	V_T	1,5	0,9	2,5	2,3	1,8
	V_R	2,0	5,6	1,3	1,5	2,6
	NRS	0,05	0,75	0,70	0,43	0,46
2 m	T_θ	12,0	10,9	10,9	7,5	10,3
	V_T	2,4	1,1	3,2	2,2	2,2
	V_R	0,4	4,9	1,9	3,5	2,7
	NRS	0,61	0,65	1,0	1,0	0,51

The mean intake temperature, θ_{inlet}, for the nocturnal period 8-9 June 1992 of 11,4°C was observed. The Eskom mast data was used to represent the mean surface inversion, but was adjusted in accordance with the tethersonde findings at the top of the inversion. The resultant potential temperature inversion was 2,7°C, from 9,5°C at ground level to 12,2°C at 120 m AGL. Substitution into Equation 3.1.1 yielded an entrainment factor of 70%. This implies that the mean inlet temperature was 1,9°C warmer than the temperature at 1,2 m AGL in the SBL.

Unfortunately, the 2-D temperature profiler was not operational during the nocturnal field excursion. As a result, together with a lack of tethersonde soundings, CT1's region of influence could not be determined for this case study.

Case Study Features

1. Easterly winds prevailed throughout the nocturnal period and a mean surface inversion of 2,7°C was observed.

2. Operation of unit 1 was stable at an average of 73,6% of its maximum generating capacity.

3. Entrainment factor of 70% of the ambient temperature inversion was observed.

4. The region of influence of CT1 could not be determined.

5. Maximum tower inflow occurs between 8 and 15 m AGL.

3.3 Case Study 2: 10 June 21:00 - 11 June 03:00

On 8 June 1992, the IOA became well established east of the country and extended over the eastern part of South Africa. A strong 850 hPa high developed and on 10 June 1992, the synoptic scale circulation of the Transvaal was dominated by this high. The 14:00 synoptic chart on 10 June 1992 is shown in Figure 3.3.1. The light winds and clear skies associated with the high presented ideal conditions for the development of a stable boundary layer.

Light winds prevailed between ground level and 40 m AGL throughout the nocturnal period and never exceeded 3 $m.s^{-1}$ at the Eskom tower. Above 40 m AGL the winds remained light, but increased to about 5 $m.s^{-1}$ at 96 m AGL. Initially, the wind was northwesterly, but became almost due northerly by 22:20. Later, the winds below 20 m AGL veered further to northeasterly, while the flow higher up the Eskom mast remained northerly.

A strong temperature inversion was observed at the start of the nocturnal period with the surface temperature of 7,1°C increasing to 11,3°C at 65 m. After midnight, the surface inversion had deepened and the top of the inversion could not be identified by the 96 m Eskom mast. The magnitude of the inversion below 96 m AGL still exceeded 3°C. Temperature and wind profiles at the mast before and after midnight, are shown in Figures

3.3.2(a) and (b) at 21:02 and 02:02, respectively. This data is considered representative of the SBL that is undisturbed by CT1, i.e. the background SBL.

Power generation unit 1 operated at an average of 79,8% of its maximum generating capacity throughout the nocturnal period. For two short intervals, 21:57 to 22:27 and 02:26 to the end of the nocturnal period, operation was above 90% of full capacity. The percentage of full capacity of operation of unit 1 is shown as a function of time in Figure 3.3.3.

Six tethersonde soundings were done during the nocturnal period. One each were carried out from sites B at 21:00 and C at 22:21, 130 m and 120 m downwind of CT1, respectively. After midnight, simultaneous upwind and downwind soundings were done at 01:00 and 02:00 from sites D and O, 280 m and 2200 m from CT1, respectively. The sites are indicated in Figure 2.1.

Site B was not directly aligned in the downwind plane of CT1. At this site, the tethersonde temperature and wind profiles in the lowest 100 m of the sounding closely resembled the background profile of the Eskom mast, Figure 3.3.2(a). A surface temperature inversion of nearly 4°C was observed below 50 m AGL, similar to the 21:02 Eskom profile. Wind speeds at site B were stronger than those recorded in the background SBL. In order to align the tethersonde site in the downwind plane of CT1, the second sounding was carried out at site C at 22:21. It is apparent that this sounding was carried out in the turbulent plume of CT1. Winds of more than 5 $m.s^{-1}$ at the surface varied markedly in direction and speed in the wake area immediately downwind of the tower. No surface temperature inversion was evident in the well-mixed almost homogeneous temperature layer close to the earth's surface. The sounding at 21:00 outside the plume and at 22:21 in the cooling tower plume are compared in Figure 3.3.4. Noteworthy is the different temperature profiles and the erratic nature of both wind speed and direction at site C, compared with the more stable profiles at B. The severe turbulence at site C resulted in the premature termination of the sounding.

In this example, site C is situated 120 m directly downwind from CT1, and clearly within the towers region of influence. Site B is 130 m from CT1, but outside the immediate downwind plane, and shows little or no SBL disturbance effects from the cooling tower. It is suggested that the heat plume and the region of influence are advected downwind under light prevailing wind conditions and the spatial area of influence of the tower is limited to the prevailing wind plane.

14:00 SAST 10-06-92

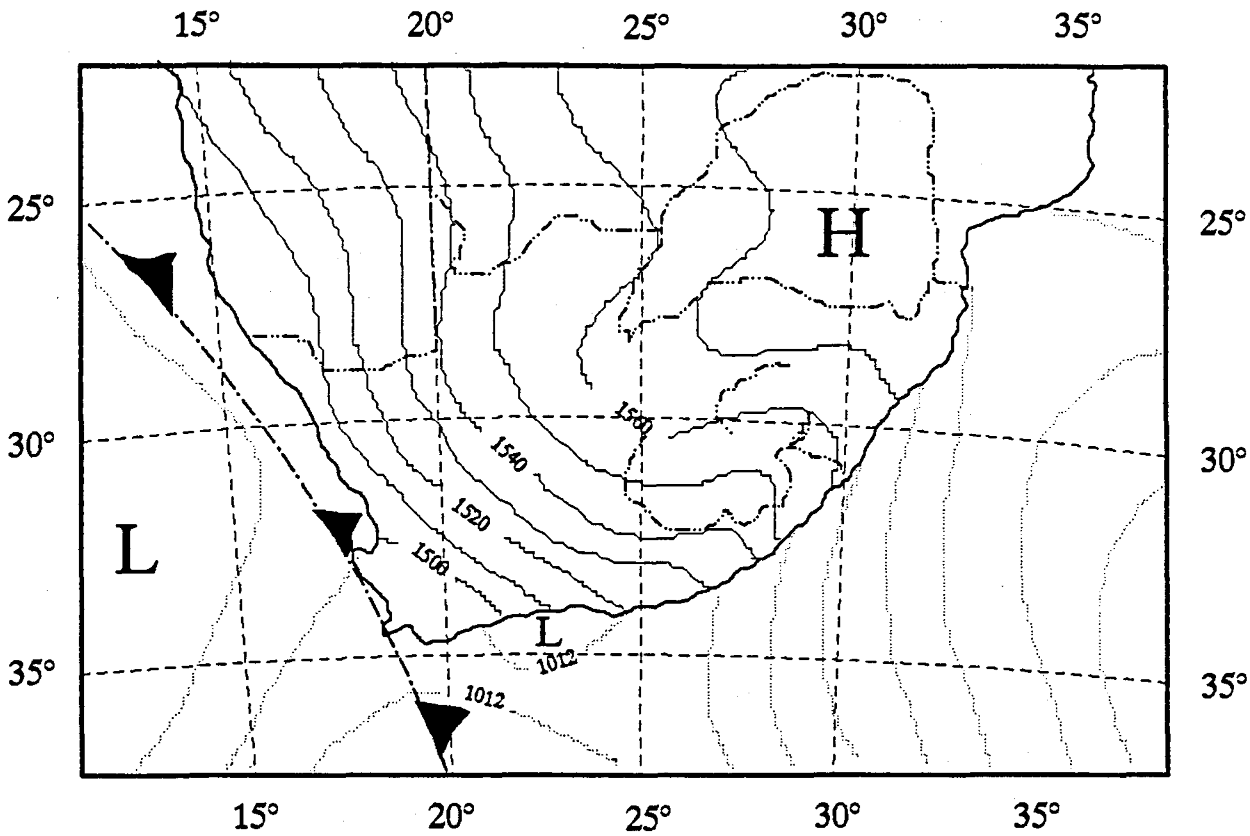

Figure 3.3.1: 14:00 synoptic chart on 10 June 1992. Isobars are shown over the ocean and 850hPa height contours over the land.

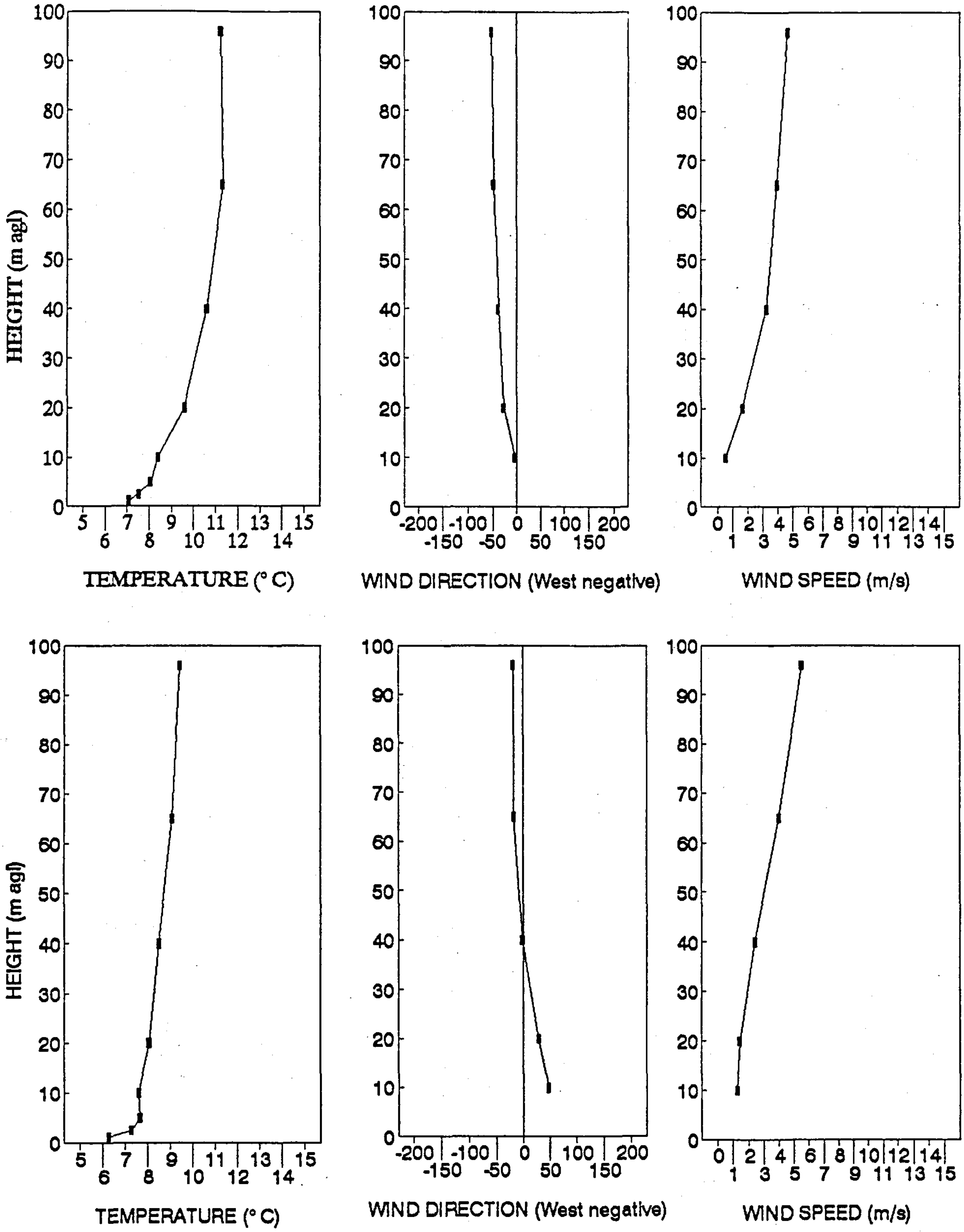

Figure 3.3.2(a): Temperature and wind profiles from the Eskom mast at: (a) 21:02 on 10 June 1992 and (b) 02:02 on 11 June 1992.

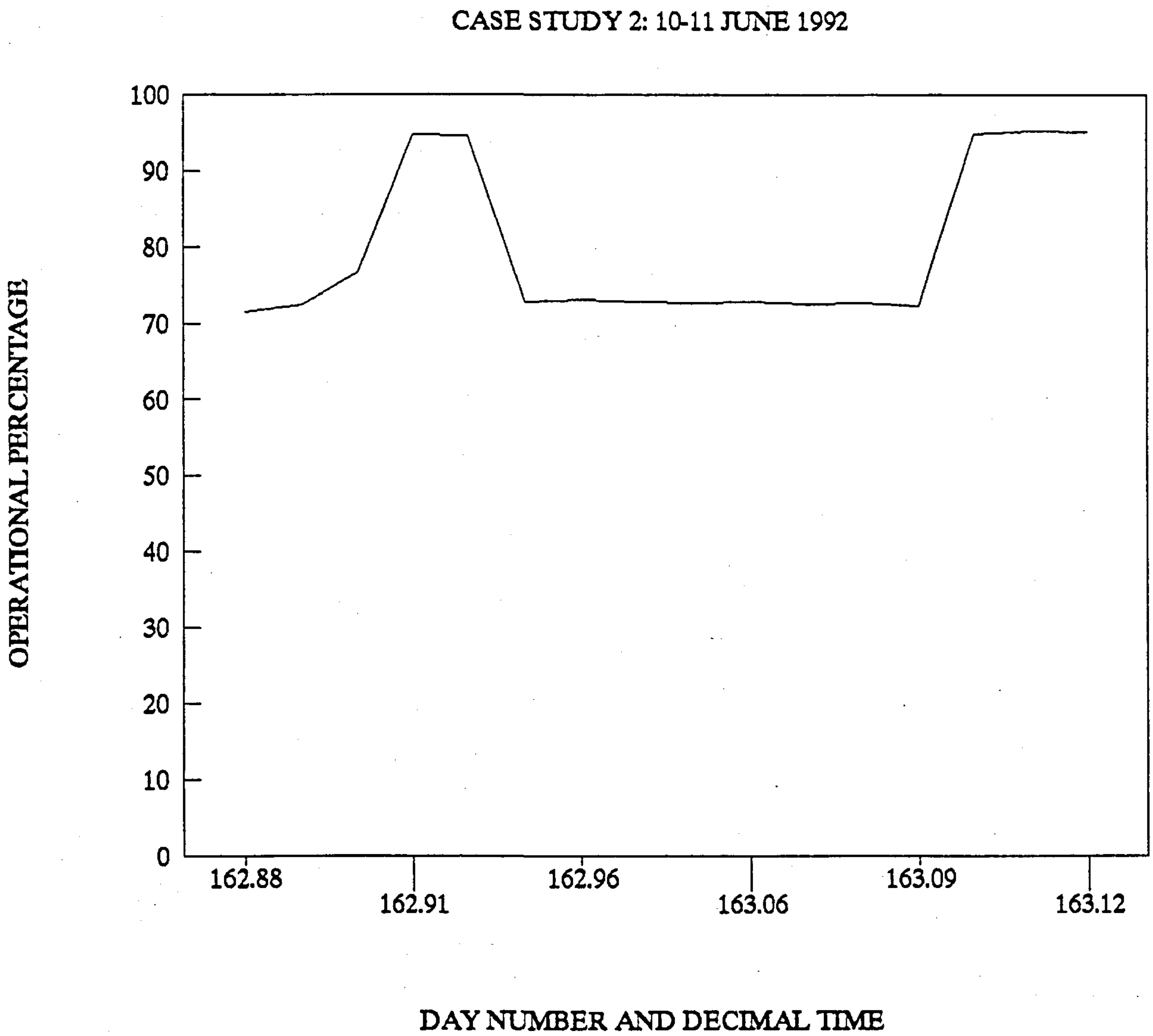

Figure 3.3.3: Percentage of full capacity of operation of unit 1 plotted against time during the nocturnal period of 10 to 11 June 1992.

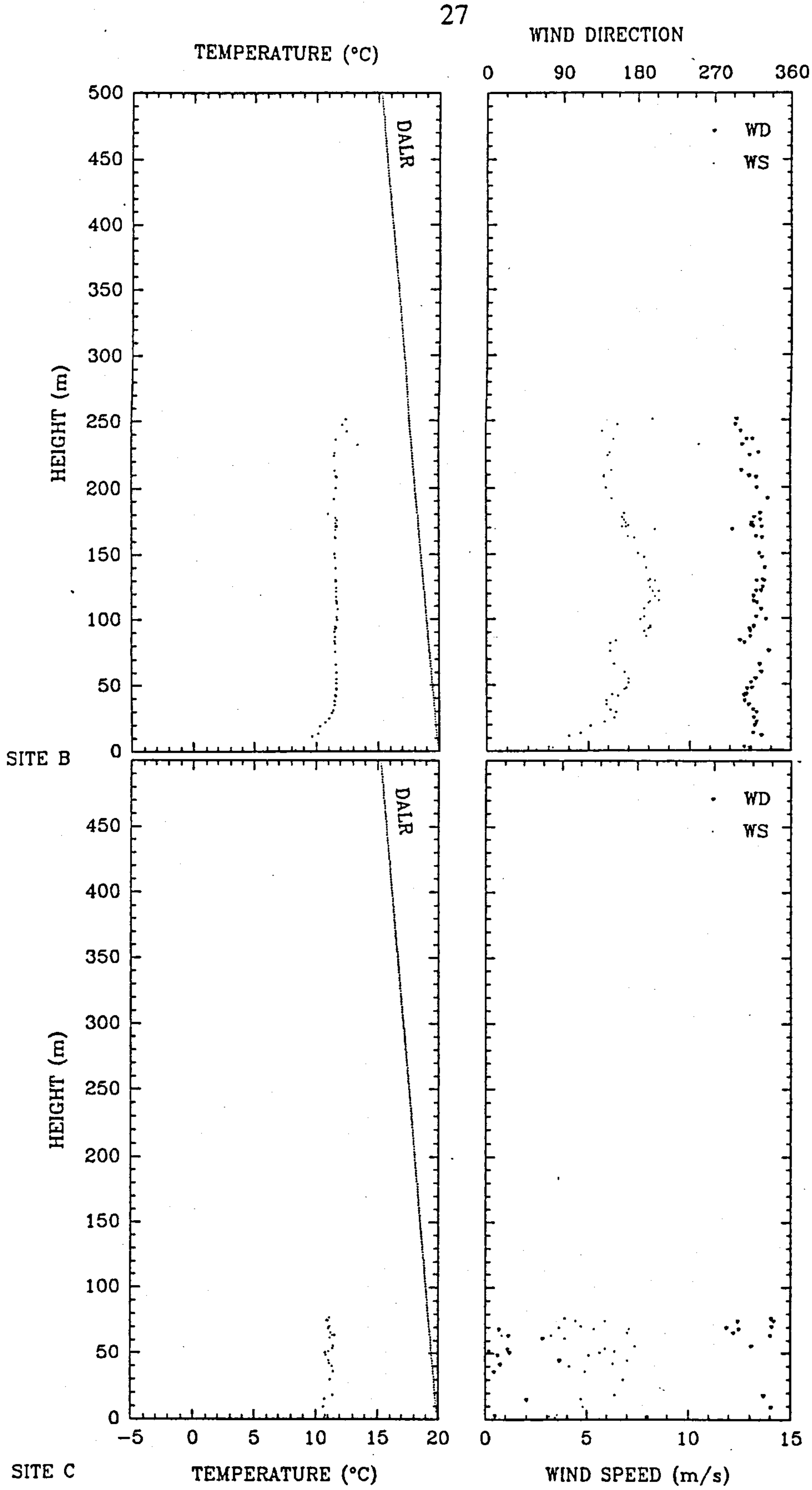

Figure 3.3.4: Tethersonde soundings at sites B and C at 21:00 and 22:00 respectively on the 10 June 1992.

The two soundings carried out at site B, well distant from Kendal, are also representative of the undisturbed SBL. A deep surface inversion was observed with the surface temperature of 5°C increasing to more than 9°C at 130 m AGL. The wind speeds increased consistently with height from being calm between ground level and 30 m AGL, to about 10 $m.s^{-1}$ above 400 m AGL. Wind direction was mostly northerly, but easterly at ground level. Similar profiles were shown by the Eskom mast after midnight. The upwind tether soundings identified the top of the inversion at 130 m, 34 m above the top of the Eskom mast.

Due to the severe turbulence experienced earlier at site C, the downwind site was moved to D after midnight. Here, 280 m from CT1, turbulence also limited the soundings at 01:00 and 02:00 to 220 m AGL and 150 m AGL, respectively. From ground level upwards on both occasions, wind speed and direction was erratic. Again, no sign of the background SBL temperature inversion was visible. Instead, a well-mixed isothermal layer was observed to the top of the soundings. As a comparison, the simultaneous soundings at 01:00 from upwind site R and downwind site D are shown in Figure 3.3.5. Noteworthy again are the markedly different temperature and wind profiles. Site D appears to lie within CT1 downwind region of influence, implying that this region extends to at least two tower lengths downwind from CT1.

The entrainment of the surface inversion into CT1 was considered for the three periods when unit 1 operated at constant, but different, output. These are tabulated with details of the inversion during the three periods in Table 3.3.1.

Table 3.3.1 Mean inlet temperature (θ_{inlet}) in °C, percentage of capacity output of unit 1 (OP), inversion details (°C) and the entrainment factor (E) for three periods during the nocturnal period 10-11 June 1992.

Time	OP				
	OP (%)	Temp. 1,2 m AGL	Inversion	θ_{inlet}	E(%)
21:57-22:27	95	6,8	4,0	10,5	93
22:42-02:11	75	4,6	4,5	10,7	135
02:26-03:00	95	4,6	4,5	9,3	104

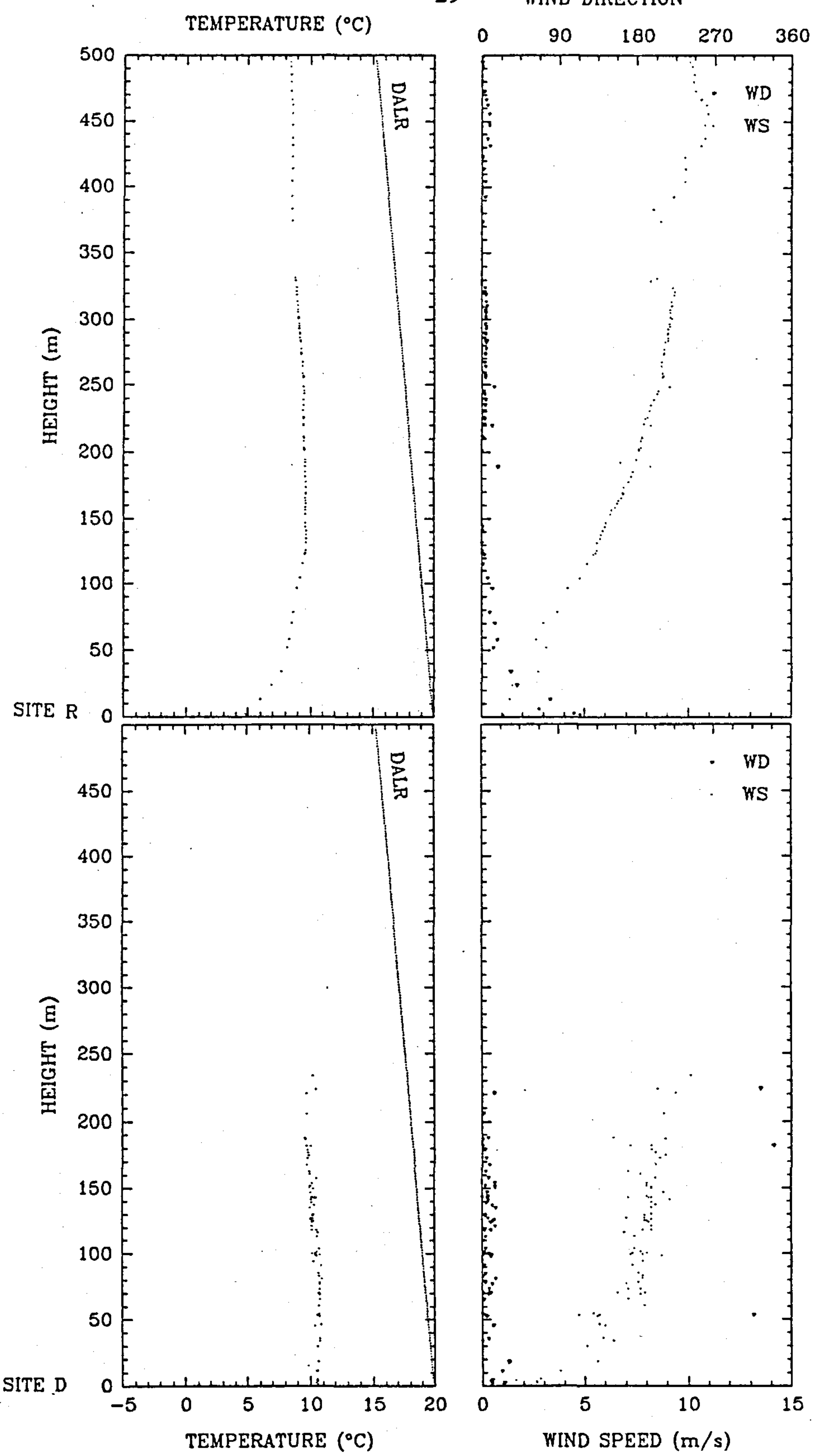

Figure 3.3.5: Simultaneous up and downwind tethersonde soundings at sites **O** and D respectively, at 01:00 on the 11 June 1992.

Entrainment factors of 93%, 135% and 104% indicate that the mean inlet temperature was 3,7°C, 6,1°C and 4,7°C, respectively, warmer than the air at 1,2 m AGL in the undisturbed SBL.

Table 3.3.2 shows the mean potential temperature and tangential and radial wind speeds at six levels of the four 22 m intake masts for the period 22:40 to 02:10. Generally, the highest temperatures were observed between 11 m and 16 m AGL. With prevailing northerly winds, the strong radial component at the northern tower is expected. Here, the strongest inflow occurs at 16 m and 22 m AGL. The relatively strong tangential components at the northern tower could be attributed to a venturi effect between CT1 and CT2, see relative positions in Figure 2.1. This is visible to a lesser degree at the eastern tower, where the Kendal Power Station buildings could also induce a venturi effect. Some outflow through the intake region occurs at the western side of CT1.

Unfortunately, the 2-D profiler was not operational. As a result, any boundary layer distortion close to CT1 could not be explored. However, the entrained air about 4 to 6°C warmer than that in the SBL inversion, suggests that no boundary layer is entrained into CT1. Instead, warmed air in the immediate tower vicinity is entrained into the intake region. This effect is stronger with the tower operating at 75% of its maximum capacity than at near full operation.

Case Study Features

1. Initially, calm wind occurred with the magnitude of surface inversion generally greater than 3°C.

2. Variable generation output of unit 1 was recorded. Two periods above 90% of capacity and one period 75% of capacity.

3. In light prevailing winds, the cooling tower heat plume seems to have the greatest effect on the SBL in the direct downwind plane.

4. CT1 region of influence extends to at least two tower lengths downwind under light prevailing wind conditions in the downwind plane.

5. Entrainment factors of 93%, 135% and 104% were found.

6. Strongest tower inflow occurs between 16 and 22 m AGL.

Table 3.3.2 Mean potential temperature (T_θ) in °C, tangential wind speed (V_T) and radial wind speed (V_R) in m.s^{-1} at the six levels of the 22 m intake masts for the period 22:40 to 02:10, 10-11 June 1992. V_T is positive clockwise, V_R is positive into the tower and NRS indicates normalised radial wind speed.

Height		N	E	S	W	Mean
22 m	T_θ	10,7	10,1	10,1	10,1	10,3
	V_T	3,2	1,7	0,7	2,2	1,9
	V_R	8,3	0,2	2,2	-0,7	2,5
	NRS	0,85	0,13	0,72	-0,82	0,22
16 m	T_θ	10,8	-	-	-	10,8
	V_T	2,6	2,8	8,8	3,1	2,3
	V_R	9,7	1,5	9,9	-0,8	3,3
	NRS	1,0	1,0	0,87	-1,0	0,49
11 m	T_θ	10,2	10,3	0,0	10,0	10,1
	V_T	2,8	3,5	2,2	2,4	2,2
	V_R	7,8	0,1	4,4	-0,2	2,5
	NRS	0,11	0,05	0,79	-0,31	0,34
8 m	T_θ	9,9	10,5	4,4	4,4	10,3
	V_T	2,6	3,0	3,3	8,8	2,2
	V_R	7,3	0,5	8,8	3,3	2,6
	NRS	0,75	0,31	0,91	-0,42	0,39
5 m	T_θ	10,1	9,8	2,2	2,2	10,1
	V_T	2,5	2,6	4,4	7,7	2,1
	V_R	6,2	0,8	7,7	4,4	2,3
	NRS	0,64	0,52	0,90	-0,43	0,4
2 m	T_θ	9,7	9,5	7,7	7,7	9,6
	V_T	3,0	3,2	5,5	0,0	2,4
	V_R	5,0	0,8	0,0	5,5	2,1
	NRS	0,51	0,56	1,0	-0,58	0,37

3.4 Case Study 3: 8 July 21:00 - 9 July 03:00

A trough of low pressure at 850 hPa, situated across the southeastern Transvaal, dominated the synoptic scale circulation during the nocturnal period 8-9 July 1992. Steep pressure gradients resulted in moderate southwesterly winds during the field excursion, which inhibited ideal formation of a stable boundary layer. The 14:00 synoptic chart on 8 July 1992 is shown in Figure 3.4.1.

Little variability was shown in the 96 m temperature and wind profiles obtained from the Eskom mast. The mean profiles for the nocturnal period are shown in Figure 3.4.2. Wind direction was consistently south-southwesterly, and increased with height from about 4 $m.s^{-1}$ at ground level to about 9 $m.s^{-1}$ at 96 m AGL. Even so, a deep inversion layer developed with the surface temperature ranging between 5°C and 6°C, increasing with height to about 8°C at 96 m AGL.

The operational output of unit 1 varied between a peak of 100% of its capacity at 22:45 and 70,4% towards the end of the period, but average output during the nocturnal period was 82%. Figure 3.4.3 shows the operational output of unit 1 as a percentage of its capacity output, plotted against time.

Only one tethersonde was deployed during the nocturnal period. Five soundings were attempted. One sounding was done at 22:00 at site E, 250 m upwind from the periphery of CT1, Figure 2.1. Due to increasing wind strength this sounding was terminated at 150 m AGL. At 23:00 a second sounding was carried out 200 m downwind of CT1 at site F. Severe turbulence resulted in the termination of the sounding at 80 m AGL. Between 01:14 and 02:20, three more soundings were done at site E. These only reached about 150 m AGL, and were terminated due to the strong winds. The four tethersonde soundings upwind of CT1 all showed the wind speed to increase steadily with height from about 2 $m.s^{-1}$ at ground level to about 8 to 10 $m.s^{-1}$ at 150 m AGL. Wind direction at ground level was southeasterly, becoming southerly at 50 m AGL. The temperature profiles showed a deep inversion layer. Often the sounding was terminated before reaching the top of the inversion. However, it was relatively weak and a 1,5°C to 2°C temperature difference existed between ground level and the top of the sounding. Figure 3.4.4 shows upwind soundings at site E at 22:00 and 02:20.

The single sounding attempted in turbulent conditions downwind of CT1 at site F reached 80 m AGL. The temperature profile was isothermal. Wind speeds increased rapidly from 2 $m.s^{-1}$ at ground level to 7 $m.s^{-1}$ at 10 m AGL. At 50 m AGL the wind speed exceeded 10 $m.s^{-1}$. The wind direction was southerly throughout the sounding. The temperature and wind profiles are shown in Figure 3.4.5 for site F at 23:00.

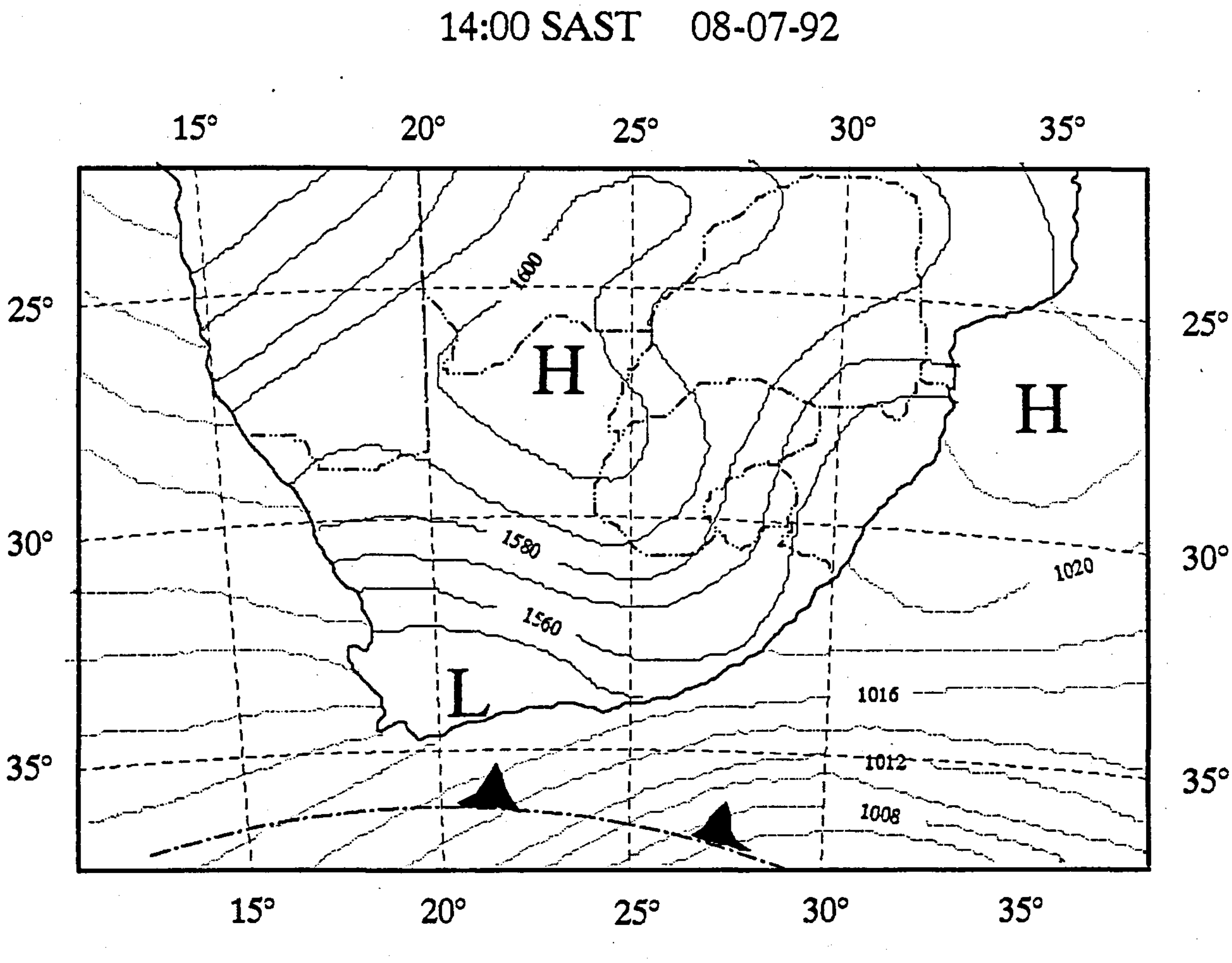

Figure 3.4.1: 14:00 synoptic chart on 8 July 1992. Isobares are shown over the ocean and 850hPa height contours over the land.

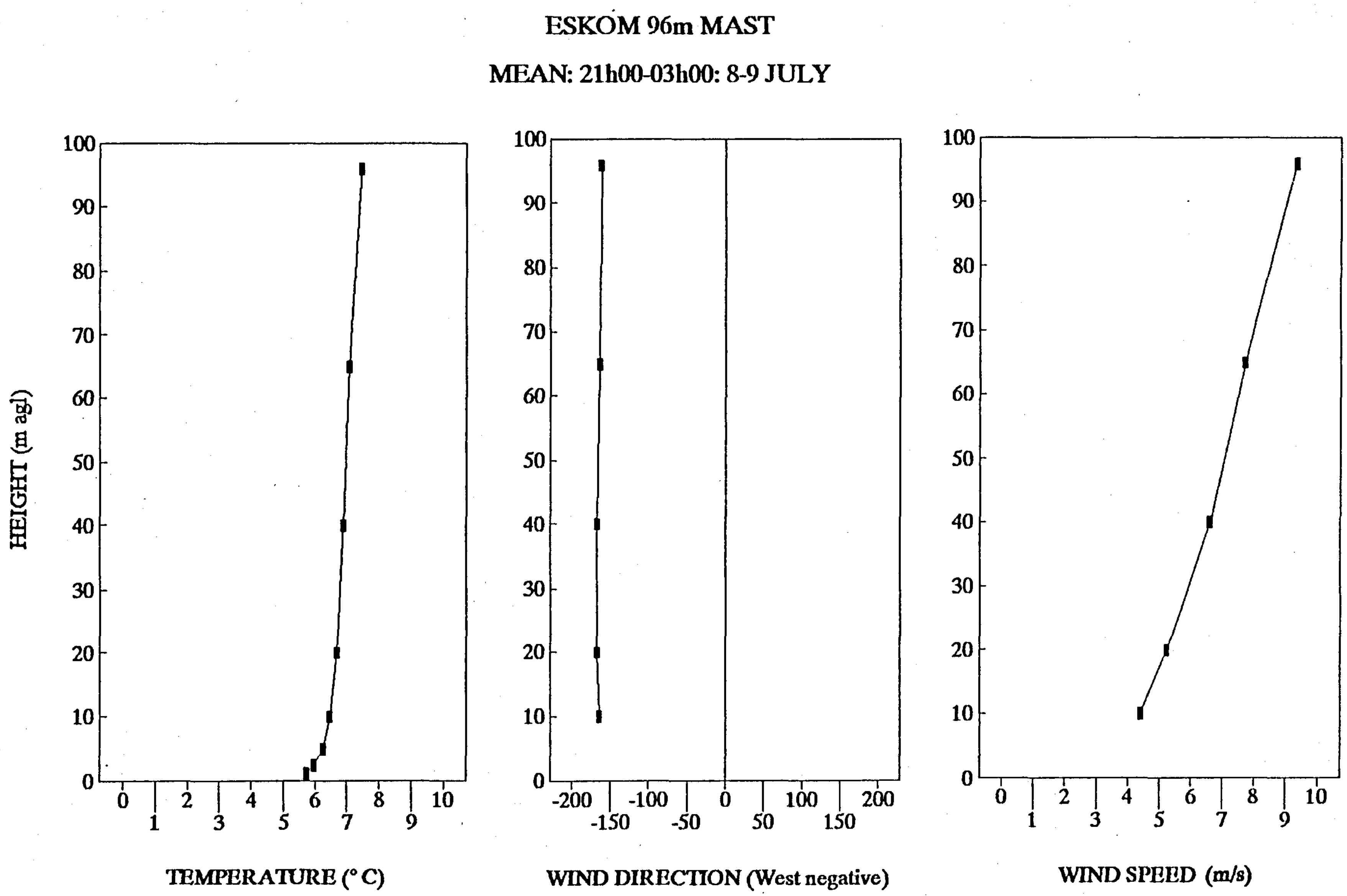

Figure 3.4.2: Mean temperature, wind direction and wind speed profiles for the nocturnal period 8 to 9 July 1992.

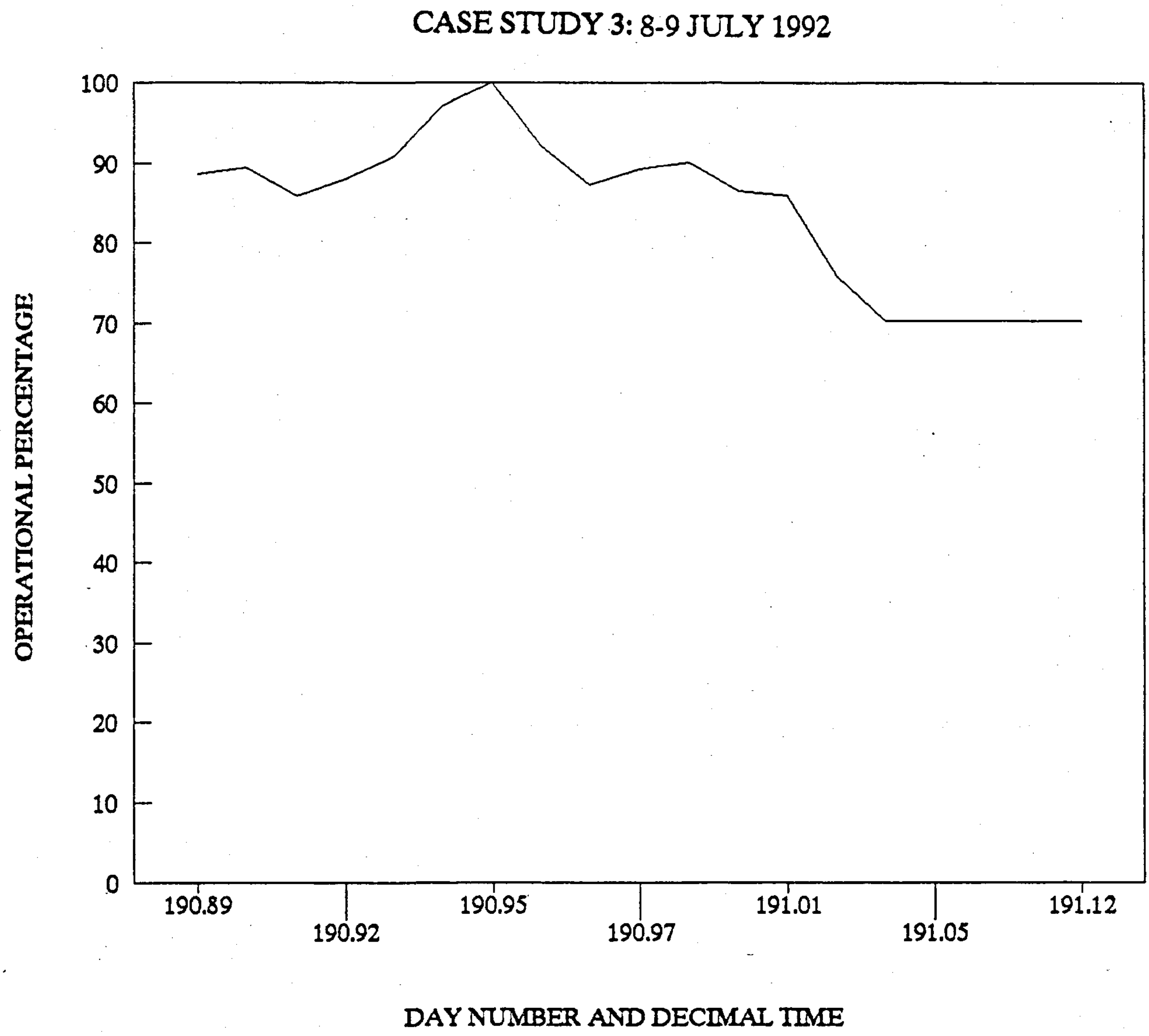

Figure 3.4.3: Operational output of unit 1 as a percentage of its output capacity, plotted against time.

Mean potential temperatures and the tangential and radial components of the wind at the four 22 m intake masts are listed in Table 3.4.1 for the six monitoring heights. The strongest tangential winds occur at the southern and western towers. As might be expected with prevailing southwesterlies, the strongest inflow is shown at the western mast, with maximum inflow at 22 m AGL. Some radial outflow occurs at the northern intake area at 16 and 22 m AGL. Figures 3.4.6(a) and (b) show the tangential and radial wind profiles at the four intake masts. At the eastern and southern masts, the temperature generally increases with height to the top of the intake region. At the western mast, a layer of air between 16 m and 22 m AGL, that is 4°C cooler than the rest of the intake air is entrained into the intake region.

Table 3.4.1 Mean potential temperature (T_θ) in °C, tangential wind (V_T) and radial wind (V_R) in $m.s^{-1}$, at the six monitoring levels on the four 22 m intake masts. Heights are m AGL. V_T is positive clockwise and V_R is positive into CT1 and NRS indicates normalised radial wind speed.

Height		N	E	S	W	Mean
22 m	T_θ	5,2	5,6	6,7	1,5	4,8
	V_T	2,0	1,1	5,9	3,8	3,1
	V_R	-0,1	0,7	2,3	6,4	2,4
	NRS	0,62	0,34	0,8	1,0	0,69
16 m	T_θ	6,0	-	-	2,2	4,1
	V_T	2,2	1,7	9,7	-	4,3
	V_R	-0,4	1,2	2,0	-	1,3
	NRS	0,74	0,57	-	-	0,66
11 m	T_θ	6,1	5,1	6,0	-	5,8
	V_T	2,0	1,9	7,4	2,4	3,3
	V_R	0,4	1,4	1,3	4,9	2,7
	NRS	0,69	0,69	1,0	0,64	0,76
8 m	T_θ	6,1	5,4	-	6,3	5,9
	V_T	2,4	1,6	-	1,4	1,7
	V_R	1,0	1,3	-	4,6	2,4
	NRS	0,92	0,64	-	0,39	0,65
5 m	T_θ	6,2	5,1	5,8	5,8	5,7
	V_T	2,6	1,4	6,3	1,6	3,0
	V_R	1,0	1,3	1,2	4,1	1,9
	NRS	0,96	0,65	0,86	0,42	0,72
2 m	T_θ	6,3	4,8	4,7	6,2	5,5
	V_T	3,0	2,0	5,9	2,1	3,2
	V_R	1,2	2,1	1,3	4,8	2,3
	NRS	1,0	1,0	0,8	0,59	0,85

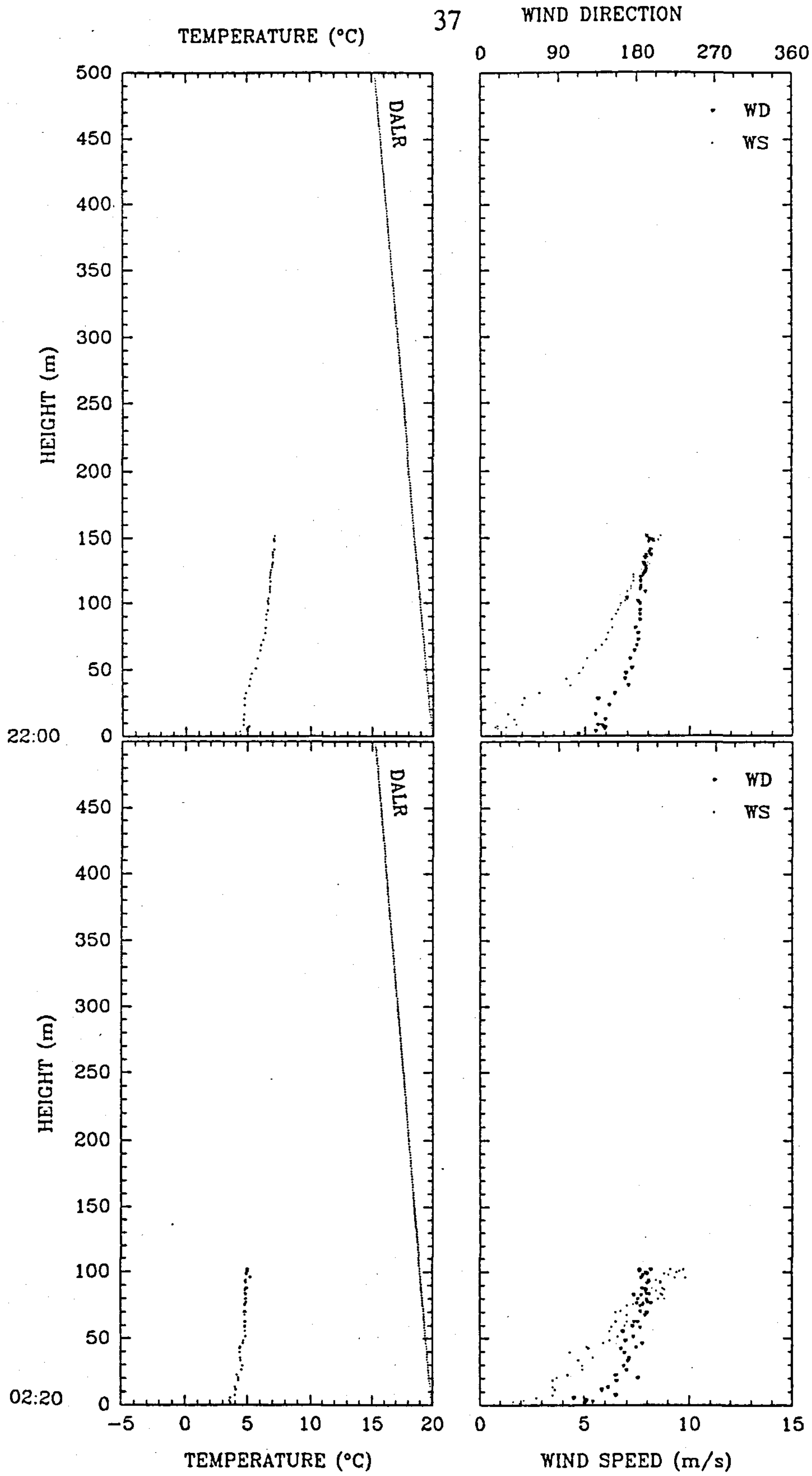

Figure 3.4.4: Tethersonde profiles from site E at 22:00 and 02:20 on 8 and 9 July 1992, respectively.

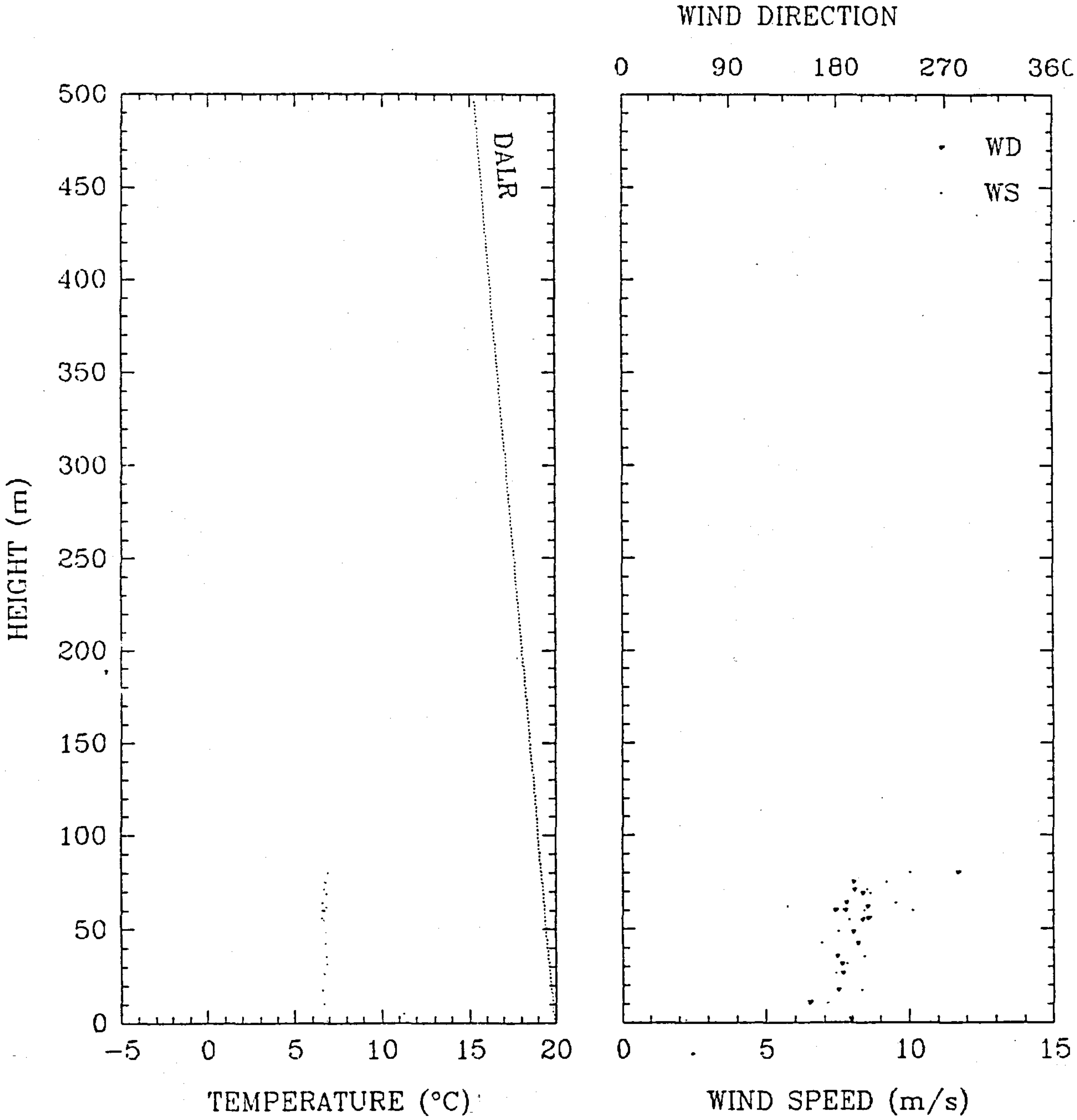

Figure 3.4.5: Tethersonde profiles from site F at 23:00 on 8 July 1992.

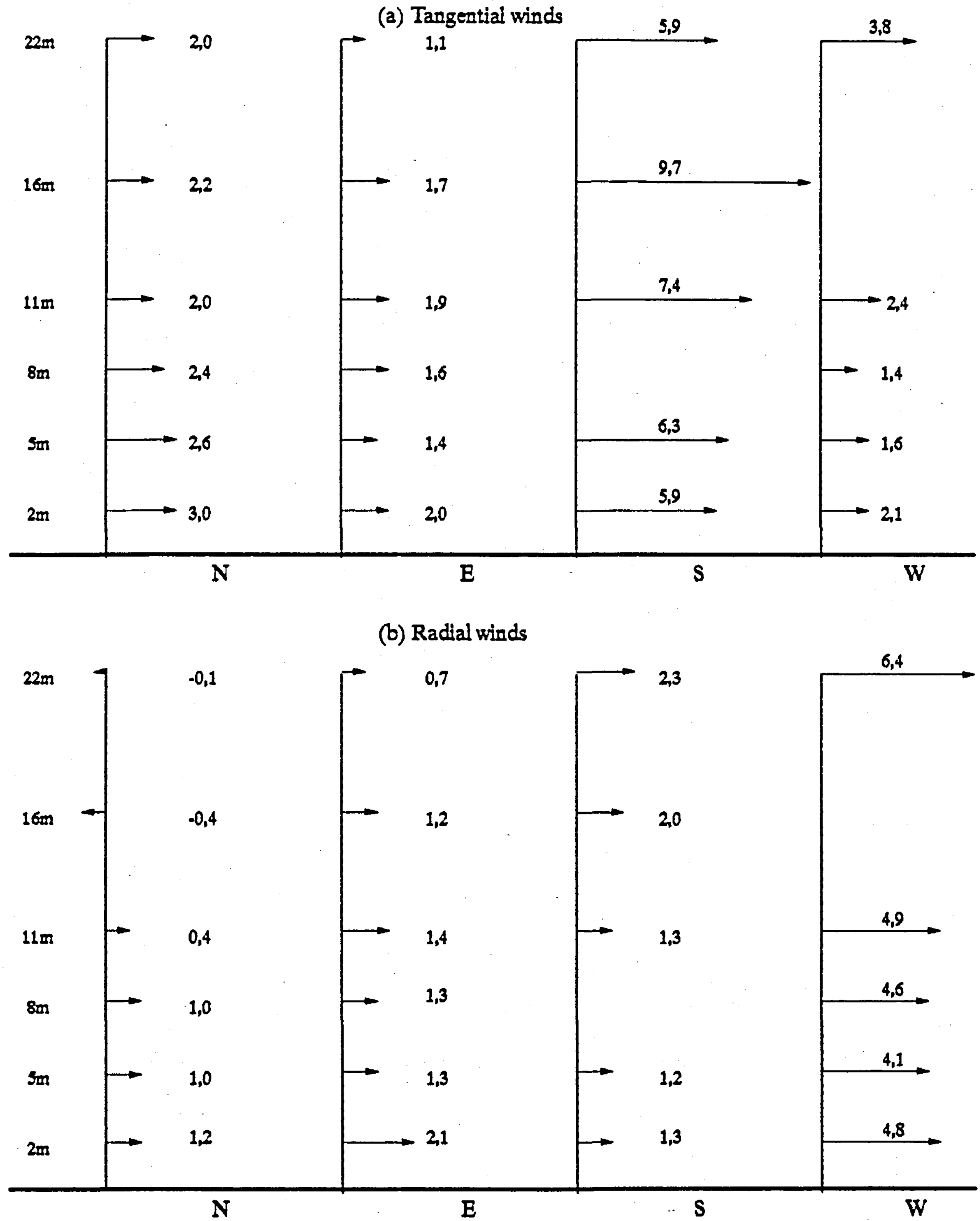

Figure 3.4.6: Mean tangential (a) and radial wind (b) components at the four 22 m masts in the in take region of CT1 for the nocturnal period 8 to 9 July 1992. Wind speeds are shown in m/s.

Using Equation 3.1.2, the mean intake potential temperature was calculated as 5,3°C. Since the Eskom tower is situated downwind of CT1 during the case study period, it was not considered representative of the background SBL. It was felt that some boundary layer disturbance by Kendal, as a whole, might influence the Eskom tower data. Rather, the average potential temperature inversion of the four upwind tethersondes was used to define θ_{min} and θ_{inv} in Equation 3.1.1. A mean surface inversion of 2,1°C was observed with the surface temperature of 3,8°C. This led to an entrainment factor of 71%. It must be noted that none of the tethersonde soundings revealed the top of the inversion. This implies that the denominator in Equation 3.1.1 is probably too small, implying in turn, that the entrainment factor may be exaggerated.

The 2-D temperature field was only operational at the end of the nocturnal period, when two recording cycles from sensors 1 to 15 were completed. The mean potential temperature field for this short period is illustrated in Figure 3.4.7(a) and listed in Table 3.4.2. Turbulence at the windward side of CT1 results in the irregular slope of the isotherms in the 2-D sensor field. A tongue of warmer air is shown above the intake area, but cooler air from the background SBL is taken up underneath this tongue into CT1. The mean tethersonde profile at site E, the one sounding at site F and the mean Eskom 96 m profile are used in Figure 3.4.7(b) to illustrate the temperature field on a larger scale in the north-south plane about CT1. Noteworthy in this diagram, is the almost homogeneous temperature layer at the leeward side of CT1 . This is a result of effective mixing in the turbulent atmosphere. Although the 2-D temperature profile data is not representative of the whole period, it has been used to provide an idea of the temperature field closer to CT1. Worthy of note at the windward side of CT1 is the compression of the SBL with much of the temperature inversion being drawn into the intake region.

Table 3.4.2 Potential temperature (°C) at the 15 sensors for the 2-D temperature profiler for the two cycles ending at 02:50 and 03:00 on 9 July 1992.

Sensor	1	2	3	4	5	6	7	8
02:00	4,6	7,2	5,0	6,9	7,1	6,2	4,4	5,4
03:00	4,2	7,2	5,3	7,0	7,1	6,2	4,1	5,4
Sensor	9	10	11	12	13	14	15	
02:50	5,7	7,3	7,8	6,3	6,9	6,6	6,5	
03:00	5,5	7,3	7,9	6,3	6,9	6,7	6,6	

From the start of the nocturnal excursion to 00:14, unit 1 operated in excess of 85% of its capacity, before dropping to 70,4% at 00:34 and which was maintained to the end of the period. The mean inlet potential temperatures for these two periods were 6,0°C and 4,7°C, respectively. Again, the upwind tethersonde soundings were used to describe the potential temperature surface inversion for these periods, to calculate the entrainment factor. During the earlier period, a 2,5°C inversion was observed with a surface temperature of 4,3°C. This led to an entrainment factor of 68%. An inversion of 3,3°C in the later period was calculated using the observed surface temperature of 3,5°C and the temperature at the top of the sounding at 22:00 was used as the top of the inversion. This assumption led to an entrainment factor of 36%. It must be stressed that both entrainment factors are subject to error, as the true magnitude of the surface inversion was not defined by the tethersonde soundings. The entrainment factors of 68% and 36% imply that the mean temperature of the intake air was 1,7°C and 1,2°C warmer than the air at 1,2 m AGL in the background SBL.

Case Study Features

1. South-southwesterly winds prevailed throughout the period, and a surface temperature inversion of 2 to 3°C developed.

2. Generating output of unit 1 varied between 100% and 70,4%.

3. Severe turbulence was observed 200 m downwind of CT1.

4. Entrainment factors of 68% at 85% of capacity generation and 36% entrainment at 70% of capacity generation were calculated.

5. The region of influence of CT1 was found to extend to approximately two tower lengths downwind of CT1.

6. Strongest tower inflow occurs at 22 m AGL.

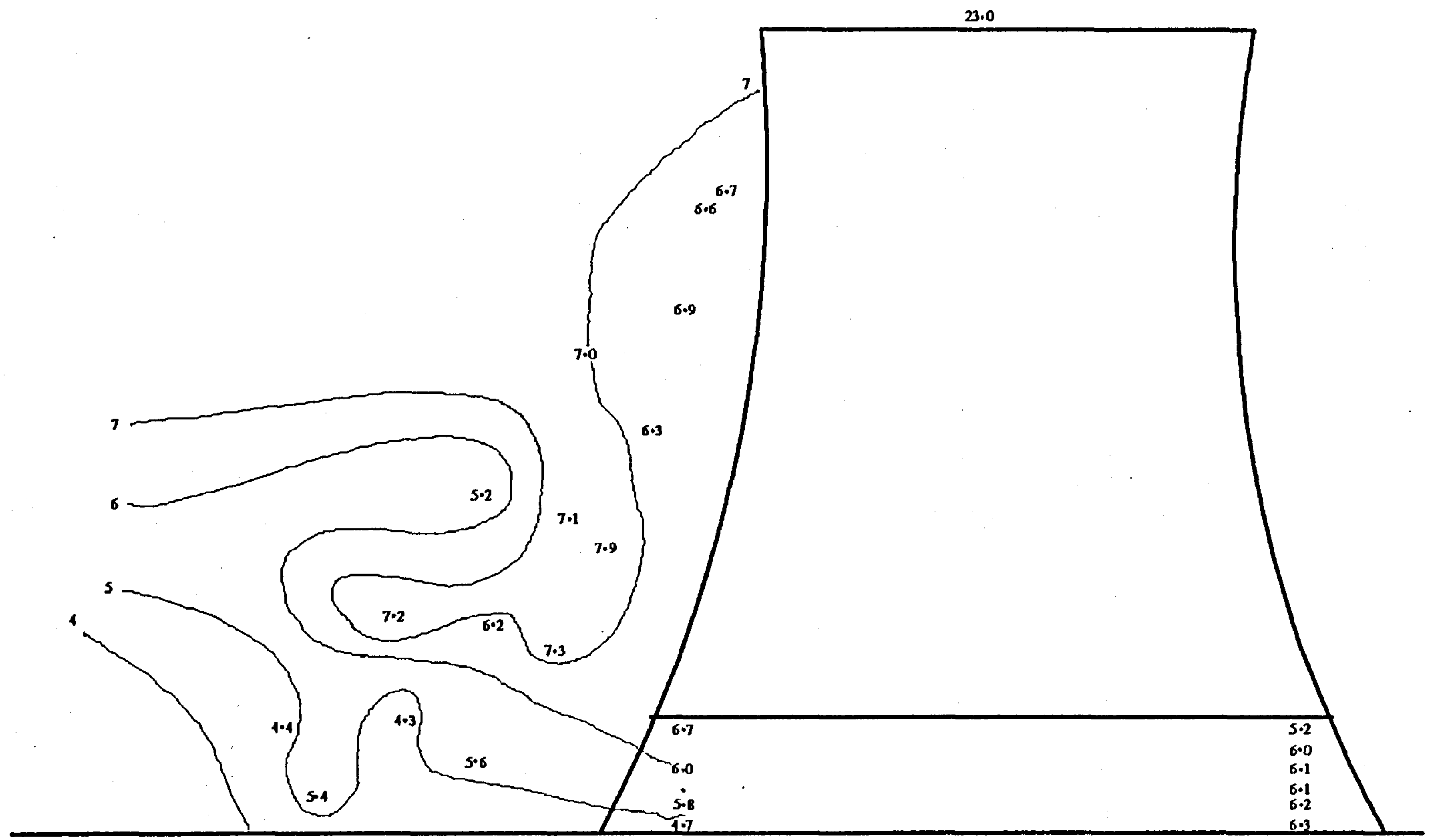

Figure 3.4.7(a): Mean 2-D temperature profile field for the period 02:50 to 03:00 on the 9 July 1992.

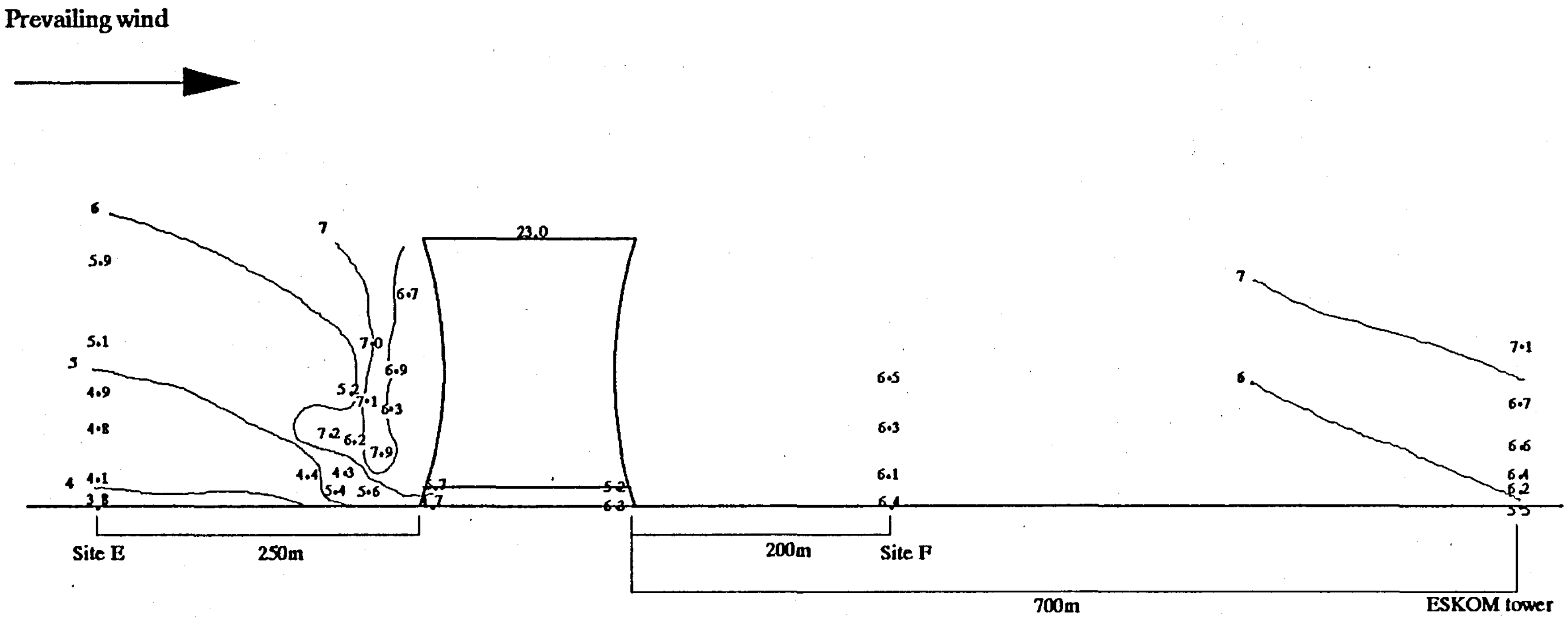

Figure 3.4.7(b): The temperature field in the north south plane from the Eskom tower to site E.

3.5 Case Study 4: 14 July 21:00 - 15 July 03:00

Strong ridging of the IOA on 11 July 1992 over the eastern parts of the country resulted in the formation of a high pressure at 850 hPa over these areas. The high became firmly established and dominated the circulation over the ETH during the case study period. The 14:00 synoptic chart for 14 July 1992 is shown in Figure 3.5.1.

No significant changes occurred in any of the monitored meteorological parameters at the 96 m Eskom mast during the nocturnal period of 14-15 July 1992. Wind speeds were generally less than 5 $m.s^{-1}$ between 10 and 40 m AGL. Above this level, speeds were in the order of 5 $m.s^{-1}$. Initially, northwesterly winds prevailed between 10 and 96 m AGL. By 23:00, the 10 m wind had become westerly, and by 01:00 westerly winds prevailed at all monitoring levels. The 96 m temperature profile did not show much variation during the nocturnal period. Concomitantly, power generation unit 1 operated in a steady mode at an average of 71,5% of its capacity, Figure 3.5.2. For these reasons, mean temperatures and wind speeds calculated over the nocturnal period are considered in this discussion.

Data from the 96 m Eskom mast, situated outside of the downwind plume, were used to determine SBL characteristics beyond the suspected region of influence of CT1. Suitable tethersonde sites upwind and downwind of CT1 were chosen to provide further information on the SBL and to examine suspected downwind effects of the cooling tower plume.

The Eskom mast, situated 685 m north of CT1 is quite well removed from Kendal and provides a good measure of the lowest undisturbed boundary layer. The mean temperature, wind direction and wind speed profiles for the nocturnal period 14-15 July 1992 are depicted in Figure 3.5.3. The standard deviation bars show little variability at the eight temperature levels. Wind speeds are also fairly constant at the five monitoring levels. The relatively larger standard deviation bars of the direction profile are attributed to the generally variable nature of light winds and a consistent backing of the wind from northwesterly to westerly.

With prevailing westerly winds, a suitable tethersonde site upwind of CT1 was located outside the Kendal grounds. This site, M in Figure 2.1, is situated about 870 m due west of CT1. Location of a suitable downwind site was impeded by the power station structures due east of CT1. Two sites, A and C in Figure 2.1, were found southeast of the cooling tower. Sites A and C are situated at about 420 m and 120 m from CT1, respectively.

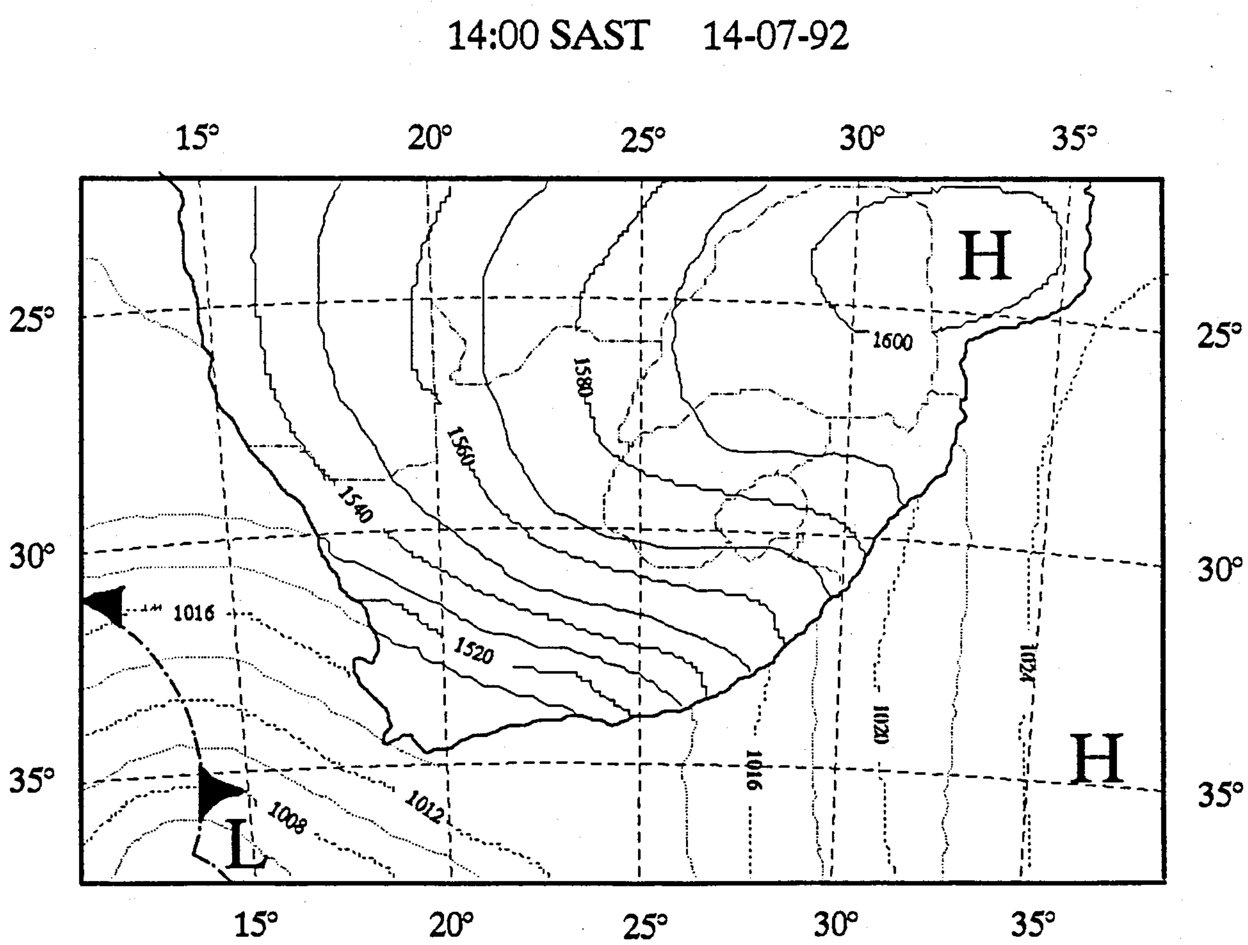

Figure 3.5.1: 14:00 synoptic chart on 14 July 1992. Isobare are shown over the ocean and 850hPa height contours over the land.

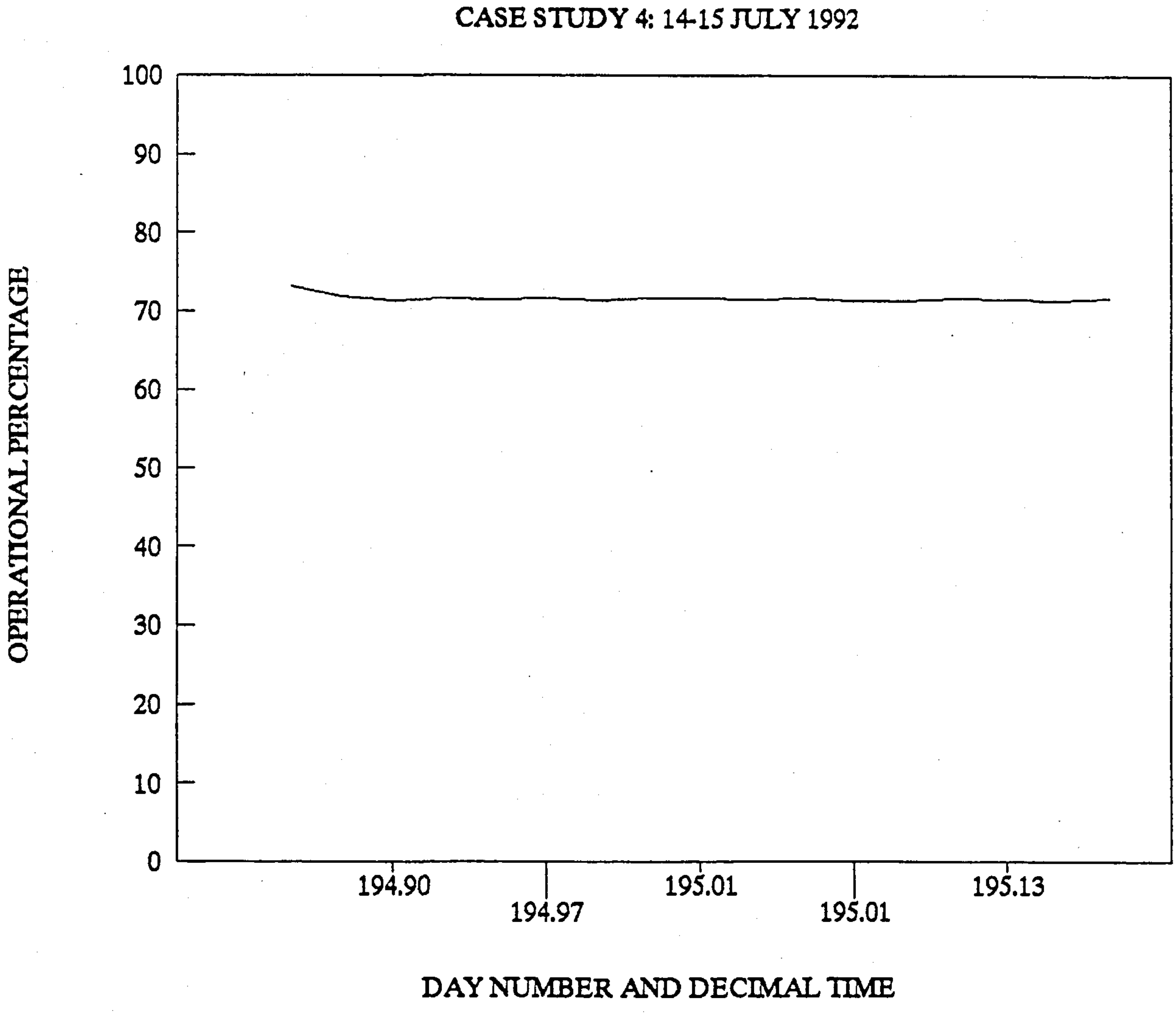

Figure 3.5.2: Percentage of maximum generation output of unit 1 during the nocturnal period 14 to 15 July 1992.

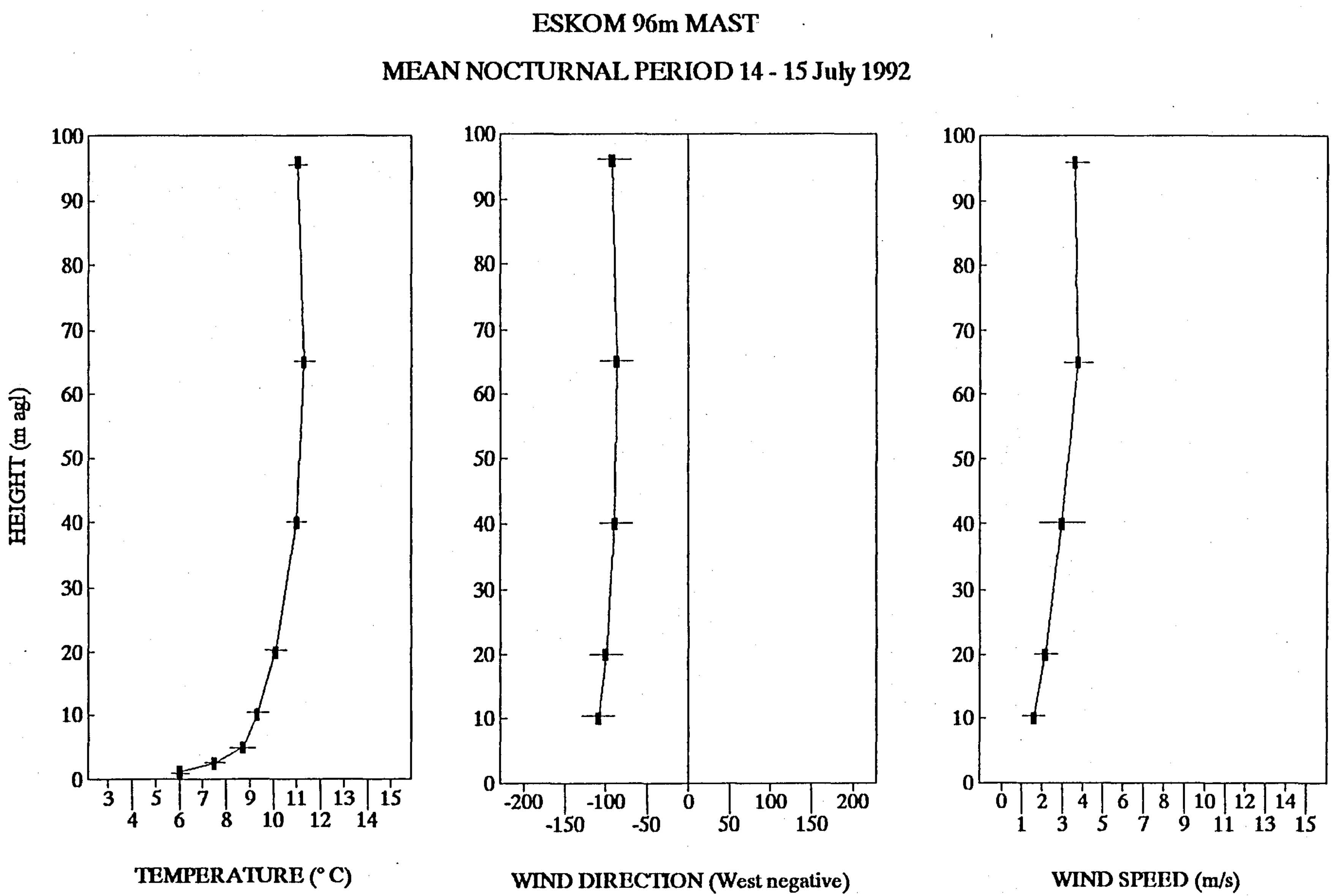

Figure 3.5.3: Mean temperature, wind direction and wind speed profiles for the nocturnal period 14 to 15 July 1992. The bars are standard deviations.

Six successful soundings were carried out at upwind site M from 23:00 to 02:58. The profiles of temperature, wind speed and wind direction obtained at the sonde, provided a good indication of the undisturbed boundary layer condition of the area surrounding Kendal.

Eight soundings were carried out downwind of CT1, starting at 22:00. Of these, three were done at site A before midnight. The remainder were carried out at site C between 01:00 and 03:00. The 22:00 downwind sounding and simultaneous upwind and downwind soundings at 23:00, 01:00, 02:00 and 03:00, are discussed here. The simultaneous vertical temperature, wind speed and wind profiles are illustrated in Figures 3.5.4(a) to (d).

22:00 - Site A:

The surface temperature of 10,9°C decreased with height through the first 12 m. This was followed by an increase in temperature to 12,3°C at 30 m AGL. From the top of the inversion, temperature remained isothermal to 128 m AGL. Beyond this level, temperature decreases with increasing height. Surface wind speeds of 2,5 $m.s^{-1}$ from the west made handling of the tether balloon difficult. Speeds increased rapidly with height to reach 5 $m.s^{-1}$ at 27 m AGL. From this level to the top of the sounding, the wind remained westerly, in the order of 5 $m.s^{-1}$.

23:00 - Site M:

Temperature increased rapidly with height from 4,1°C at the surface to 8,3°C at 98 m AGL. This was followed by a slower increase to 9,3°C at 171 m AGL. Above this, the temperature was mainly isothermal with increasing height to the top of the sounding at 283 m AGL. Wind speeds were calm below 10 m AGL. Above this level, light northwesterlies prevailed, with a maximum wind speed of 3,7 $m.s^{-1}$ at 141 m AGL, Figure 3.5.4(a).

23:00 - Site A:

The surface temperature of 7,7°C decreased slightly with height through the first 7 m AGL, after which it increased to 11,5°C at 51 m AGL. An isothermal layer was evident to 144 m AGL. Above this, a slow decrease in temperature occurred to 10,3°C at the top of the sounding, 322 m AGL. The light southwesterly winds at the surface increased steadily with height and veered to reach 4,7 m.s^{-1} at 77 m AGL from the west. Above this level, wind speed and direction remained steady, Figure 3.5.4 (a).

01:00 - Site M:

Temperature increased with height from 7,7°C at the surface to 10,9°C at 201 m AGL. Above this level, temperatures decreased slowly with height to a value of 9,6°C at 501 m. Wind speeds were calm below 44 m AGL, and increased gradually to 5,1 m.s^{-1}, from the north-northwest, at the top of the sounding, Figure 3.5.4(b).

01:00 - Site C:

A temperature inversion was evident below 57 m AGL, with temperatures at the surface of 5,4°C increasing to 11°C. The temperature profile above this level was isothermal to 143 m AGL, then decreased slowly to 10,5°C at 217 m AGL, the top of the sounding. The wind profile did not change much from the 23:00 profile, Figure 3.5.4(b).

02:00 - Site M:

From a surface temperature of 6,7°C, temperature increased to 9,4°C at 123 m AGL. Above this level, it remained isothermal to 234 m AGL, before decreasing slowly to 8,7°C at 406 m. Winds were calm below 57 m AGL, at which level a sharp increase occurred with speeds increasing to 5 m.s^{-1} at 68 m. They remained at these speeds to the top of the sounding, Figure 3.5.4(c).

02:00 - Site C:

The surface temperature of 6,5°C increased to 10°C at 37 m AGL. Above this level, the profile remained isothermal to the top of the sounding, 170 m AGL. The west-southwesterly surface wind of 1,5 m.s^{-1} increased rapidly with height and reached 4,7 m.s^{-1} at the top of the inversion. At this level the wind had backed to southwesterly. From 37 m AGL to the top of the sounding, southwesterly winds in the order of 5 m.s^{-1} prevailed. Increasing turbulence resulted in the early termination of the sounding, Figure 3.5.4(c).

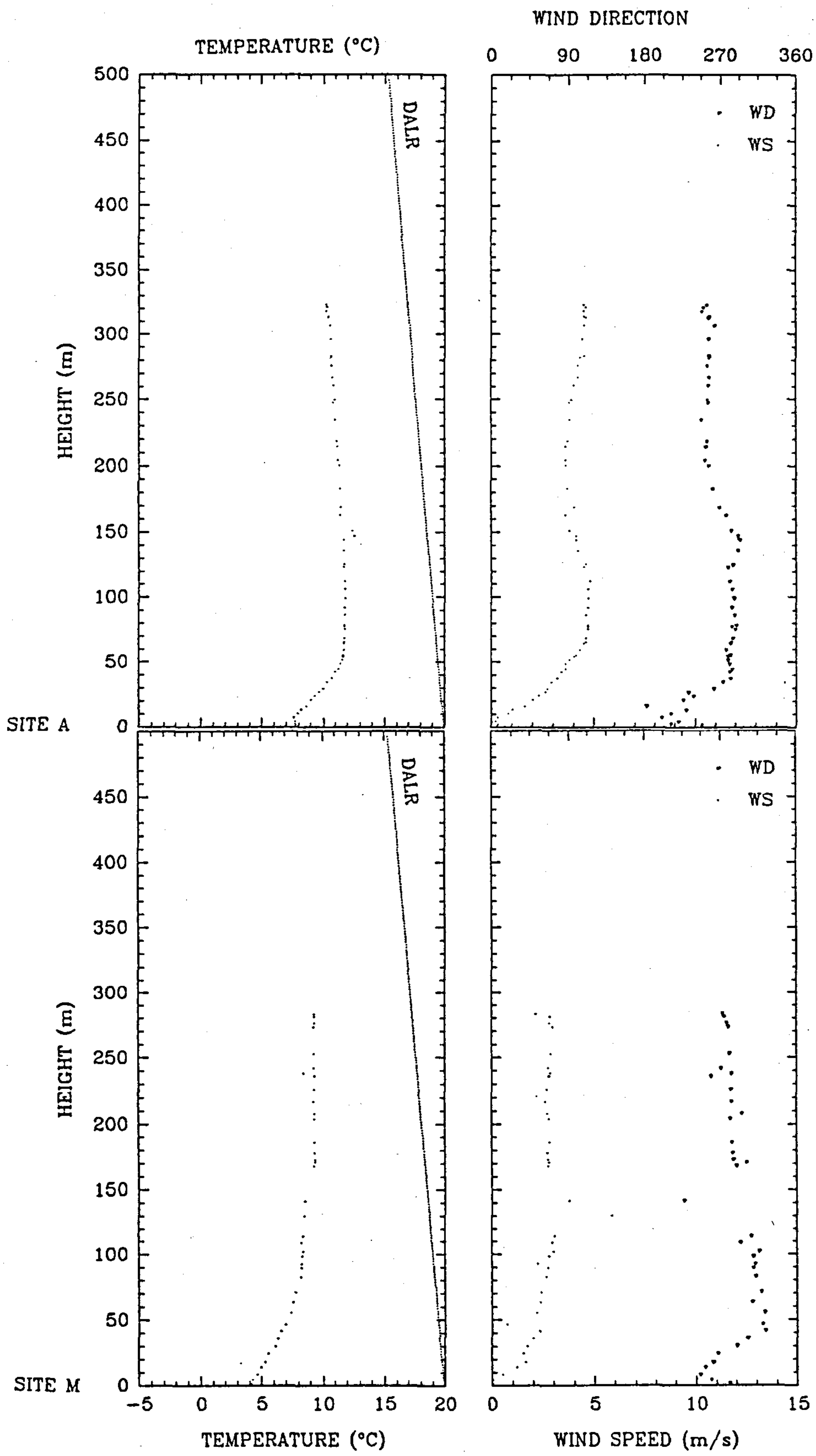

Figure 3.5.4(a): Simultaneous soundings at sites A and M at 23:00 on 14 July 1992.

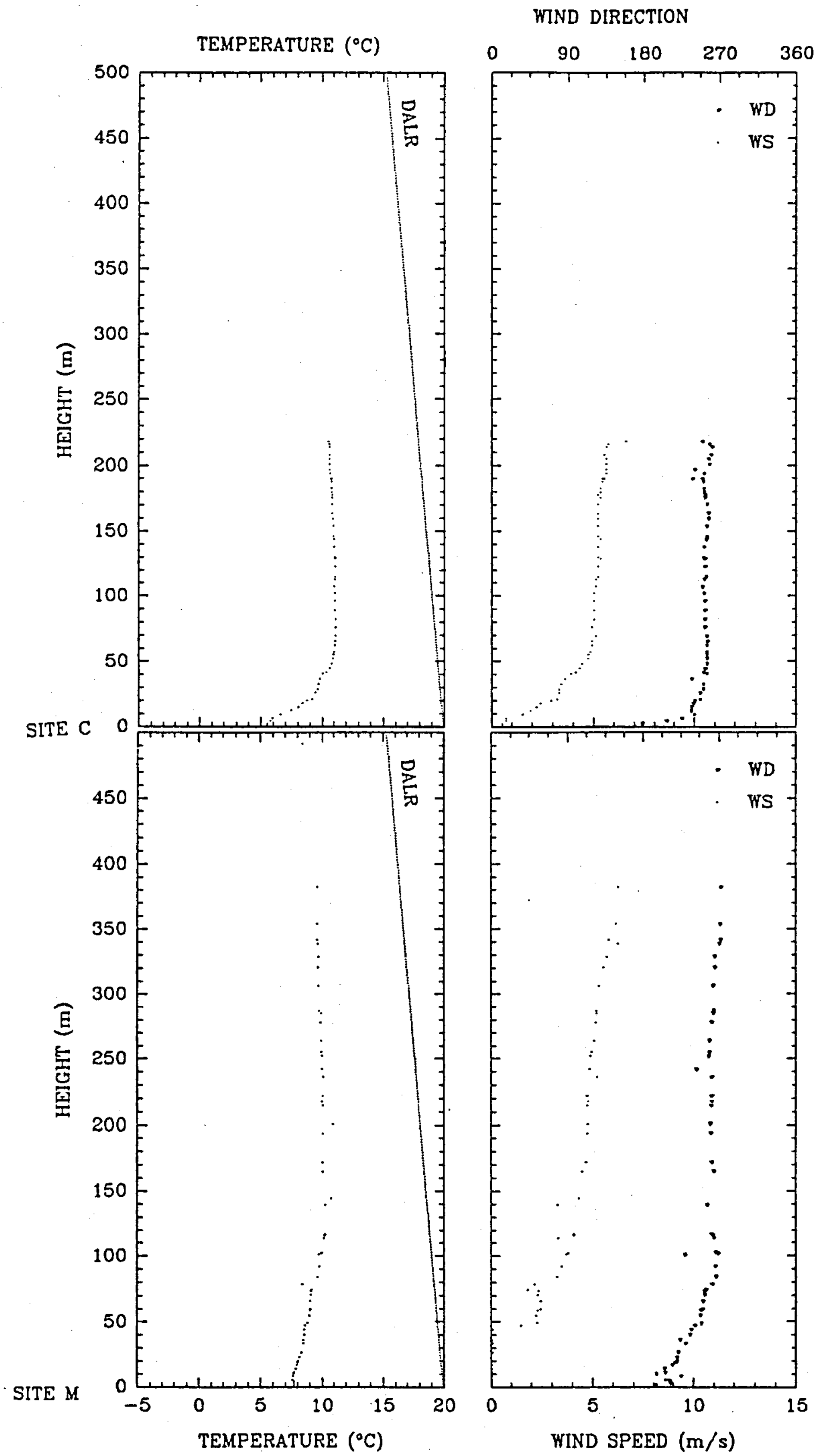

Figure 3.5.4(b): Simultaneous soundings at sites C and M at 01:00 on 15 July 1992.

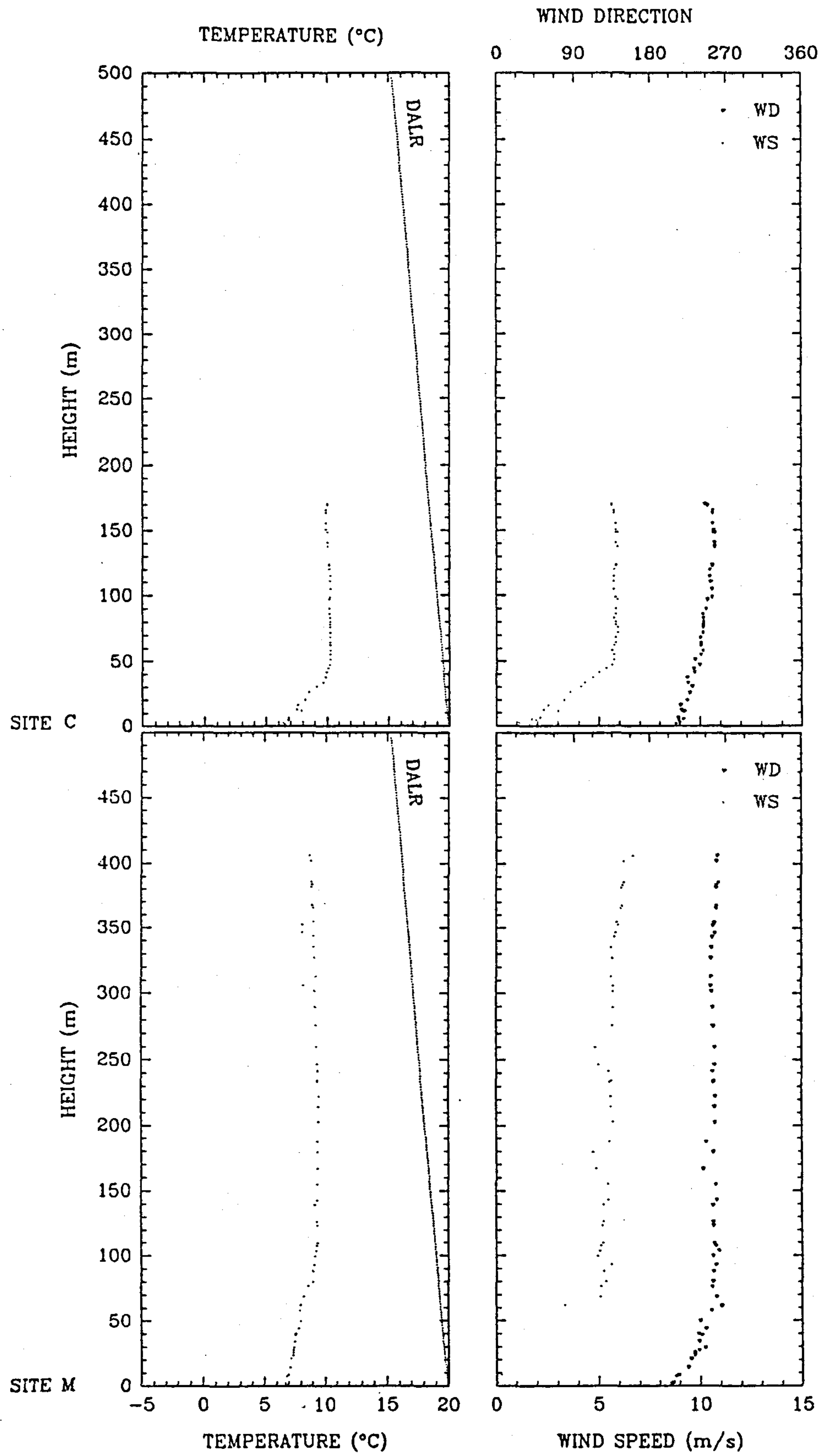

Figure 3.5.4(c): Simultaneous soundings at sites C and M at 02:00 on 15 July 1992.

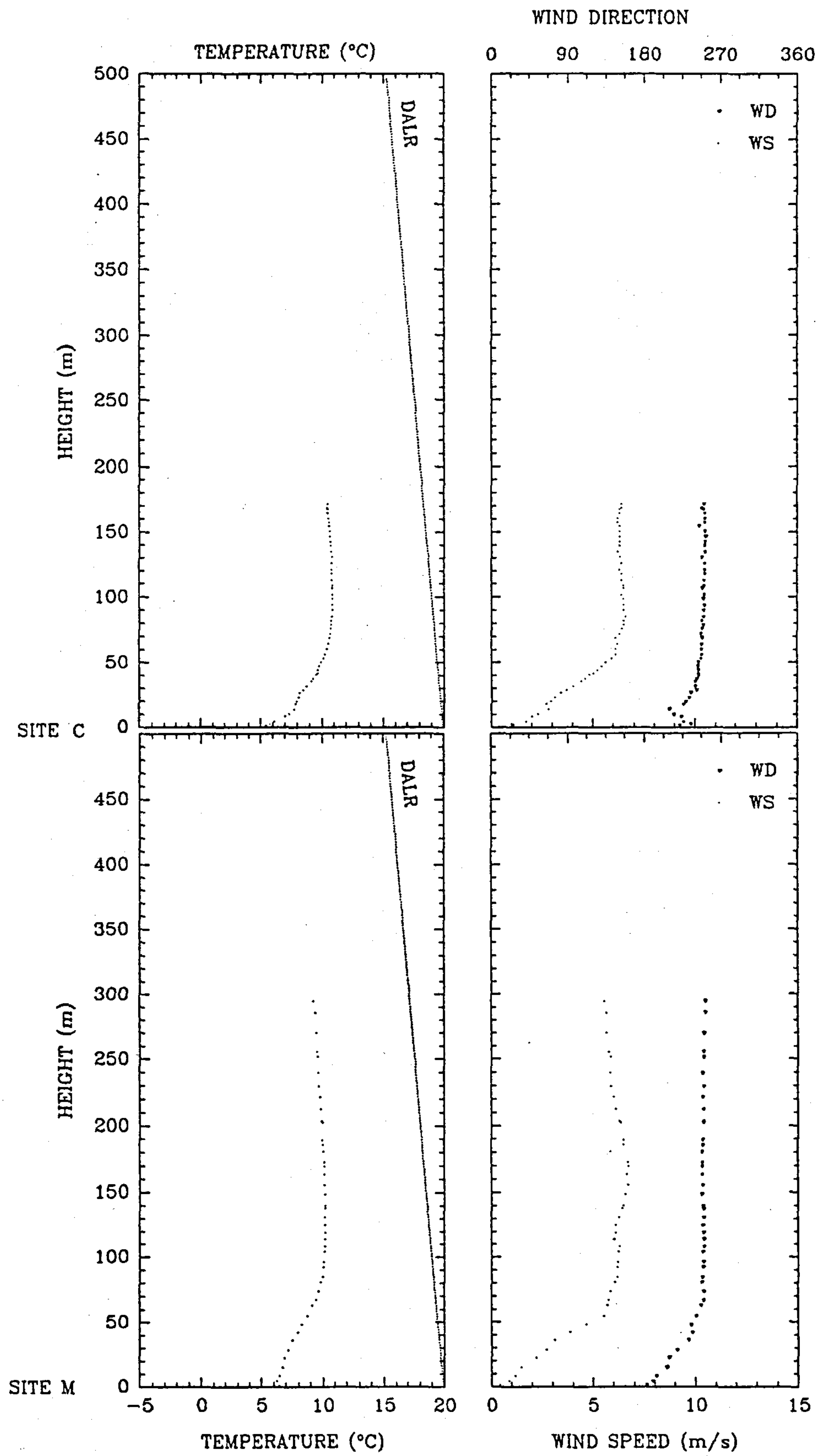

Figure 3.5.4(d): Simultaneous soundings at sites C and M at 03:00 on 15 July 1992.

02:58 - Site M:

Temperature increased from 6,4°C at the surface to 10,2°C at 113 m AGL. Above this level, a gradual decrease occurred to the top of the sounding, where 9,3°C was recorded. Winds were calm at the surface, increasing steadily to about 6 $m.s^{-1}$ at 80 m AGL. These speeds were maintained above this level, Figure 3.5.4(d).

03:00 - Site C:

A surface temperature inversion of 4,1°C was observed, reaching to 40 m AGL. Above this relatively sharp increase, a slower increase occurred with temperature reaching 1,3°C at 89 m AGL. Beyond this level to the top of the sounding, 171 m AGL, the temperature profile was isothermal. The wind increased steadily and veered from southwesterly 1,1 $m.s^{-1}$ at the surface to speeds in the order of 6 $m.s^{-1}$ from the west-southwest at 75 m AGL. Above this level, they remained constant, Figure 3.5.4(d).

Comparison between the upwind and downwind soundings are made with reference to Figure 3.5.5. The distance to the sites are scaled according to the size of CT1. Two noteworthy differences are evident between the upwind and downwind soundings in all four examples.

(i) The magnitude of the surface inversion is similar at both sites, but a noticeable difference in the inversion depth occurs. At the upwind site, the top of surface temperature inversion varies between 110 m AGL and 200 m AGL. Downwind of CT1 the corresponding height varies between 30 m AGL and 90 m AGL.

(ii) The wind speed profiles at the upwind and downwind sites differ. The upwind site is characterised by calm winds close to the surface, with a sudden wind speed shear at about 30 m AGL. Above this level, the flow is nearly laminar. At the downwind site, wind speeds generally increase gradually with height to the top of the inversion, above which flow is nearly laminar.

In the undisturbed boundary layer upwind of CT1 (Site M), thermal stratification occurs with the colder, more dense air close to ground-level forming a layer over which the gradient southwesterly wind flows. This is shown by the wind shear with height at Site M, just above the coldest air. At the downwind Site C, 120 m from CT1, turbulence is introduced as the wind flows around the cooling tower and other structures at the power station. Thermal stratification downwind of CT1 cannot take place, and wind with turbulence occurs throughout the profile. The calm winds at 23:00 at Site A, 420 m from CT1, suggest that turbulence has decreased and the conditions shown at Site M are being approached.

The above discussion and comparison illustrates that the stable boundary layer, depicted by the upwind tethersonde profiles, is distorted downwind of CT1. During the case study period, the mean potential temperature of the four sensors in the exit plane of CT1 was 30,2°C. Downwind advection of the resultant heat plume from CT1 introduced warmer air to the downwind profile, lowering the top of the temperature inversion, e.g. at 01:00 temperatures of 10°C occur at 200 m upwind of CT1, while downwind, advection of the heat plume results in these temperatures occurring at 50 m AGL.

Surridge and Hayton (1985) found the region of influence of the Grootvlei cooling towers, serving 200 MW units, to be approximately a tower length from the tower periphery under calm wind conditions. Swanepoel and Held (1990), using an acoustic sounder, found evidence of the cooling tower heat plume at Kendal (660 MW) to extend to about two tower lengths from the tower base under light prevailing winds. In this case study, Site C, 120 m from CT1's periphery, is well within CT1 region of influence. With prevailing gradient winds of about 5 $m.s^{-1}$ at plume level, the region of influence appears to be distorted downwind and evidence of the tower heat plume is shown at Site A, 420 m from CT1. However, at this distance, the turbulent effects of CT1 on the SBL seem to be reduced, with some thermal stratification evident, shown by a layer of colder dense air with calm winds at the surface. From the above discussion, it appears that the region of influence of CT1 on the SBL extends to about two tower lengths from the tower periphery in gradient wind conditions of 5 to 6 $m.s^{-1}$. At this distance there is evidence of the SBL reforming.

Due to the stable meteorological conditions and stable operation of unit 1, mean temperature and wind data are used to discuss inflow at the four 22 m intake masts. These means are presented in Table 3.5.1 for the six sensor heights.

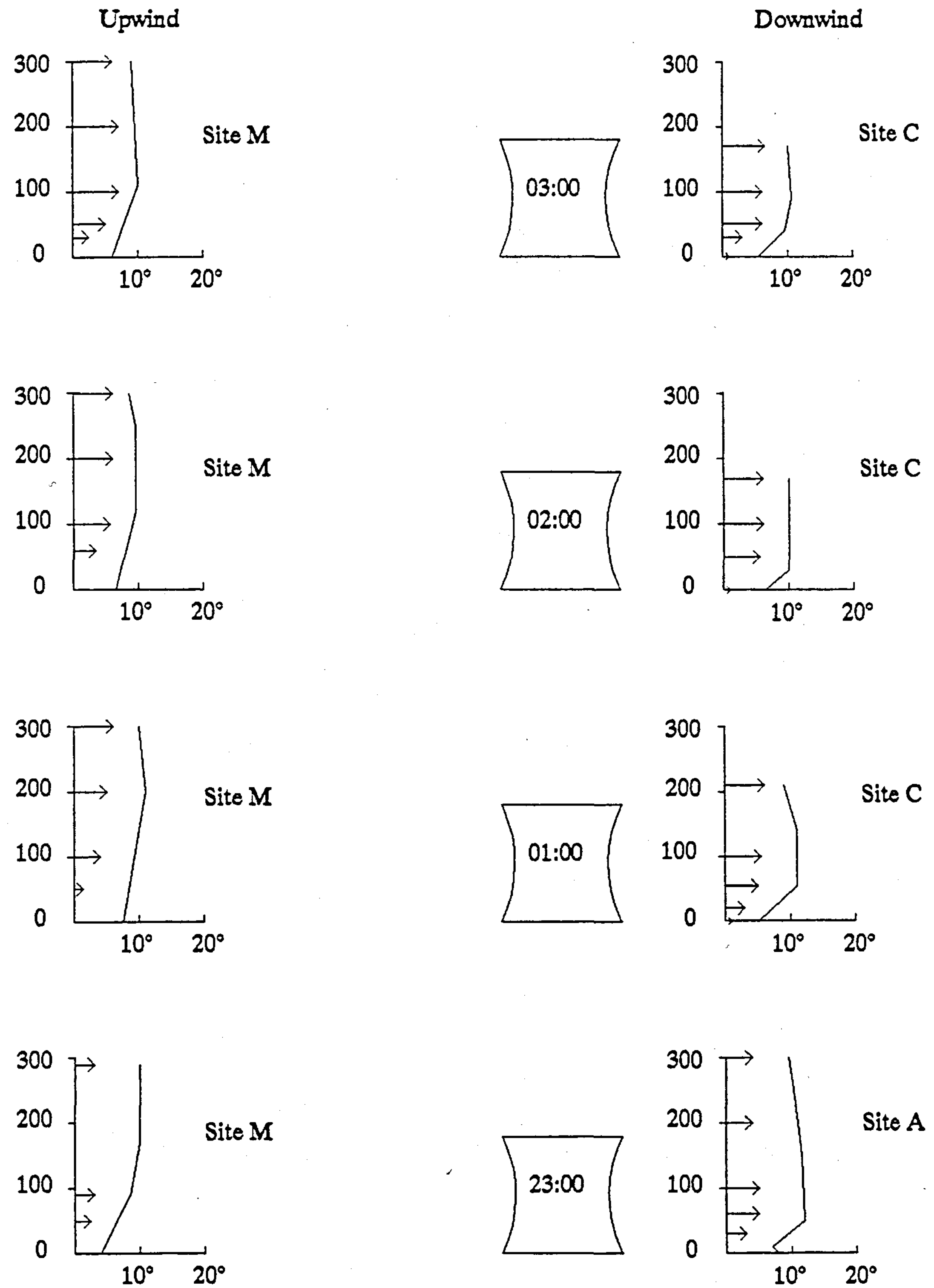

Figure 3.5.5: Comparison between up and downwind soundings for the nocturnal period 14 to 15 July 1992. The lengths of the arrows indicates the relative wind speed.

Table 3.5.1 Mean potential temperature (T_θ) in °C, tangential wind speed (V_T) and radial wind speed (V_R) in $m.s^{-1}$ from the four 22 m masts during the nocturnal period 14-15 July 1992. Heights are m AGL. V_T positive is clockwise, V_R positive into the tower. NRS is the normalised radial wind speed.

Height		N	E	S	W	Mean
22 m	T_θ	11,1	10,6	10,6	-	10,8
	V_T	1,6	-1,9	1,3	-	1,6
	V_R	2,0	1,0	2,1	-	1,7
	NRS	0,6	0,83	0,7	-	0,71
16 m	T_θ	11,3	-	-	-	11,3
	V_T	4,2	-1,7	2,1	-	2,7
	V_R	3,6	0,8	2,2	-	2,2
	NRS	1,0	0,67	0,73	-	0,80
11 m	T_θ	10,8	10,4	9,8	-	10,3
	V_T	3,9	-1,8	1,8	-	2,5
	V_R	3,0	0,7	2,2	-	2,0
	NRS	0,83	0,58	0,78	-	0,71
8 m	T_θ	10,4	10,6	-	-	10,5
	V_T	3,0	-1,6	-	-	2,3
	V_R	2,7	0,7	-	-	1,7
	NRS	0,75	0,58	-	-	0,67
5 m	T_θ	10,3	10,3	9,5	13,9	10,0 (without W)
	V_T	2,7	-1,7	1,2	6,8	2,6
	V_R	2,4	1,0	2,2	4,3	3,0
	NRS	0,67	0,67	0,83	0,98	0,80
2 m	T_θ	9,9	10,1	8,6	14,6	9,5 (without W)
	V_T	3,6	-1,8	1,7	4,2	2,8
	V_R	2,7	1,2	3,0	6,4	3,3
	NRS	0,75	1,0	1,0	1,0	0,94

At all levels the radial wind flows are into CT1. Unfortunately, no data was recorded from 8 to 22 m on the western mast, but at 2 and 5 m, the radial wind component is somewhat accelerated from the calm winds at these levels in the undisturbed boundary layer at Site M. The radial winds are illustrated in Figure 3.5.6 . The strongest inflow occurs between 1 and 16 m AGL.

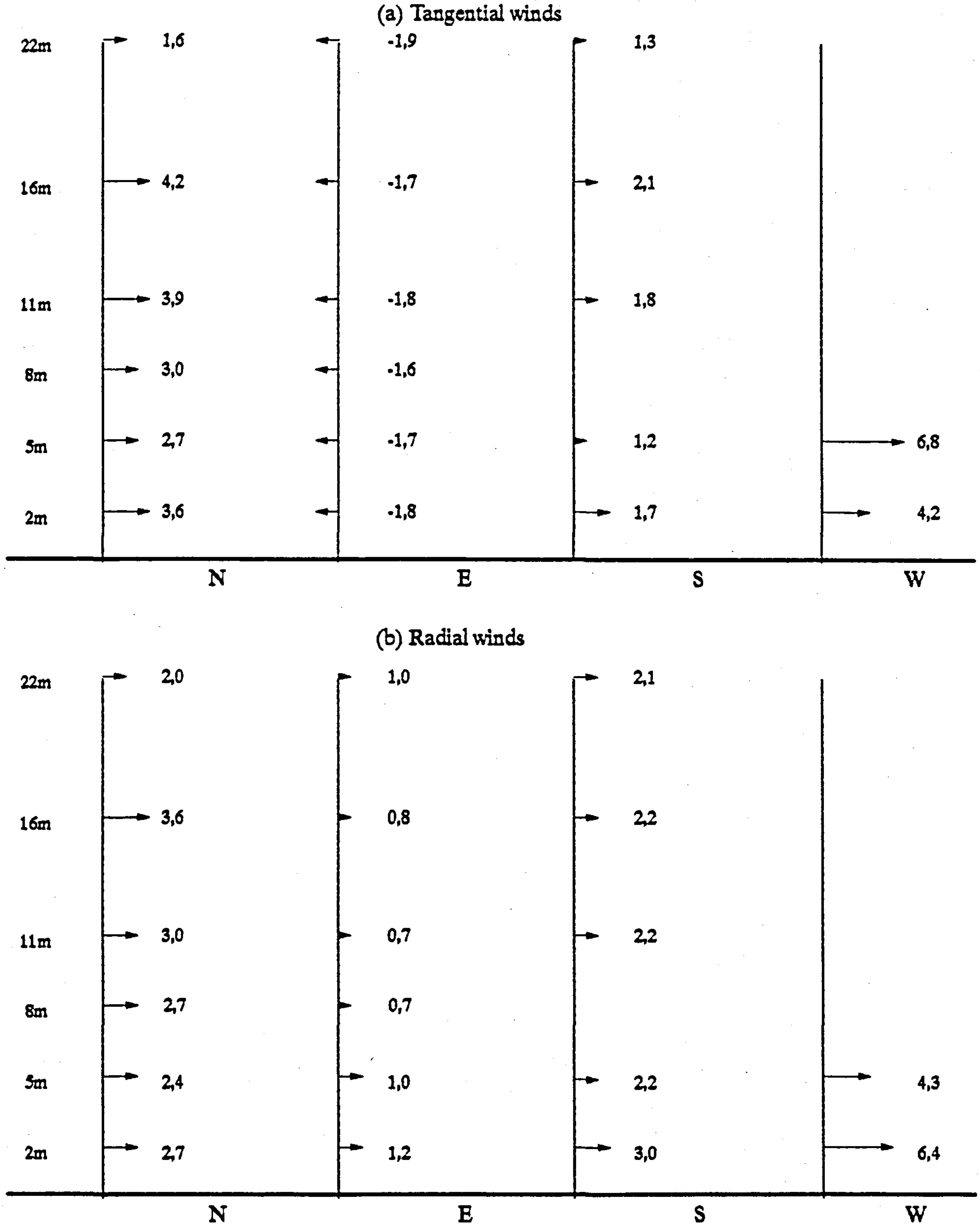

Figure 3.5.6: Mean tangential (a) and radial wind (b) components at the four 22 m masts in the intake region of CT1 for the nocturnal period 14 to 15 July 1992. Wind speeds are shown in m/s.

The tangential wind components, listed in Table 3.5.1 and shown in Figure 3.5.6, indicate turbulence at the downwind (eastern) side of CT1. Tangential flow at all levels is clockwise, except at the downwind eastern side where anticlockwise flow is indicated. The power station structures at the eastern side of CT1 may play a role in this phenomenon. From the current data, wind flow around CT1 cannot be accurately assessed. Generally, temperature increases with height between the bottom and top of the masts, except for the upwind western mast, where the temperature decreases with height, and is 4°C to 5°C warmer than at the other masts.

The two-dimensional temperature line was operational from 01:20 to 02:50 on 15 July 1992. Data was received from 15 of the 19 sensors, with the sensor line nearest to CT1 not functional. The average temperatures for this period are listed in Table 3.5.2, with sensor numbers corresponding to sensor positions in Figure 2.3.

Table 3.5.2. Mean potential temperatures (°C) for the period 01:20 to 02:50 from the two-dimensional temperature field sensor.

Sensor	Temperature	Sensor	Temperature
1	9,6	9	10,4
2	11,5	10	10,9
3	10,5	11	10,9
4	10,4	12	10,7
5	10,6	13	10,5
6	10,7	14	10,2
7	9,7	15	10,3
8	9,3		

With a westerly wind prevailing during the nocturnal period, the 2-D temperature field and tethersonde sites A and C were approximately in the same radial plane downwind of CT1. Site M was situated in the same radial plane upwind of CT1. Tower intake temperatures in the southeasterly plane are represented by the mean between the eastern and southern 22 m towers. Using temperature data from the two-dimensional field, tethersondes, tower intake masts and exit temperature of the plume, the mean temperature field downwind of CT1 is illustrated in Figure 3.5.7. The background conditions are given by the Eskom mast which is not in the same radial plane as the other data sources.

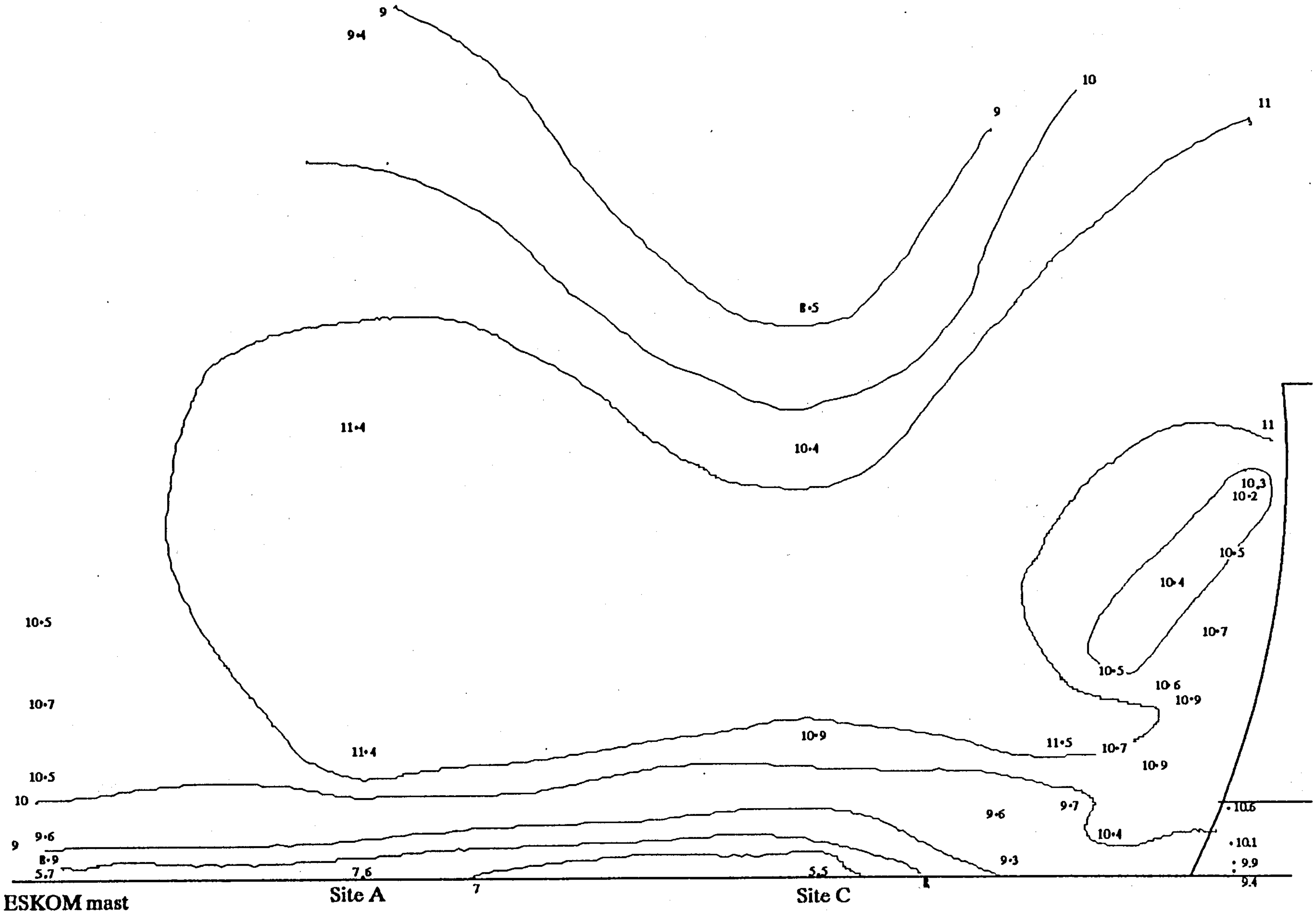

Figure 3.5.7: Temperature field in the downwind radial plane of CT1.

The undisturbed SBL north of CT1 indicates a temperature inversion of 5,0°C between ground-level and 65 m AGL. At Site A, 420 m from CT1, the top of the inversion was recorded at 50 m AGL and the temperature at the top of the inversion was nearly 1°C warmer than the background. Similarly, at Site C, 120 m from CT1, the top of the inversion occurred at 50 m AGL.

Closer to CT1, the two-dimensional field shows further depression of the temperature inversion towards the tower intake. A tongue of warm air from the heat plume is shown to extend downward into the two-dimensional field close to CT1. Concurrently, cooler air of surface origin appears to circulate close to the tower, between the intake area and the top of the tower. This is shown as a "pool" of air cooler than 10,5°C. Beyond this pool and above the surface inversion, an extensive layer of air that is warmer than the background air is evident. It appears that this air forms part of the tower heat plume advected downward and downwind of CT1 by the prevailing westerly winds. This more detailed study of the temperature field downwind of CT1 also indicates that the field of influence of the cooling tower extends to approximately two tower lengths from the tower periphery. The downward advection of the heat plume to below the tower exit plane was also noted by Swanepoel and Held (1990) using an acoustic sounder.

Using the upwind soundings and the 96 m Eskom mast, the average background surface inversion of 3,9°C was obtained. Mean temperature at 1,2 m AGL was 6,1°C, and the corresponding temperature at the top of the inversion was 10,0°C. After applying the necessary weighting factors, the mean inlet temperature to CT1 during the nocturnal period was calculated as 8,8°C. These temperatures yielded an entrainment function of 69%, implying that the mean inlet temperature was 2,7°C warmer than the air at 1,2 m AGL in the SBL.

Case Study Features

1. Prevailing northwesterly, becoming westerly, winds throughout the field excursion. A surface temperature inversion of 3-5°C was observed.

2. Constant power generation of 71,5% of maximum capacity occurred throughout the period.

3. Region of influence of CT1 extended about two tower lengths downwind under light prevailing wind conditions.

4. Inversion entrainment factor of 69%.

5. Strongest air inflow into CT1 was between 11 and 16 m.s^{-1}.

3.6 Case Study 5: 16 July 21:00 - 17 July 03:00

The synoptic circulation during this case study period was dominated by a well-established high pressure system at 850 hPa, situated over the northeastern parts of the country. The 14:00 synoptic chart for 16 July 1992 is shown in Figure 3.6.1. This presented ideal conditions for the maintenance of a stable boundary layer during the nocturnal period.

At the start of the monitoring period, Kendal's unit 1 was operating at above 80% of its capacity. Between 22:16 and 22:36, this dropped to 70% of capacity, which was maintained to the end of the nocturnal study period. Due to the change in operational output of unit 1, this case study is discussed in two parts. The first, from 21:00 to 22:17, when the average operation was 92% of capacity. The second, from 22:36 to 03:00, when the average operation was 71% of capacity. Figure 3.6.2 shows the operational percentage of unit 1 during the nocturnal period.

Typical of the dominant 850 hPa high pressure over the study region is that the stable boundary layer conditions prevailed throughout the nocturnal period. Hence, temperature and wind data recorded by the 96 m Eskom mast showed little variation.

3.6.1 21:00 - 22:17: 16 July 1992

During this period, two simultaneous tethersonde soundings were carried out at sites F and D, 200 m upwind and 280 m downwind of CT1, respectively, at approximately 22:00. The resultant temperature and wind profiles are shown in Figure 3.6.3. With prevailing north-easterly winds during this period, the 96 m Eskom mast, situated 685 m north of CT1, was roughly upwind. The temperature and wind profiles from the mast at 21:58 are shown in Figure 3.6.4.

The upwind sounding and the Eskom mast describe the undisturbed boundary layer. At both sites, the wind at the surface was light northeasterly, backing a little with height. Wind speeds were generally less than 5 m.s^{-1}, except at site F, where above 200 m AGL wind speeds approached 7 m.s^{-1}. The average upwind potential temperature profile exhibited a surface inversion of 1,3°C, from a surface temperature of 9,6°C to 10,9°C at 33 m AGL.

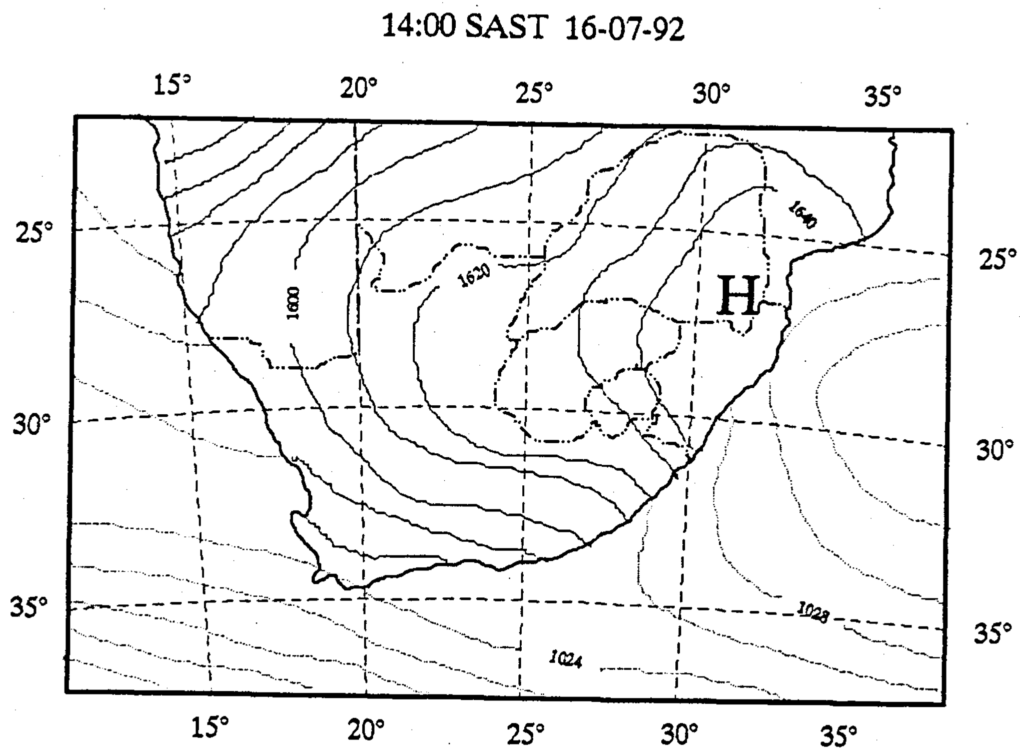

Figure 3.6.1: 14:00 Synoptic chart for 16 July 1992.

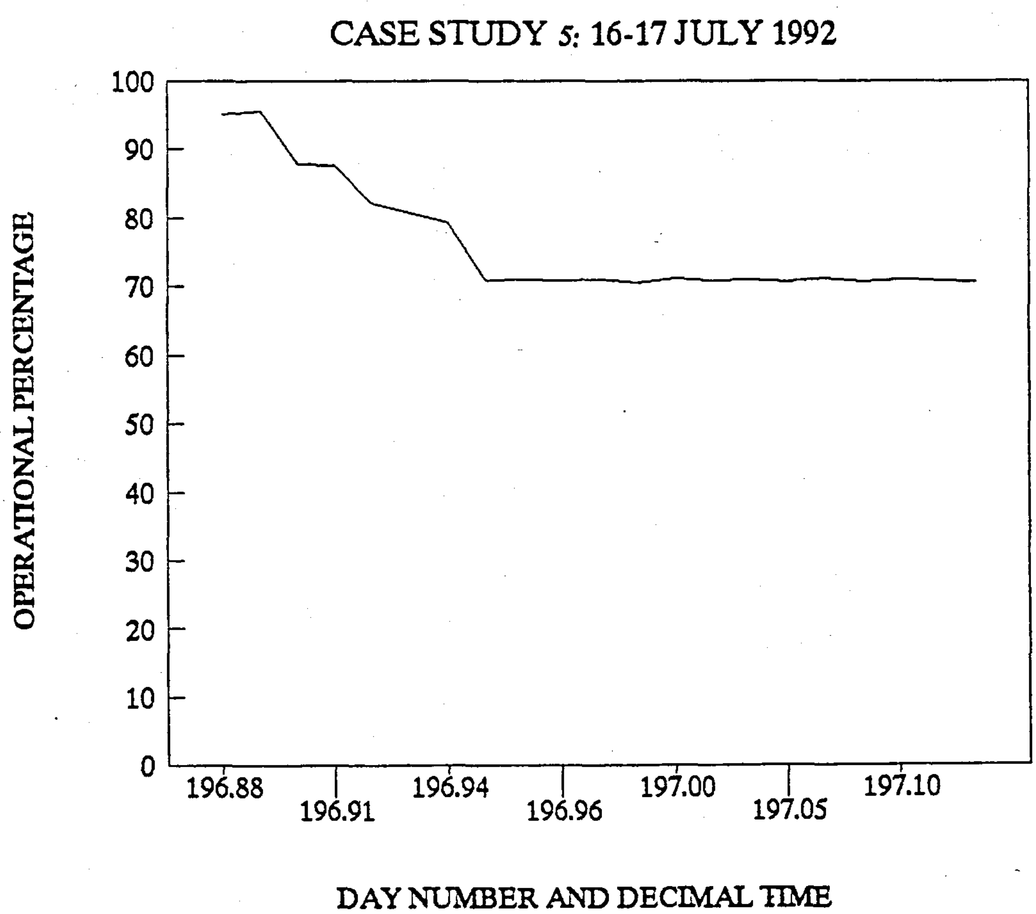

Figure 3.6.2: Operational performance of unit 1.

The 22:00 tethersonde sounding, 280 m downwind of CT1 at site D, exhibited different temperature and wind profiles to that of the upwind sounding. An isothermal layer was evident from ground level to about 100 m AGL. Above this level, the temperature decreased slowly with increasing height. An interesting feature is illustrated in the upwind wind profile, Figure 3.6.3, at site F. Below 50 m AGL and above 150 m AGL, the wind direction exhibits the same northerly component of the background SBL, shown by the upwind sounding and the Eskom 96 m mast. At these levels, the wind speeds also resemble those of the upwind soundings. Between 50 and 150 m AGL, a considerable amount of turbulence was encountered during the sounding. This turbulence is illustrated by the erratic and rapidly changing wind direction.

Evidence of distortion of the background SBL by CT1 is evident in the downwind tethersonde profiles. The background SBL surface inversion of 1,3°C is non-existent at 280 m downwind of CT1. Turbulence in the lee of the cooling tower provided sufficient mechanical mixing to prevent cooling of the air in contact with the ground and the formation of a surface inversion. A well-mixed isothermal layer prevailed. In this instance, CT1's region of influence extends to about two tower lengths from the tower periphery.

Fifteen sensors on the two-dimensional temperature line on the southeastern side of CT1 were operational during this period. Temperatures recorded at 22:00 are listed in Table 3.6.1, where the sensor numbers correspond with the positions indicated in Figure 2.3.

Table 3.6.1 Two-dimensional potential temperatures at 22:00, 16 July 1992

Sensor	1	2	3	4	5	6	7	8
Temperature (°C)	11,9	12,1	12,1	11,4	12,5	11,5	11,6	11,0
Sensor	9	10	11	12	13	14	15	
Temperature (°C)	11,8	11,9	11,0	12,2	11,1	11,1	12,2	

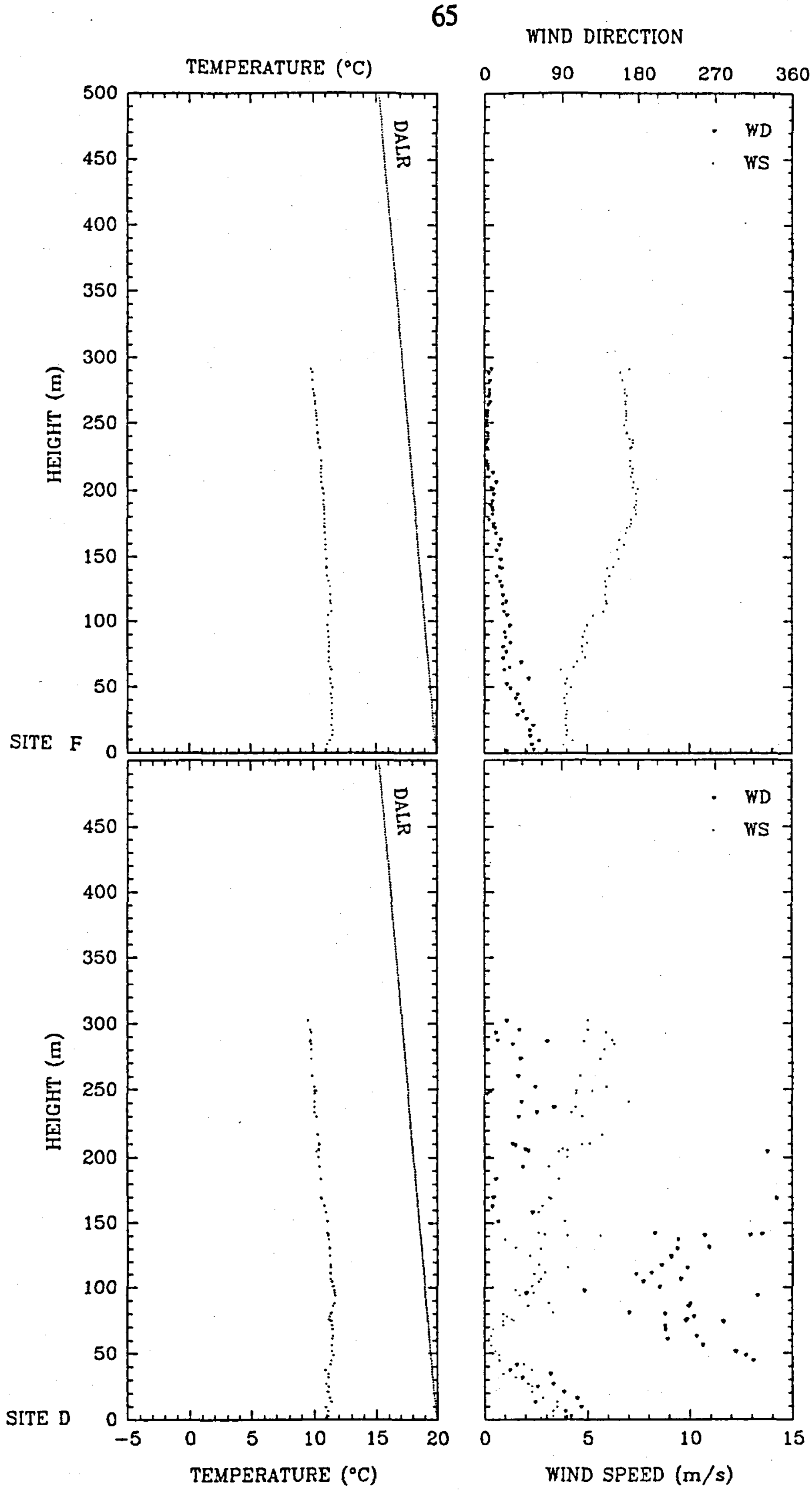

Figure 3.6.3: Up and downwind tethersonde profiles at 22:00 at sites F and D respectively.

ESKOM 96 m MAST

16 JULY 1992: 21h58

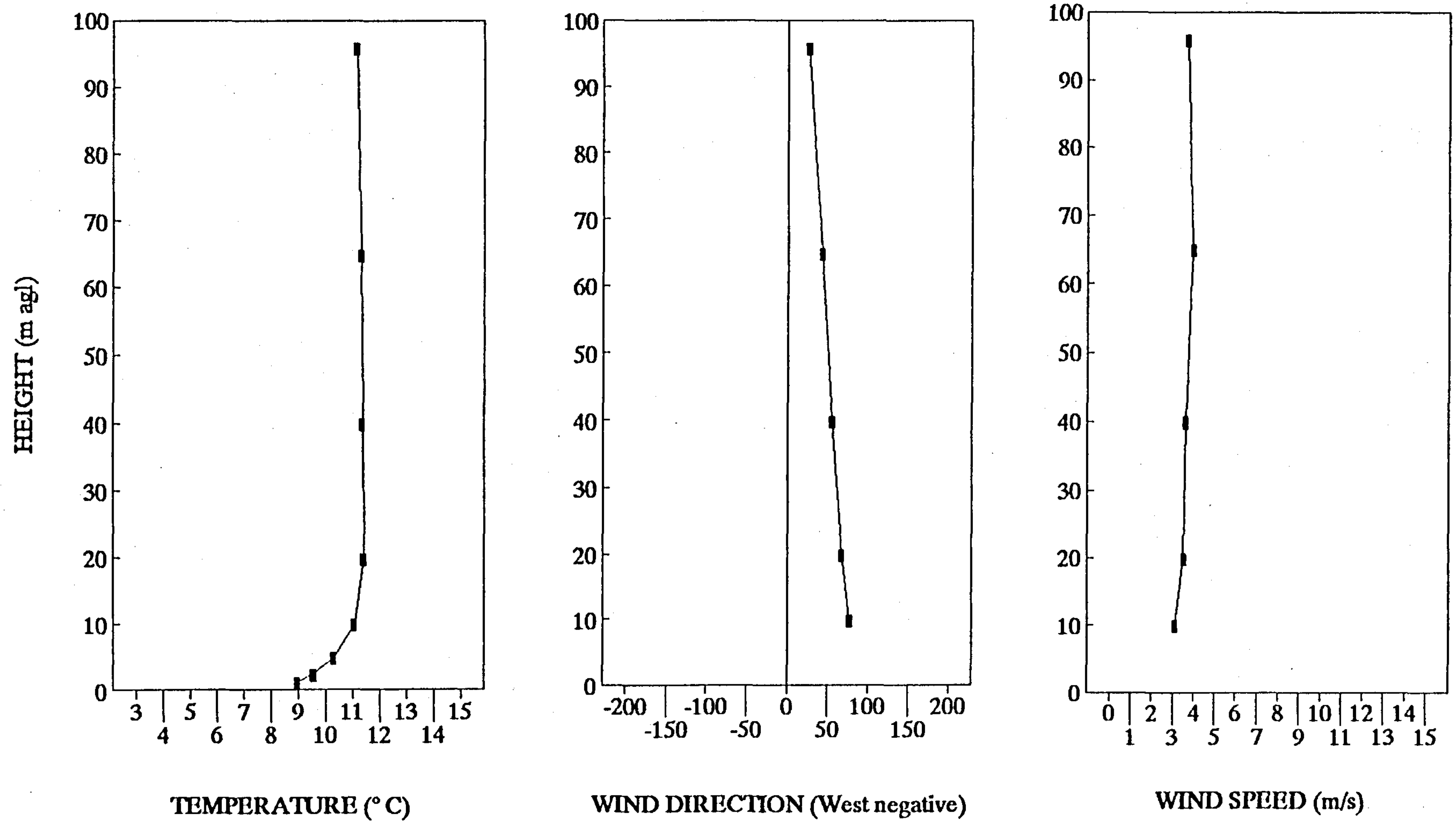

Figure 3.6.4: Eskom mast profiles at 21:58.

In describing the two-dimensional temperature field in the north-south radial plane about CT1, the 2-D temperature profiler and the intake masts are used to illustrate the temperature field close to CT1, Figure 3.6.5(a). The temperature field further from CT1, Figure 3.6.5(b), is described using tethersonde profiles and the 96 m Eskom mast data and the close field information from Figure 3.6.5(a). At the upwind side of CT1, the Eskom mast and the tethersonde sounding from site F are used to describe the background SBL. The northern 22 m intake mast describes the temperature field at the upwind side of the intake area. Downwind of CT1, the tethersonde sounding from site D and the 2-D temperature profiler are used. The mean temperatures of the eastern and southern 22 m masts provide a measure of the temperature field in the intake area, that is, in the same radial plane as the 2-D profiler and site D. Temperatures at 22:00 from the relevant 22 m masts are listed in Table 3.6.2.

Table 3.6.2 Potential temperature at six levels in CT1's intake region, from the 22 m masts.

Position	Height (m AGL)					
	2	5	8	11	16	22
N	12,0	12,3	9,2	9,5	12,2	12,0
E	11,9	12,0	12,3	11,9		11,9
S	11,6	12,0	11,7	11,4		11,6

The temperature field close to CT1 shows the heat plume advected downward at the lee side of the cooling tower by the prevailing wind into the rêgion of the 2-D temperature profiler. A tongue of air warmer than 12°C extends downward to just above the tower intake region, Figure 3.6.5(a). This is also shown by the temperature field on the larger horizontal scale in Figure 3.6.5(b). On the larger scale, the heating range effect of the cooling tower is evident. Almost the entire area within 200 m of either side of CT1 is warmer than the background SBL. Under the light prevailing wind conditions, the cooling tower exhibits almost a symmetrical distortion of the SBL. Temperatures in the intake region at the upwind side show a layer of cooler air between 8 and 11 m AGL. This is possibly of surface origin.

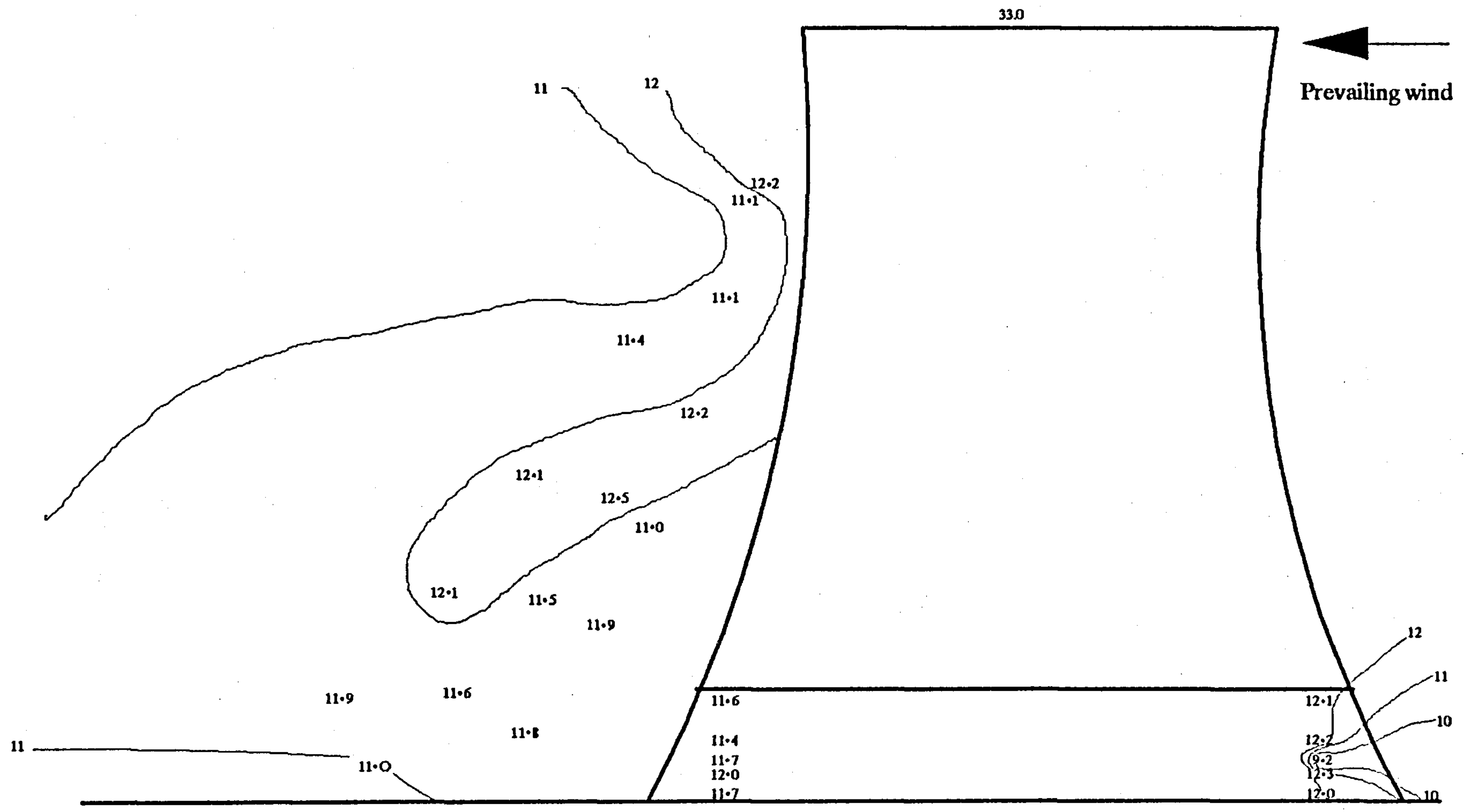

Figure 3.6.5(a): Temperature field close in to cooling tower No. 1 at 22:00.

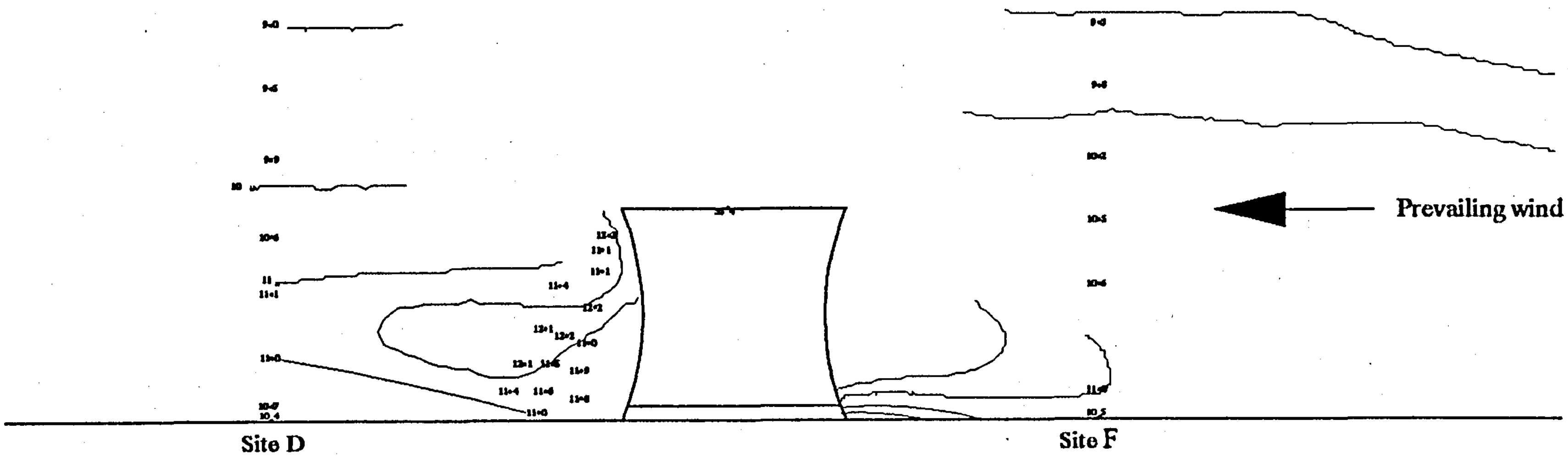

Figure 3.6.5(b): Temperature field about CT1 in the north-south radial plume at 22:00.

The mean intake potential temperature of 11,9°C during the period 21:00 to 22:10 was calculated using Equation 3.1.2. By using the average upwind temperature inversion, an entrainment value of 140% is calculated. During this period, unit 1 was operating at an average of 92% of its capacity. The temperature fields illustrated in Figure 3.6.5(a) and (b) show that there is no significant entrainment of the boundary layer, but rather air from the heat island created around CT1 is being circulated back into the tower intake.

In Table 3.6.3, the mean temperature and tangential and radial components at the six levels at the intake mast are listed. The stronger tangential component at the eastern tower possibly indicates a venturi effect of the northerly wind between CT1 and cooling tower 2. The clockwise orientation of all the tangential components indicate rotation of air around CT1 and the possible formation of a closed vortex system. All the radial components are directed inward and are generally stronger than the tangential components.

Table 3.6.3 Mean potential temperature (T_θ) in °C, tangential wind speed (V_T) and radial wind speed (V_R) in m.s^{-1} from the four 22 m intake masts, during the period 21:00 to 22:10, 16 July 1992. Heights are m AGL, NRS is the normalised radial wind speed. V_T is positive clockwise, V_R is positive into the tower.

Height		N	E	S	W	Mean
22 m	T_θ	12,3	12,1	11,8	-	12,1
	V_T	0,5	3,2	1,5	-	1,7
	V_R	2,5	1,4	2,4	-	2,1
	NRS	0,3	1,0	0,5	-	0,6
16 m	T_θ	12,6	-	-	-	12,6
	V_T	1,5	3,4	1,0	-	2,0
	V_R	9,6	2,0	2,4	-	4,7
	NRS	1,0	0,92	1,0	-	0,97
11 m	T_θ	9,3	11,9	11,8	-	11,0
	V_T	2,5	3,2	0,8	-	2,2
	V_R	1,2	2,0	2,5	-	1,9
	NRS	1,0	0,7	0,3	-	0,37
8 m	T_θ	9,1	12,2	12,1	-	11,2
	V_T	2,2	2,6	-	-	2,3
	V_R	1,0	2,2	-	-	1,6
	NRS	0,1	0,6	-	-	0,35
5 m	T_θ	12,1	12,0	12,2	9,4	12,1*
	V_T	2,5	2,4	1,0	0,6	2,0*
	V_R	1,2	2,0	2,7	0,36	2,0*
	NRS	0,14	0,6	0,7		0,48*
2 m	T_θ	11,9	11,9	11,6	9,9	11,8*
	V_T	1,0	2,9	0,8	1,3	1,6*
	V_R	5,5	2,0	2,9	3,9	3,5*
	NRS	0,64	0,6	0,7	1,0	0,65*

* Without W.

3.6.2 22:36: 16 July 1992 - 03:00: 17 July 1992

The prevailing wind direction in the background SBL, indicated by the Eskom mast, was northeasterly at 10 m AGL, but backed with height to be northerly at 96 m AGL. Wind speeds throughout this period were light, varying between 2 and 4 $m.s^{-1}$ between 10 and 96 m AGL. The mean 96 m wind profiles for the period are shown in Figure 3.6.6. Figure 3.6.6 also shows the mean temperature profile for the period. A mean potential temperature inversion of 2,8°C exists between the surface and 65 m AGL.

From the start of the period to midnight, simultaneous tethersonde soundings were carried out upwind and downwind of CT1. Three soundings were done, each at sites O and D, 1300 m upwind, and 280 m downwind of CT1, respectively.

A comparison between the upwind and downwind soundings produces similar conclusions to that of the comparison of soundings discussed in Section 3.6.1, when unit 1 operated at 92% of capacity. At site O, a well-developed surface temperature inversion was observed, with the surface temperature of about 7°C increasing to about 10°C at 30 m AGL. Wind speeds increased gradually with height from calm surface winds to about 7 $m.s^{-1}$ at 300 m AGL. Easterly winds at the surface backed to northerly above 50 m AGL. The sounding at 23:42 illustrates the profiles typical of this period, Figure 3.6.7. Concurrently, the downwind soundings exhibited little or no surface temperature inversion. Wind direction below 150 m AGL was variable, and speeds were generally light. Above 150 m AGL, the wind speed increased to values similar to those at site O and became consistently northerly. Only above 150 m AGL are conditions representative of the background SBL exhibited. The downwind sounding at 23:41 is shown in Figure 3.6.7.

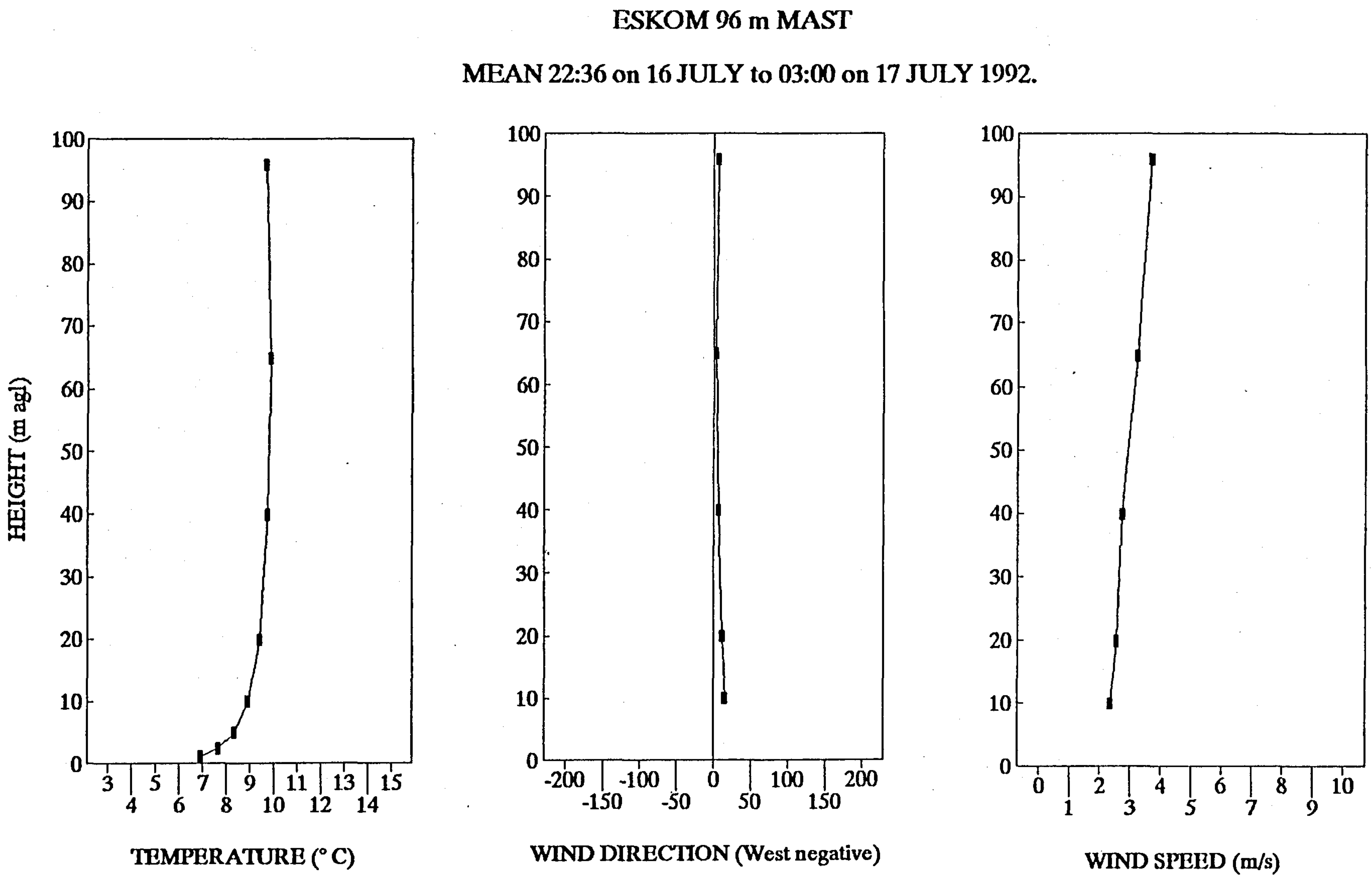

Figure 3.6.6: Mean temperature and wind profiles from the Eskom mast from 22:36 to 03:00 on the 16 to 17 July 1992.

Examination of the simultaneous tethersonde soundings at downwind sites D and P, 280 m and 900 m from CT1, respectively, provide a better perception of the downwind region of CT1. The mean 96 m Eskom mast profiles, Figure 3.6.8, are used to represent the background SBL and the soundings are compared with these. At the closer of the two sites, site D, a surface temperature inversion of between 1,5°C to 2°C, is exhibited with the inversion top at about 40 m AGL. This is somewhat weaker than the background inversion of 2,8°C at a height of 65 m AGL. The winds at site D were light throughout the profile, reaching a maximum of 5 $m.s^{-1}$ above 300 m AGL. The wind direction at the surface was generally southerly throughout the period. With the background winds generally northeasterly, this towerward flow at site D indicates some turbulent wake effect in the lee of CT1. Above 50 m AGL, the wind direction veers through west, becoming ultimately northerly at about 200 m AGL, i.e. the background northerly flow is resumed again above 200 m AGL.

Further downwind from CT1, the temperature and wind profiles are typical of the background SBL and so no evidence of CT1's influence is apparent. The 65 m deep surface temperature inversion, shown for the background by the Eskom mast, is exhibited up to 60 m AGL at site P. Wind speeds at this site increase gradually with height from calm winds at the surface to about 7 $m.s^{-1}$ at 300 m AGL and wind direction changes from easterly at ground level, back to northerly with increasing height. The similarity between the Eskom tower profiles and the soundings at site P show SBL conditions 700 m north and 930 m south of CT1, respectively. No indications of SBL distortion are evident six tower lengths downwind of CT1 at site P. Figure 3.6.8 shows the 03:00 and 03:11 soundings from sites D and P, respectively.

During this period, the mean inlet potential temperature to CT1 was 10,2°C. The entrainment function yielded an entrainment factor of 133% of the 2,8°C potential temperature inversion. This implies that the entrained air was significantly warmer than the air at 1,2 m AGL in the SBL.

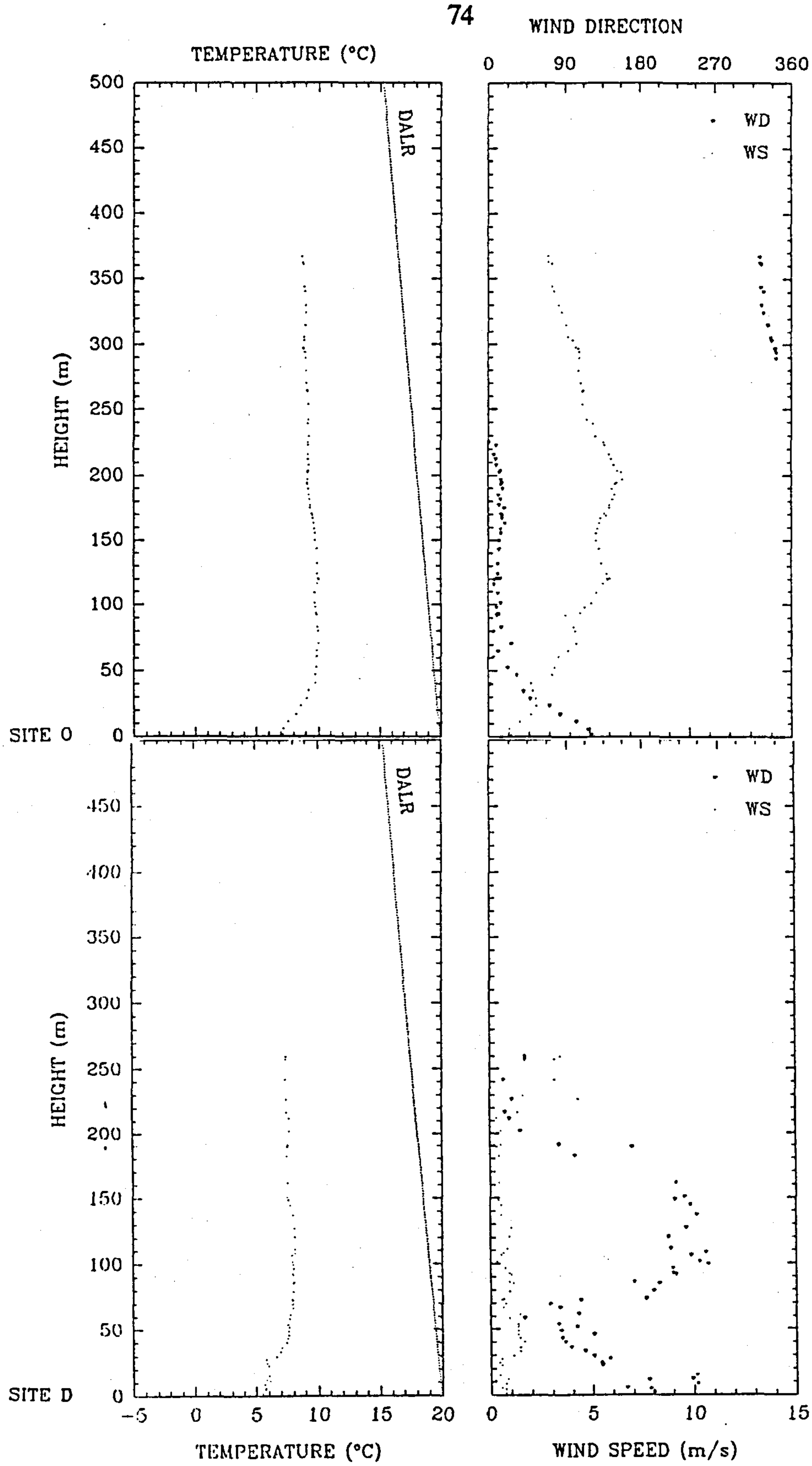

Figure 3.6.7: Upwind sounding, site O, at 23:42 and the downwind sounding, site D, at 23:41

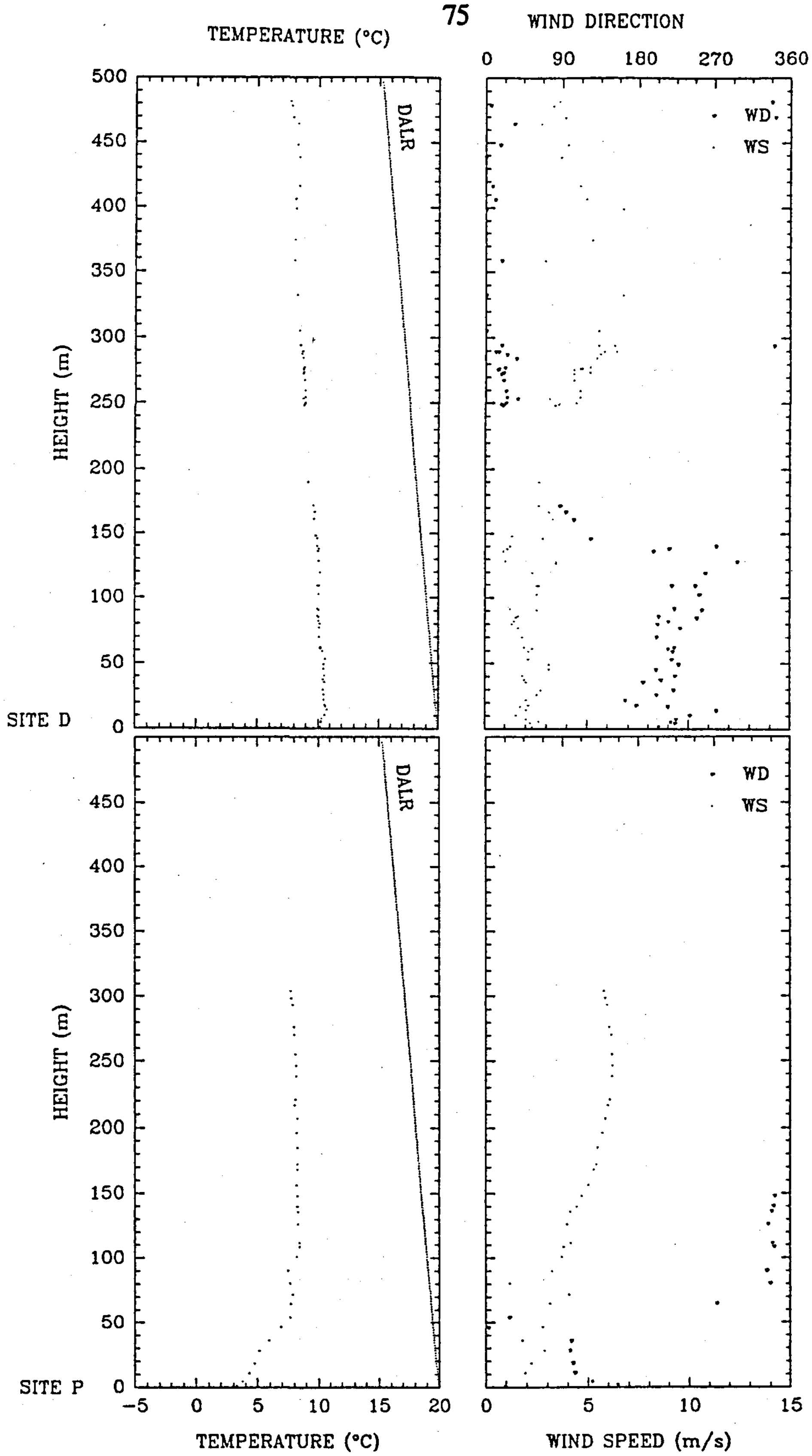

Figure 3.6.8: Downwind sounding at 03:00 and 03:11 from site D and P, respectively.

The mean two-dimensional temperature field close to CT1 during the period is illustrated in Figure 3.6.9(a). The actual values are tabulated in Table 3.6.4. The temperature field in the north-south plane about CT1, from the Eskom mast in the north to tethersonde site P in the south, is illustrated in Figure 3.6.9(b). In these two diagrams, the SBL distortion by the cooling tower is shown with temperatures in the intake region far warmer than anywhere in the surrounding boundary layer. Under perfect stable boundary layer conditions with light northerly prevailing winds at plume exit height, only a small downwind distortion of the heat plume occurs. It is apparent that no air from the cooler surrounding boundary layer is taken up into the cooling tower. Air within the closed heat island around CT1 is entrained into the tower intake, resulting in the enhanced entrainment factor.

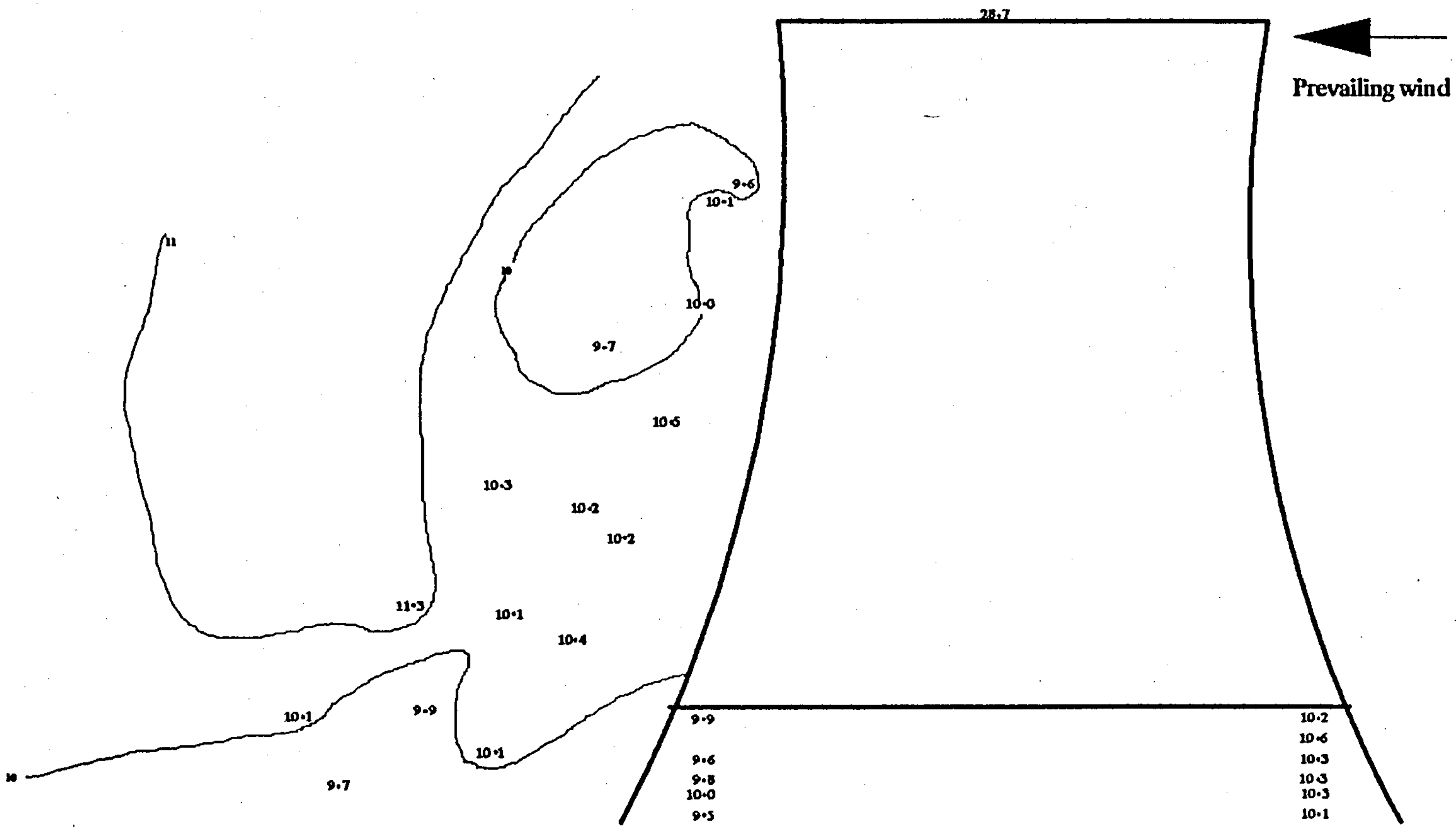

Figure 3.6.9(a): Temperature field close in to cooling tower No. 1 during the period 22:36 to 03:00 on the 16 and 17 July 1992.

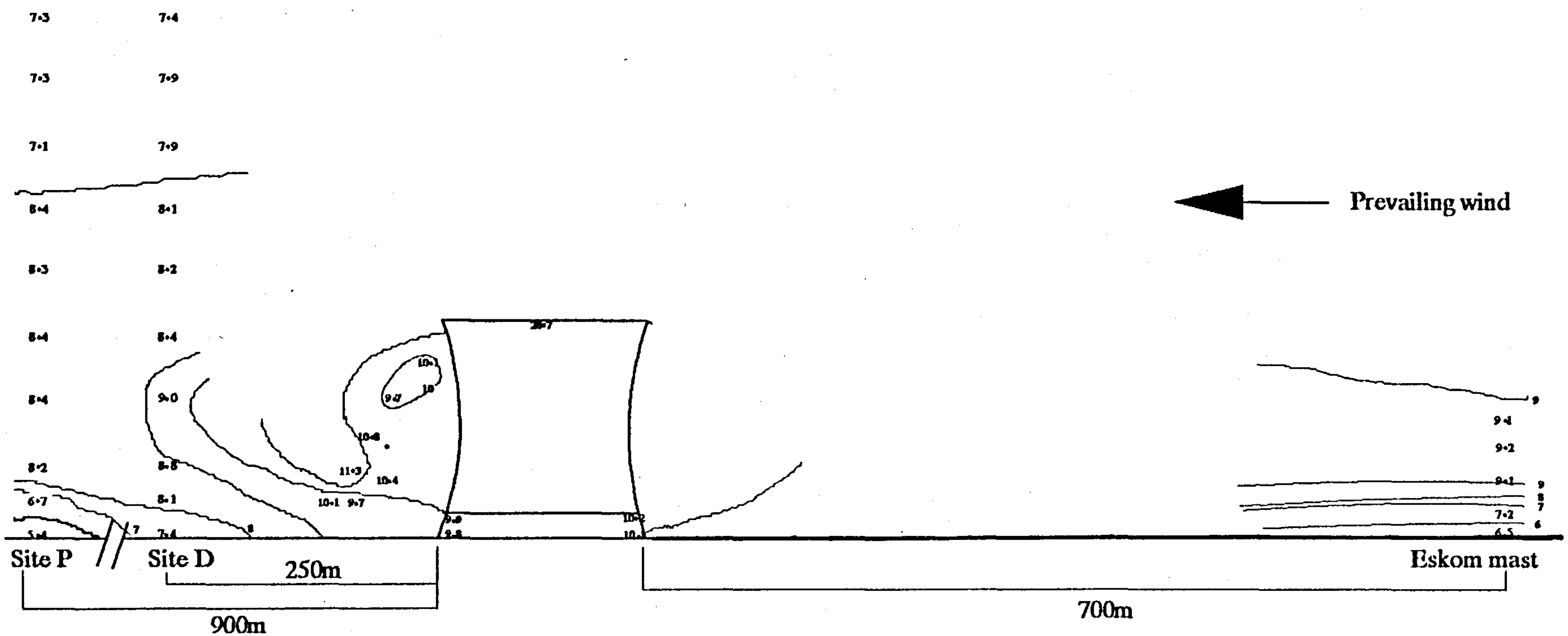

Figure 3.6.9(b): Temperature field about CT1 in the north - south radial plane from the Eskom mast to tethersonde site P.

Table 3.6.4 Mean potential temperature (T_θ) in °C, tangential wind speed (V_T) and radial wind speed (V_R)in m.s^{-1} from the four 22 m intake masts, during the period 22:10 to 03:00, 16-17 July 1992. Heights are m AGL. V_T is positive clockwise, V_R is positive into the tower.

Height		N	E	S	W	Mean
22 m	T_θ	10,2	10,0	9,7	-	10,0
	V_T	0,5	3,8	1,9	-	2,1
	V_R	3,8	2,0	2,5	-	2,8
	NRS	0,6	0,74	1,0	-	0,78
16 m	T_θ	10,6	-	-	-	10,6
	V_T	3,4	2,9	1,8	-	2,7
	V_R	6,4	2,7	2,1	-	3,7
	NRS	1,0	1,0	0,87	-	0,96
11 m	T_θ	10,3	9,8	9,4	-	9,8
	V_T	2,3	2,6	1,2	-	2,0
	V_R	2,1	2,7	2,3	-	2,4
	NRS	0,33	0,99	0,95	-	0,76
8 m	T_θ	10,3	10,1	9,6	-	10,0
	V_T	2,1	2,1	-	-	2,1
	V_R	2,0	2,6	-	-	2,3
	NRS	0,32	0,95	-	-	0,64
5 m	T_θ	10,3	10,3	9,7	14,0	10,1*
	V_T	0,8	5,0	0,8	-2,9	2,2*
	V_R	5,0	-0,8	2,3	1,6	2,3*
	NRS	0,78	-0,3	0,95	0,51	0,48*
2 m	T_θ	10,1	10,1	9,0	14,5	9,9*
	V_T	0,7	3,8	0,7	-3,5	1,5*
	V_R	4,7	-0,7	2,4	3,1	2,1*
	NRS	0,74	-0,3	0,99	1,0	0,48*

* Without W.

Case Study Features

1. Ideal SBL conditions prevailed with calm surface winds, but a small surface temperature inversion was observed.

2. Unit 1 operated at 95% and 71% of its capacity from 21:00 to 22:17 and 22:36 to 03:00, respectively.

3. Severe distortion of the SBL is evident around CT1 and entrainment factor of 104% and 133% occurred, respectively, for these two periods.

4. Boundary layer distortion is almost symmetrical about CT1 to more than one tower height distance. No downwind evidence of SBL distortion was found six tower lengths from CT1.

3.7 Case Study Summary

The main objectives of the experiment at the Kendal Power Station were to determine the extent to which CT1 affected the stable atmospheric boundary layer, and to determine the amount of inversion entrainment into CT1. To achieve this end, the field stage of the experiment was carried out in June and July 1992, the time of the year most conducive to stable atmospheric boundary layer conditions on the Highveld. Temperature and wind profiles were monitored at four points in the tower intake region, over the full vertical extent of this region. Further, tethersonde systems were deployed up- and downwind of the cooling tower, to examine the horizontal extent of its region of influence. A two-dimensional temperature profiler was used to examine the temperature field towards the cooling tower intake region. This section highlights common features found in the individual case studies discussed in the preceding five sections. Interesting but relevant features unique to a single case, are also reviewed.

All the results presented show that the stable atmospheric boundary layer is significantly distorted in the vicinity of CT1. The degree of distortion and the horizontal extent of the region of influence of the tower depend on the nature of the prevailing wind and on the output of the tower's generating unit, i.e. the tower load.

In calm or light wind conditions an almost symmetrical distortion of the SBL develops around the dry-cooling tower. The region of influence is most pronounced within one tower height (165 m) distance from the tower. Some distortion is evident at two tower heights distance from the tower. Typical background stable boundary layer conditions are non-existent in the heat island. A closed system is apparent in which warm air recirculates through the tower. No evidence of cooler air from the outer stable boundary layer entering the tower was found. This is borne out by entrainment factors of larger than 100%. In the calm wind situations, larger entrainment factors were observed at lower outputs from unit 1.

The two-dimensional temperature field about CT1 in Figure 3.6.9(b), depicts the severe distortion of the SBL. Air in circulation around the tower is significantly warmer than the air in the background stable boundary layer. An interesting observation with the light wind situation is that greater entrainment factors were found at lower tower generating output. At about 70% output greater entrainment factors occur than at about 90% output. The implication is that, at near maximum generating capacity, the induced cooling tower draught impinges slightly on the distorted SBL, drawing in some outside air.

In prevailing wind conditions the cooling tower's region of influence and its heat plume are advected downward and downwind. This effect is most pronounced within two tower heights distance in the downwind plane from the cooling tower. Within this area, severe turbulence was experienced. The temperature inversion on the up- and downwind sides of the cooling tower were markedly different, see Figure 3.5.4. Usually, the inversion height is lowered by the downward advection of the heat plume, but under severe conditions, turbulence and mixing erode the inversion entirely and an isothermal layer results. Distant from the tower, a marked thermal stratification occurs in which the coldest most dense air forms a plume over which the gradient winds move. Calm winds occur within the coldest lowest layer, above which a shear in wind speed was observed. In the disturbed boundary layer no shear occurred and less thermal stratification was noted. The vertical wind profiles downwind of the cooling tower showed wind speeds increasing considerably with height.

The two-dimensional temperature field about CT1 under prevailing wind conditions is shown in Figure 3.5.7. Noteworthy in the diagram is the downward and downwind advection of the heat plume, the upwind thermal stratification and the difference in upwind and downwind temperature and wind profiles.

Contrary to the upwind tethersonde soundings, those attempted downwind of the tower proved difficult in the turbulence induced by the tower. This was especially marked when thermal turbulence in the heat plume was complimented by mechanical turbulence in the lee of the cooling tower. A series of two soundings, one just outside the downwind plume of the cooling tower, and one directly downwind, showed that most of the effect of the plume is restricted to the downwind plane.

Entrainment factors under prevailing wind conditions are usually in the order of 70%. An entrainment factor of 36% was observed, but the full extent of the surface temperature inversion could not be determined in this case. This implies that the air entrained into CT1 is warmer than that measured at 1,2 m AGL in the undisturbed stable boundary layer.

Entrainment factors and the corresponding output from unit 1 during the case studies are shown in Table 3.7.1. The four entrainment factors greater than 100% all occurred in light wind situations. Note that the highest entrainment values occur at tower operation loads of about 70% of the maximum. Comparison of the data contained in Table 3.7.1 indicate that, with prevailing winds, cooler air is entrained into the tower, but under calm conditions, severe SBL distortion occurs around the tower, and the induced draught is insufficient to draw air into the tower from outside the island. As a result, warmer air is used in the cooling process.

Table 3.7.1 Entrainment factors, corresponding output from unit 1 as a percentage of maximum capacity and mean boundary layer wind conditions during the case study periods.

Time	Entrainment (%)	Unit 1 output (%)	Wind conditions
21:00 - 03:00 8-9 June	70	74	Easterly
21:57 - 22:27 10 June	93	95	Calm
22:42 - 02:11 10-11 June	135	75	Calm
02:26 - 03:00 11 June	104	95	Calm
21:00 - 03:00 8-9 July	71	82	Southwesterly
21:00 - 00:14 8-9 July	68	85	Southwesterly
00:34 - 03:00 9 July	36	70	Southwesterly
21:00 - 03:00 14-15 July	69	72	Northwesterly
21:00 - 22:17 16 July	140	92	Calm
22:36 - 03:00 16-17 July	133	70	Calm
Mean	92	81	

At the lee side of CT1, a pool of cooler air was observed between the tower's upper lip and the intake area. This cooler air was not entrained into the tower, but circulated above the intake in the induced eddies.

The relative performance of CT1 under the different SBL conditions that were encountered during the field excursions, was determined using data supplied by Eskom and the DB Thermal Characteristic Curve for Natural Draught C. Tower, (Eskom drawing No. 0 64/6510), Schmitz and Landers (1992). The characteristic curve considers the ambient atmospheric conditions and flow rate of water to the cooling tower and the expected temperature of the water after the cooling process. In other words, for given ambient conditions, if the actual water temperature after the cooling process is cooler (or warmer) than the expected water temperature, then the cooling tower was more (or less) efficient.

Mean water temperature into CT1, mean actual temperature of the cooled water out of CT1, the expected temperature of the cooled water according to the characteristic curve and the difference between actual cooled water temperature and the expected value are listed in Table 3.7.2 for six periods discussed in Sections 3.2, 3.3, 3.5 and 3.6. Those in Section 3.4 are excluded as the entrainment factors are unreliable. The water flow rate as a percentage of maximum (80 000 m^3 hr^{-1}) is also listed.

The data in Table 3.7.2 will be discussed with reference to the entrainment factors and prevailing winds, listed in Table 3.7.1. During the light wind situations with entrainment factors of 135% and 133% on 10-11 June and 16-17 July, CT1 did not function as well as expected and the cooled water was 2,3°C and 2,6°C, respectively, warmer than expected. In the two lesser distorted SBL situations, where entrainment was 104% and 140% respectively on 11 June and 16 July, CT1 operated at close to the expected performance characteristics. On these occasions, the water was cooled to 0,6°C and 0,7°C below the respective expected values. During the earlier period on 10 June, a light wind situation, CT1 cooled the water to 2,6°C below the expected value. These three occurrences suggest that, although the SBL was severely distorted around CT1, some coolant air entered the tower intake in another plane.

Table 3.7.2 Water temperatures (°C) into and out of CT1, the expected cool water temperature according to characteristic curves and the difference between actual cool and expected cool water (δT). δT is negative for tower water cooler than expected. Flow is the rate of water flow to CT1.

Time	Flow (%)	Water temperature (°C)			
		In	Actual out	Expected out	δT
21:00 - 03:00 8-9 June	82	38,7	28,5	31,4	-2,9
21:51 - 22:27 10 June	86	41,9	30,1	32,7	-2,6
22:42 - 02:11 10-11 June	85	38,0	28,4	26,1	2,3
02:26 - 03:00 11 June	85	40,9	28,8	29,4	-0,6
21:00 - 03:00 14-15 July	76	37,5	28,0	26,1	1,9
21:00 - 22:17 16 July	74	43,0	31,7	32,4	-0,7
22:36 - 03:00 16-17 July	74	35,2	25,7	23,1	2,6

During the periods 8-9 June and 14-15 July, CT1 entrained 70% and 69% of the nocturnal inversion, respectively. Even so, a marked difference in tower performance was observed. During the first period, cooling to 2,9°C below the expected water temperature occurred, but in the later period CT1 did not perform as well and the cooled water was observed to be 1,9°C warmer than expected. This observation is not fully understood, but prevailing winds may play a role in the varying tower performance. Easterly winds prevailed during the June period, which resulted in cooling beyond expectation. Northwesterly winds prevailed during the July period, possibly inducing a venturi effect between CT1 and CT2 and entraining some of the heat plume into CT1. This could have a negative effect on CT1's performance, resulting in the cooled water being warmer than expected. Some indication of inter-tower activity may be borne out in this example.

4. CONCLUSIONS

To conclude this study, it is pertinent to refer back to the initial objectives and comment on the degree of success achieved with each.

The prime objective was to repeat the Swanepoel and Held (1990) experiment under typical winter stable boundary layer conditions. This objective was met during five nocturnal field excursions, two of which proved to be ideal stable boundary layer conditions. The remaining objectives to monitor temperature and air flow inside the cooling tower, over the whole cross-section of the intake area and to use two tethersonde systems, deployed simultaneously during three of the five field excursions, were met in the field phase of the experiment. Furthermore, cooling tower performance figures were monitored during the field experiment by Eskom staff. Lastly, the data collected and reported on will provide evaluation material for the models being developed by the University of Stellenbosch.

Kendal Power Station's CT1 was found to have a significant influence on the surrounding stable boundary layer. The region of influence usually extends symmetrically to beyond one tower height distance from the cooling tower, but with prevailing winds in the boundary layer, this region can extend to more than two tower heights distance in the downwind plane. With prevailing winds about the tower, about 70% of the observed inversion is entrained into the tower intake. During calm conditions, a closed heat island develops around the tower and no entrainment of cooler air from the stable boundary layer into the tower intake region was observed.

The reason for using the entrainment function in this study was twofold. Firstly, to determine the degree of entrainment of the observed temperature inversion into the cooling tower. Secondly, to facilitate a comparison with the Grootvlei study (Surridge and Hayton, 1985), and with earlier work at Kendal (Swanepoel and Held, 1990).

The Grootvlei Power Station study considered the influence of a cooling tower, serving a 200 MW unit, on the stable boundary layer. Surridge and Hayton (1985) found the region of influence of the cooling tower to extend to about one tower height distance from the tower periphery. They also observed inversion entrainment factors of between 35% and 76%. The average entrainment observed was 54% of the observed temperature inversion magnitude.

In their study, Swanepoel and Held (1990) had difficulty quantifying the entrainment into the Kendal Power Station's CT1, serving a 660 MW unit. Nevertheless, in conditions not entirely representative of the stable boundary layer, they observed the entrainment to fluctuate between 50% and 78%. The region of influence of the cooling tower was found to extend to at least 270 m from the tower periphery.

This study shows that the mean entrainment of the temperature inversion at Kendal Power Station's 660 MW cooling tower of 92% is significantly higher than that at the 200 MW Grootvlei Power Station. The higher Kendal entrainment figure is due to the occurrence of entrainment factors of larger than 100% with severe distortion of the stable boundary layer. This feature was not encountered at Grootvlei nor during the earlier Kendal study. The ideal stable boundary layer conditions experienced in this study did not occur during the field phase of the earlier Kendal work. The field of influence of the Kendal cooling tower was found to extend to about two tower heights distance from the tower periphery under calm conditions. This was found to extend to about three tower heights under prevailing winds at the plume exit. A marked downward and downwind advection of the tower heat plume was noted. Both the region of influence and the entrainment factors observed under prevailing wind conditions agree with those found by Swanepoel and Held (1990).

Considering the plan diagram of Kendal Power Station, Figure 2.1, and the observed range of influence of CT1, a considerable amount of tower interaction might occur under certain wind conditions. For example, with prevailing northerly winds, CT1 is situated within CT2's region of influence, and vice versa with southerly winds. The same argument will affect CT2 and CT3, with prevailing north-northeasterly and south-southwesterly winds. Under calm wind conditions, the heat islands around each cooling tower will certainly overlap between the towers. That from CT1 will overlap with that from CT2, and likewise between CT2 and CT3. Certainly, the findings in this report indicate that the inter-tower spacing is probably insufficient to prevent interaction between the cooling tower under calm wind conditions and in conditions of prevailing winds from selected quadrants. This interaction could reduce tower efficiency by disturbing the stable boundary layer and supplying air warmer than that in the undisturbed boundary layer to an adjacent cooling tower.

Under the different prevailing weather conditions during the field experiment, different degrees of cooling tower performance were observed. With unit 1 operating at near full capacity during the closed heat island situation in a stable boundary layer, the cooling tower did not perform as well as predicted by the cooling tower characteristic performance curves. When easterly winds prevailed the tower performed better than predicted, but performed at below expectations with northwesterly winds. This finding suggests some tower interaction. The extent of the tower interaction under various stable boundary layer conditions encountered, should be considered when planning the layout of natural-draught dry-cooling towers for future power stations.

5. REFERENCES

SCHMITZ W and LANDERS M. TRI Eskom, Personal Communication.

SURRIDGE A D (1981). Wind and temperature fields measured around two dry-cooling towers at Grootvlei Power Station, CSIR Report, ATMOS/82/20.

SURRIDGE A D (1982). On measurement of atmospheric winds, Boundary-Layer Meteorology, **24**, 421-428.

SURRIDGE A D and HAYTON D (1984). Some results of experimental studies into dry cooling systems at coal-fired electric power generating stations in South Africa, CSIR Report, ATMOS/84/2.

SURRIDGE A D and HAYTON D (1985). Interaction between a natural draught dry-cooling tower and the stable boundary layer, CSIR Report, ATMOS/85/3.

SWANEPOEL D J deV and HELD G (1990). Interaction between the stable boundary layer and a natural draught dry-cooling tower at Kendal Power Station, CSIR Report, EMA-C 90144.

TYSON P D, PRESTON-WHYTE R A and DIAB R D (1976). Towards an inversion climatology of southern Africa: Part 1, Surface inversions, South African Geographical Journal, **58**, 2, 151-163.

APPENDIX 1: 22 m MAST ANEMOMETER CALIBRATION

Anemometer No.	Regression line			Anemometer No.	Regression line		
	Coeff.	Const.	Correlation (R)		Coeff.	Const.	Correlation (R)
214	66,863	6,511	0,9997	208	64,357	6,688	0,99995
228	63,325	7,951	0,99996	226	61,276	4,529	0,99996
159	65,181	4,727	0,99994	138	64,796	7,754	0,99994
132	62,708	5,609	0,99997	004	67,416	6,687	0,99995
153	62,146	4,491	0,99998	157	62,375	6,826	0,99996
224	62,044	10,135	0,99993	161	66,906	3,159	0,99995
128	67,993	11,522	0,99996	231	64,531	13,992	0,99995
243	66,277	7,457	0,99994	013	74,342	-16,184	0,99995
213	66,254	3,672	0,99997	193	63,935	3,923	0,99995
158	68,164	5,571	0,99994	197	62,831	5,301	0,99997
183	65,035	8,488	0,99995	142	61,824	-0,842	0,99992
178	65,949	6,795	0,99994	187	63,026	10,592	0,99997
219	60,700	8,300	0,99997	222	66,997	6,291	0,99997
205	65,406	9,078	0,99993	242	62,605	-0,681	0,99995
167	68,730	-22,968	0,99994	140	65,628	8,295	0,99995
245	64,603	8,104	0,99995	152	66,906	9,259	0,99995
211	62,348	1,845	0,99997	145	64,098	10,746	0,99998
196	62,557	7,148	0,9997	215	61,332	21,286	0,99998
144	64,157	6,334	0,9997	181	64,875	7,669	0,99993
230	63,833	4,648	0,9994	185	68,266	5,324	0,99995
206	56,407	18,350	0,9997	201	66,086	3,162	0,99995
195	61,679	5,647	0,9996	207	63,886	6,569	0,99995
229	65,986	5,341	0,9996	223	62,090	6,978	0,99994
306	66,902	5,709	0,9996	233	63,326	7,462	0,99994

An example of the calibration of one of the above sensors is given on the next page. The crosses plotted show real values against measured values, while the line is the best fit which constants are tabulated above.

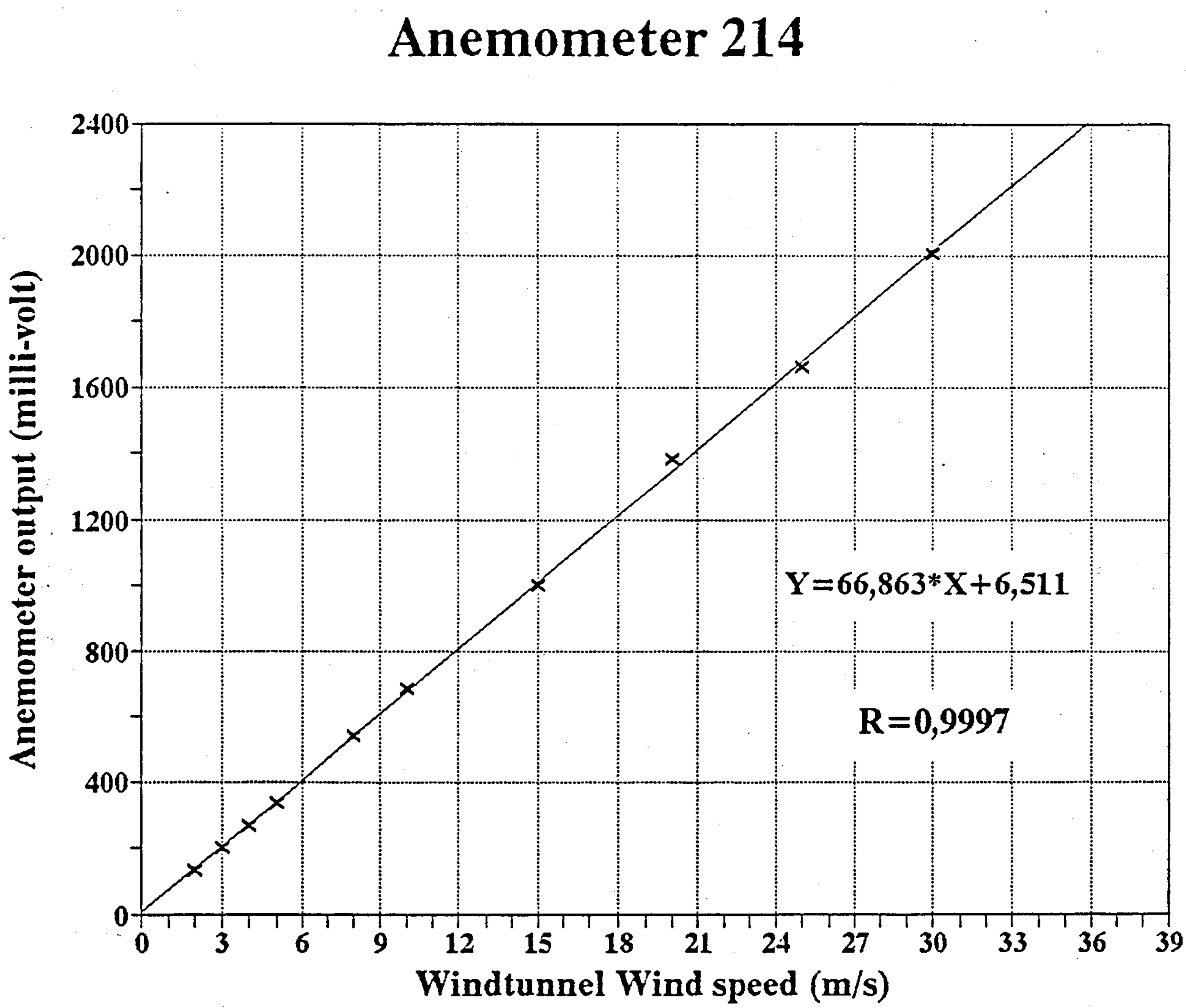
Anemometer 214
Anemometer output (milli-volt)
2400
2000
1600
1200
800
400
0
0
3
6
9
12
15
18
21
24
27
30
33
36
39
Windtunnel Wind speed (m/s)
Y=66,863*X+6,511
R=0,9997

APPENDIX 2: 22 m MAST TEMPERATURE SENSOR CALIBRATION.

Tower temp sensor No.	Regression line		
	Coefficient	Constant	Correlation (R)
247	0,790	4,447	0,9997
338	0,921	2,081	0,9993
336	1,066	-1,248	0,9989
337	0,927	1,745	0,9996
307	0,997	0,381	0,9992
334	0,874	2,828	0,9999
308	0,957	1,213	0,99995
216	0,958	0,795	0,9994
306	0,896	2,089	0,9955
202	0,904	2,128	0,9970
330	0,915	1,897	0,9974
197	0,893	1,898	0,9953
218	0,901	2,332	0,9996
310	1,864	2,934	0,9976
249	0,089	-1,807	0,9992
190	0,891	2,258	0,9964
333	0,902	1,902	0,9976
335	0,911	1,971	0,9987
200	0,979	0,770	0,99995
331	0,921	2,049	0,9986
210	0,929	1,686	0,9983
309	0,925	1,851	0,9998
245	1,079	-1,739	0,9995
201	0,877	2,555	0,9999

An example of the calibration of one of the above sensors is given on the next page. The crosses plotted show real values against measured values, while the line is the best fit which constants are tabulated above.

Thermistor 338

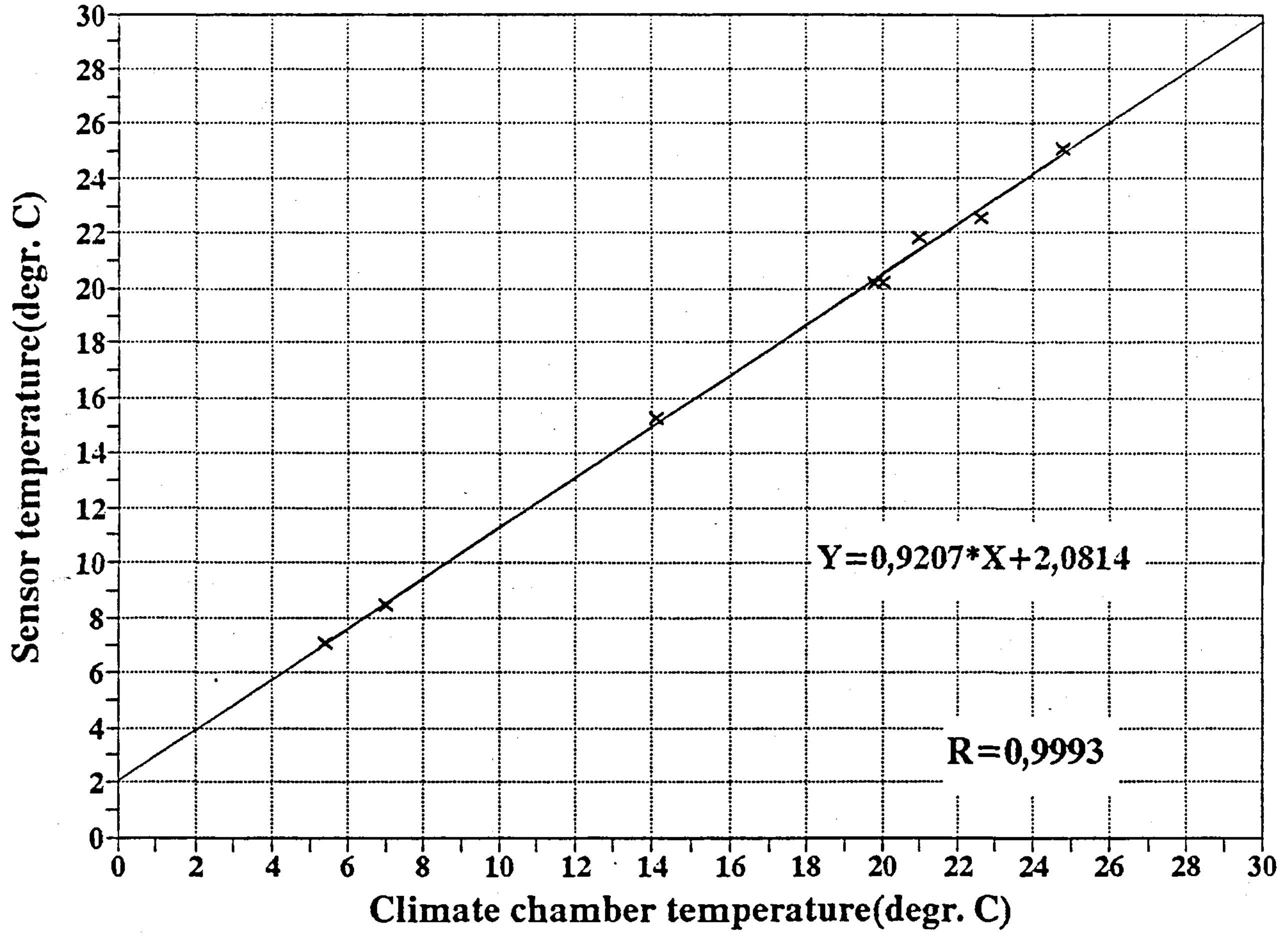

APPENDIX 3: 2-DIMENSIONAL TEMPERATURE SENSOR CALIBRATION.

2-Dim. temp sensor No.	Regression line		
	Coefficient	Constant	Correlation (R)
1	16,321	203,913	0,9962
2	17,460	206,967	0,9986
3	15,192	209,427	0,9988
4	16,929	223,490	0,9962
5	14,928	247,399	0,9977
6	15,957	226,517	0,9970
7	16,207	209,973	0,9982
8	15,975	224,547	0,9975
9	15,097	230,056	0,9997
10	16,026	240726	0,9952
11	15,644	239,018	0,9990
12	15,957	211,775	0,9973
13	15,270	223,677	0,9990
14	15,179	212,999	0,9987
15	15,265	209,939	0,9997
16	14,969	220,649	0,9998
17	15,447	230,502	0,9997
18	15,299	234,906	0,99990
19	14,950	246,247	0,99996
20	15,223	249,433	0,9998

An example of the calibration of one of the above sensors is given on the next page. The crosses plotted show real values against measured values, while the line is the best fit which constants are tabulated above.

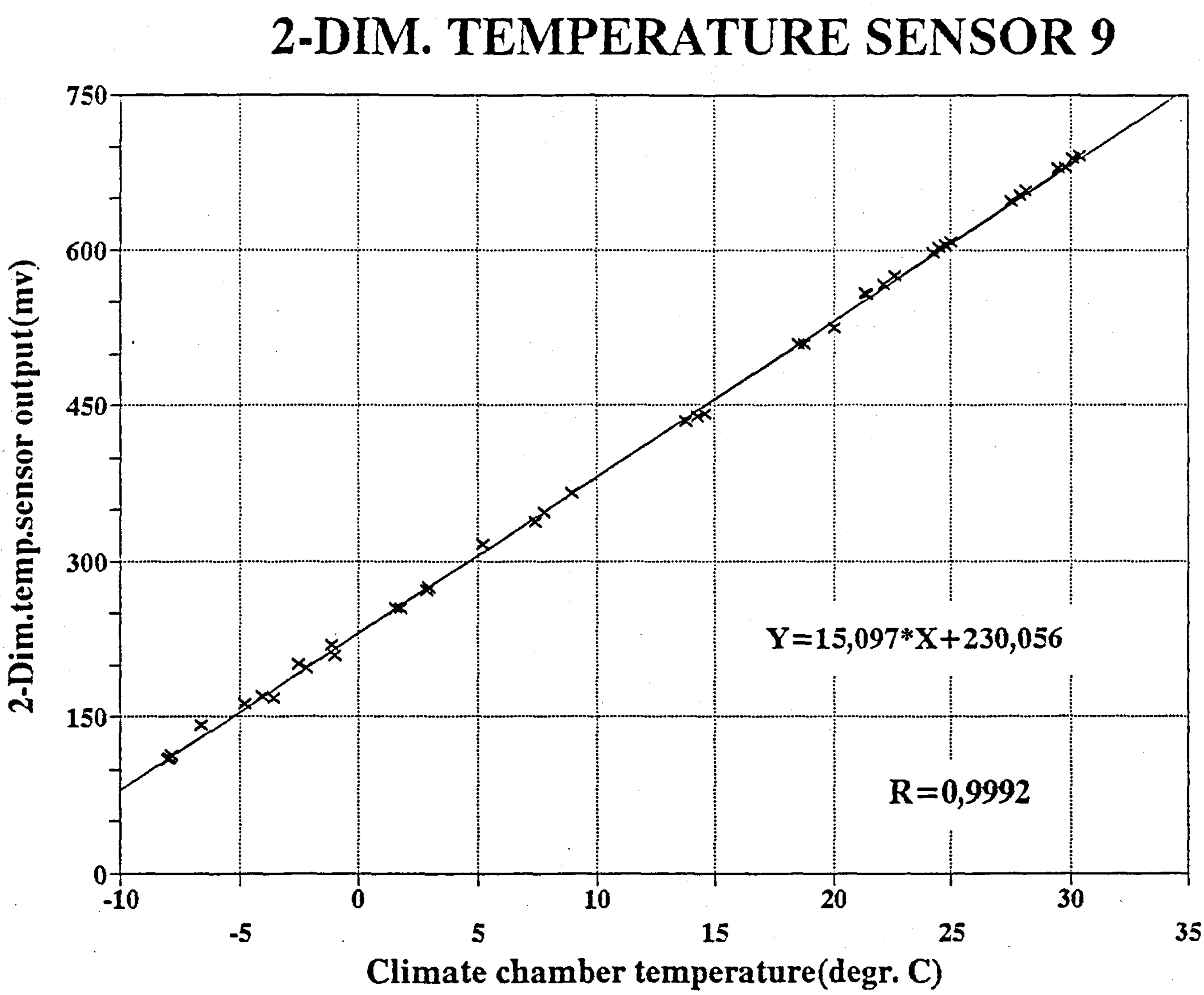
2-DIM. TEMPERATURE SENSOR 9
750
600
450
300
150
0
-10
-5
0
5
10
15
20
25
30
35
2-Dim.temp.sensor output(mv)
Climate chamber temperature(degr. C)
Y=15,097*X+230,056
R=0,9992